



**A CUBESAT MISSION FOR MAPPING SPOT BEAMS OF GEOSTATIONARY
COMMUNICATIONS SATELLITES**

THESIS
MARCH 2015

Jacob A. LaSarge, Second Lieutenant, USAF

AFIT-ENY-MS-15-M-247

**DEPARTMENT OF THE AIR FORCE
AIR UNIVERSITY**

AIR FORCE INSTITUTE OF TECHNOLOGY

Wright-Patterson Air Force Base, Ohio

DISTRIBUTION STATEMENT A.
APPROVED FOR PUBLIC RELEASE; DISTRIBUTION UNLIMITED.

The views expressed in this thesis are those of the author and do not reflect the official policy or position of the United States Air Force, the Department of Defense, or the United States Government.

This material is a declared work of the U.S. Government and is not subject to copyright protection in the United States

A CUBESAT MISSION FOR MAPPING SPOT BEAMS
OF GEOSTATIONARY COMMUNICATIONS SATELLITES

THESIS

Presented to the Faculty

Department of Aeronautics and Astronautics

Graduate School of Engineering and Management

Air Force Institute of Technology

Air University

Air Education and Training Command

in Partial Fulfillment of the Requirements for the
Degree of Master of Science in Astronautical Engineering

Jacob A. LaSarge, B.S., Mechanical Engineering

Second Lieutenant, USAF

March 2015

DISTRIBUTION STATEMENT A
APPROVED FOR PUBLIC RELEASE; DISTRIBUTION UNLIMITED

AFIT-ENY-MS-15-M-247

A CUBESAT MISSION FOR MAPPING SPOT BEAMS
OF GEOSTATIONARY COMMUNICATIONS SATELLITES

THESIS

Jacob A. LaSarge, B.S., Mechanical Engineering
Second Lieutenant, USAF

Committee Membership:

Dr. J. T. Black
Chair

Dr. L. B. King
Member

Dr. G. L. Duke
Member

Abstract

As space-rated technologies become more compact and more readily available over time, the concept of accomplishing space missions with smaller nanosatellite-class spacecraft becomes increasingly feasible. This research focuses specifically on a CubeSat mission to assist with radio frequency (RF) domain verification; that of characterizing and mapping K-band (and lower frequency) spot beams from communications satellites in geostationary orbit. By flying a constellation of CubeSats through the edges of spot beams originating from geostationary communication satellites, the spot beam's coverage area will be characterized.

This research conducts a mission feasibility assessment, identifies the principle mission requirements to complete a spot beam mapping CubeSat mission, and examines various constellation configurations that are able to complete the spot beam mapping mission effectively. It was found that certain spot beam mapping CubeSat constellations performed better than others, specifically regarding mapping time, responsiveness to changing conditions, spot beam detection capability, and overall mapping resolution. Constellations with CubeSat formations that used specific spacing between themselves in an orbital plane could be synchronized to produce spot beam maps with excellent resolution; however constellations with a single plane of evenly-spaced CubeSats or particular Walker constellations from 350 – 500 km could produce better results over shorter durations. Separating CubeSats into planes tended to mix responsiveness and overall map resolution depending on conditions.

Acknowledgements

I wish to enthusiastically acknowledge my thesis advisor; Dr. Jonathan Black, for his outstanding assistance in helping me put together this project, and supplying excellent ideas and feedback throughout the process. The recommendations, conference proposals, and general insight were incredibly useful and much appreciated.

I also wish to thank the members of my thesis committee for their enduring support --- I'd like to acknowledge Dr. Brad King, for providing exceptional guidance and support through my undergraduate years of learning the particulars of small satellite operations, now including my shot at a Master's degree. I would also like to extend my cordial thanks to Dr. Gary Duke, for his willingness to assist and serve on my committee.

Finally, I wish to acknowledge the on-campus individuals who provided assistance, in both academic and military advice, through this process --- especially Dr. Black's team of faculty, contractors, and PhD students, who also provided me with excellent advice, guidance, and support over the past year and a half.

Jacob A. LaSarge

Table of Contents

Abstract	iv
Acknowledgements	v
Table of Contents	vi
List of Figures	viii
List of Tables	xi
List of Abbreviations	xii
I. Introduction	1
1.1 Problem Statement	2
1.2 Current CubeSat Research	3
1.3 Scope / Application	4
1.4 Assumptions	6
1.5 Methodology	7
1.6 Research Merit	7
1.7 Thesis Overview	8
II. Background	10
2.1 Spot Beam Mapping Mission Context	10
2.2 The CubeSat Standard	12
2.3 CubeSat Missions and Concepts	13
2.4 Mission Simulations for Optimization and Modeling	18
2.5 Domain Verification at GEO	19
2.6 Spot Beam Mapping Mission Requirements	20
2.7 Orbit & Constellation Propagation	23
2.8 Spot Beam use at GEO	27
2.9 Sources of Error / Mitigation	28
2.10 Performance Metrics	30
2.11 CubeSat Capability	34

2.12	Spot Beam Mapping Applications	36
2.13	Summary	37
III.	Methodology, Design and Development	39
3.1	Problem Overview.....	39
3.2	Model / Environment Simulation.....	41
3.3	Spot Beam Models	43
3.4	Algorithms / Software Tools	48
3.5	Performance Measurements and Variables.	56
3.6	CubeSat System Metrics	68
3.7	Summary	72
IV.	Results and Analysis	73
4.1	Data Parameters and Trade-offs	74
4.2	Scenario Results (Single-plane constellations)	75
4.3	Scenario Results (Walker Constellations and Multiple Planes).....	83
4.4	Effects of Changing Altitude.....	87
4.5	Effects of Changing Number of CubeSats	90
4.6	Effects of Changing # of Planes.....	92
4.7	Effects of Changing Payload Data Rate	93
4.8	Effects of Changing Inclination	98
4.9	Effects of Changing Duration	104
4.10	Transmitter Position Requirement	107
4.11	Summary	113
V.	Conclusion	115
5.1	Recommendations for Future Work.....	118
	Appendix A: MATLAB Scripts.....	120
	Vita.....	153

List of Figures

Figure 1: Spot Beam Mapping CubeSat Constellation (red) for detecting and mapping spot beams emitted from GEO (yellow/green).	2
Figure 2: MEPSI, 2U Cubesat [<i>USAF</i>]	13
Figure 3: CSTB-1 [<i>Boeing</i>]	14
Figure 4: 6U CubeSat form factor example [<i>AFIT</i>]	16
Figure 5: Spot beam mapping orbit traces showing a visual representation of the difference between “revolution” gap distances and orbit “pass” gap distances.	25
Figure 6: Collect Lat/Lon/Alt and Time information when within spot beams, and received power is high enough.....	40
Figure 7: Intelsat Galaxy 28... Formerly known as Intelsat Americas 8... Formerly known as Telstar 8... on SSL's LS-1300S bus. [<i>SSL</i>]	41
Figure 8: Spot beam model created for North America, using Galaxy 28's Ku-Band beam pattern.	42
Figure 9: Intelsat Galaxy 28 Ku-band spot beams as modeled in STK.	46
Figure 10: Geo-CommSat-II (notional) Ku- and Ka-band spot beams as modeled in STK.	47
Figure 11: Flowchart depicting the simulation side of the spot beam map generation process.....	49
Figure 12: Flowchart showing the process used to obtain the final spot beam maps for analysis.....	51
Figure 13: Earth-Centered, Earth-Fixed coordinate axes used for beam map point translation.	52
Figure 14: "In plane" geometry used for mapping space-based LLA data points to the ground.	54
Figure 15: Geometry used for inclination limit calculation.....	62
Figure 16: Geometry driving angular measurement resolution and the payload sampling rate.....	64
Figure 17: Example of orbital coverage gaps in compiled beam map. (Circled in red)	67
Figure 18: OV-1 for the CubeSat spot beam mapping mission.....	69
Figure 19: SBM mission profile transition diagram.	70
Figure 20: G-28 Space map data points as overlay (blue) with calculated ground map (black), coverage over North America and Hawaii.	76

Figure 21: G-II Space map data points as overlay (blue) with calculated ground map (black), coverage over the pacific.....	77
Figure 22: 3-D Space and ground beam data maps superimposed on the globe, as recorded by the CubeSat SBM constellation from G28 transmitter (left) and G-II transmitter (right).	78
Figure 23: 3-D space and ground beam data maps superimposed on the globe, from G-28's North America beams, zoomed in.....	79
Figure 24: Shorter duration (24 hour) collect, using parameters: 350km 68 inc. 1 plane 6 satellites even spacing.	81
Figure 25: Space/Ground 3D Map with "less informative" data collects. Cfg: 450km, 68deg inc, 1 day, 5 sec data rate, 1 plane, 1 sat.....	83
Figure 26: 350km 6/3/2 Walker Constellation Spot Beam Map -- Galaxy 28 North America Region.	84
Figure 27: 350km, 68inc, 3day, 5sec, 2plane, 3sats/plane, even spacing	85
Figure 28: "Clean" spot beam map constellation result from mapping G-II beams. Constellation: 68 deg, 350km, 3 days, 5 sec, 1 plane, 6 sats, 20 deg sep. Compare to known G-II beams, note missing beams.	86
Figure 29: Coverage gap sizes at mission altitudes for single plane constellations using 3 or 6 CubeSats -- 1 day of collects compared to 3 days of collection.	88
Figure 30: Coverage gap sizes at mission altitudes for 6-2-3 and 6-3-2 Walker constellations -- 1 day of collects compared to 3 days of collection.	89
Figure 31: Relative coverage gap sizes obtained from changing the number of single plane CubeSats at tested mission altitudes.	91
Figure 32: 400km altitude Ku-band spot beam collection passes over the Gulf of Mexico using different payload sampling rates. Left: 1 second per sample, Right: 10 seconds per sample.	93
Figure 33: Ground-based spot beam map accuracy for changing payload data sampling rates, for the mission altitudes.....	94
Figure 34: Minimum sampling rate needed for given spot beam sizes. Assumes 3 data points are required for each pass.....	98

Figure 35: Inclination: 68 deg. Walker 6-3-2 Constellation at 400km, simulated for 24 hours.	99
Figure 36: Inclination: 75 deg. Walker 6-3-2 Constellation at 400km, simulated for 24 hours.	100
Figure 37: Inclination: 82 deg. Walker 6-3-2 Constellation at 400km, simulated for 24 hours.	101
Figure 38: Inclination: 90 deg, polar. Walker 6-3-2 Constellation at 400km, simulated for 24 hours.	102
Figure 39: Inclination: 97.1 deg. Walker 6-3-2 Constellation at 400km, simulated for 24 hours.	103
Figure 40: Inclination: 28 deg. Walker 6-3-2 Constellation at 400km, simulated for 24 hours.	104
Figure 41: Obtained 24-Hour ground-based spot beam map over North America for a single plane of six CubeSats orbiting at 350 km, 68 deg. inclination, with 5 samples/sec sampling rate.....	105
Figure 42: Obtained 72-hour ground-based spot beam map over North America for a single plane of six CubeSats orbiting at 350 km, 68 deg. inclination, with 5 samples/sec sampling rate.....	106
Figure 43: Attitude knowledge error effects on GEO position error covariance determination.	107
Figure 44: 3D View of bearing estimates from CubeSat to GEO Transmitter during a spot beam pass, unfiltered, with GEO orbit distance constraint. (75 samples @ 5 seconds/sample).....	110
Figure 45: Filtered CubeSat position determination of Galaxy 28 along ECEF X-Axis. Data shown for single beam pass over North America, sampled at 5 seconds/sample, with 2 degrees of attitude knowledge error.	111
Figure 46: Filtered CubeSat position determination of Galaxy 28 along ECEF Z-Axis. Data shown for single beam pass over North America, sampled at 5 seconds/sample, with 2 degrees of attitude knowledge error.	112

List of Tables

Table 1: Mission Level requirements, listed with threshold and objective values for the spot beam mapping CubeSat mission.....	21
Table 2: Constraints applied to the CubeSat spot beam mapping mission.	22
Table 3: Typical satellite antenna sizes for Ku- and Ka- band transponders [13].	43
Table 4: LLA position vectors of Galaxy 28 and G-II.....	52
Table 5: CubeSat constellation variables used within the spot beam mapping mission scenarios	56
Table 6: Constants / Variables used within STK's lifetime tool to compute expected lifetime of the Spot Beam Mapping 6U CubeSats.....	58
Table 7: Results of lifetime simulations for various orbits. Assumed fully loaded (12kg) 6U CubeSat.	59
Table 8: Results of lifetime simulations for mission orbit altitudes. Assumed “lightly” loaded (6kg) 6U CubeSat.....	60
Table 9: Test variables for the Single Plane Constellation resultant beam maps shown.	75
Table 10: Selected sample of result information demonstrating single plane constellation capabilities for 3-day collection duration.....	80
Table 11: Selected sample of results demonstrating single plane constellation capability for 24-hour collection duration.	82
Table 12: Results for varying number of satellites within one plane, using collection durations of 1 and 3 days.	90
Table 13: Sample of results by adding CubeSat planes for constant 6 total satellites, with collection durations of 1 and 3 days, 400km alt.	92
Table 14: GPS information: Necessary data storage size determined by <i>constant</i> collection durations and payload sampling rate.	95
Table 15: Ground map geometric error and angular bearing error based on GEO position error estimate. 350km altitude results shown.....	109
Table 16: Favorable spot beam mapping configuration for Ku- and Ka-band spot beam map generation, following with research assumptions and derived requirements.....	116

List of Abbreviations

λ_T	=	Transmitter Longitude
ψ_S	=	Rotation angle from vertical to space point
$1U$	=	One Unit CubeSat Standard Volume
$3U$	=	Three Unit CubeSat Standard Volume
$6U$	=	Six Unit CubeSat Standard Volume
AOA	=	Angle of Arrival
$ADCS$	=	Attitude Determination and Control System
$Comm-Sat$	=	Communications Satellite
$COTS$	=	Commercial Off-The-Shelf
$CSV (.CSV)$	=	Comma Separated Values
DPD	=	Direct Position Determination
$ECEF$	=	Earth-Centered, Earth-Fixed
$FPGA$	=	Field Programmable Gate Array
$G-28$	=	Intelsat Galaxy 28
$G-II$	=	Geostationary Communications Satellite No. 2
GEO	=	Geostationary Earth Orbit
GGA	=	Global Positioning System Fixed Data
GPS	=	Global Positioning System
$HPBW$	=	Half-power beam width
IRF	=	Instantaneous Received Frequency
ITU	=	International Telecommunications Union
LEO	=	Low Earth Orbit

<i>LLA</i>	=	Latitude, Longitude, Altitude
<i>MMT</i>	=	Mission Modeling Tool
<i>MSDOS</i>	=	Microsoft Disk Operating System
<i>NASA</i>	=	National Aeronautics and Space Administration
<i>NMEA</i>	=	National Marine Electronics Association
<i>MSIS-00</i>	=	Mass Spectrometer Incoherent Scatter (2000)
<i>PACS</i>	=	Payload Alert Communications System
<i>P-POD</i>	=	Poly-Picosatellite Orbital Deployer
<i>PSC/CSD</i>	=	Planetary Sys. Corp. Canisterized Satellite Dispenser
<i>PU</i>	=	Pattern Unit
<i>RF</i>	=	Radio Frequency
<i>RSO</i>	=	Resident Space Object
<i>SBM</i>	=	Spot Beam Mapper
<i>SSA</i>	=	Space Situational Awareness
<i>STK</i>	=	Systems Tool Kit
<i>SWAP</i>	=	Size, Weight, and Power
<i>TDOA</i>	=	Time Difference Of Arrival
<i>TRL</i>	=	Technology Readiness Level

A CUBESAT MISSION FOR MAPPING SPOT BEAMS OF GEOSTATIONARY COMMUNICATIONS SATELLITES

I. Introduction

As space becomes an increasingly congested, contested, and competitive environment, the importance of space-based capabilities only increases over time [1]. The concept of added capability in space is especially relevant for spacecraft operating in or near Geostationary Earth Orbit (GEO), where demand for orbital slots is high and space is becoming increasingly limited. As more spacecraft are launched into the GEO belt, the chance of fatal collisions or interference between spacecraft increases [2]. This interference and additional congestion includes the radio-frequency (RF) domain, with global satellite communications taking advantage of numerous and ever-increasing number of spot beams of varying frequencies and pointing locations [3].

Thus, mapping and locating the space-based position of spot beams from communications satellites in geostationary orbit may enhance global RF beam pattern knowledge by providing reasonable estimates of beam location, gain, and frequency information useful for verifying, monitoring, and/or identifying spot beam coverage areas. Conversely, the spot beam mapping mission may also allow areas of lacking spot beam coverage to be identified.

The nano-satellite form factor known as the “CubeSat” [4] has been selected as a project constraint in an effort to follow the trend of attempting to reduce the cost and complexity of the space missions when compared to large, aggregated space systems [5].

Therefore, this research will identify the mission capabilities that are necessary to produce spot beam maps with CubeSats, and will also introduce a software tool to collect, compile and allow analysis on collected space-based GPS data within spot beams.

1.1 Problem Statement

The primary product of this thesis is to analyze the feasibility of completing a spot beam mapping mission with a 6U CubeSat form factor. The mission will specifically be mapping signals from geostationary transmitters with transponder frequencies up to the Ka-band, for the purpose of identifying areas of interfering signals or areas of poor ground coverage. The formal mission statement for the spot beam mapping CubeSat is to *Detect and map the boundaries of geostationary (GEO) communication satellites' spot beams at a target frequency by flying a CubeSat(s) through the spot beams at a low earth orbit (LEO) altitude.* Figure 1, below, shows an earth view of the spot beam mapping mission concept.

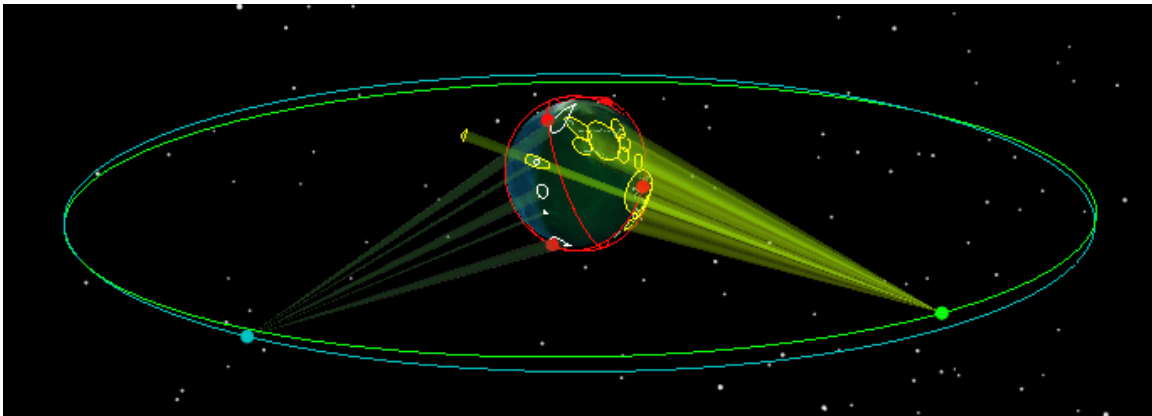


Figure 1: Spot Beam Mapping CubeSat Constellation (red) for detecting and mapping spot beams emitted from GEO (yellow/green).

The following questions for research or further study of the spot beam mapping CubeSat mission are derived from the mission statement:

- Can spot beam coverage areas from Comm-Sats in the GEO belt be adequately mapped by CubeSats flying through the beams in LEO?
- How do various constellations and orbital parameters affect the overall capability of the spot beam mapping mission?
- What on-board capabilities must a spot beam mapping CubeSat have in order to complete the mission?

This thesis addresses those questions, including additional concerns related to spot beam mapping, in order to determine spot beam mapping mission feasibility given a CubeSat form factor.

1.2 Current CubeSat Research

The CubeSat-scale platforms of the small satellite community have significantly advanced efforts in reducing complexity and cost for space missions that do not necessarily require satellites larger than a school bus [6]. Although 1U - 3U CubeSats with payloads have been flown in quantity, the 6U CubeSat bus offers comparable simplicity and ease of integration with at least double the volume and mass capacity [7]. This extra size, weight, and power (SWAP) capacity allows for larger, more robust payloads as well as the possibility to implement larger and more capable bus components, including star trackers and larger Attitude Determination and Control Systems (ADCS), with added capability. Recent research and design projects conducted at the Air Force

Institute of Technology have shown that beneficial missions and capabilities can be derived from nanosatellite-class spacecraft [8].

The small satellite community has been studying various missions on nanosatellite-class spacecraft, in a similar manner to AFIT CubeSat research. For example, the Australian Centre for Space Engineering Research created the Biarri GPS Receiver Project [9], a 3U CubeSat mission testing space rated GPS receivers in an attempt to improve reported spatial position determination accuracy. Similarly, GPS information is vital for the spot beam mapping mission, as positions of spot beams are determined through GPS data. CubeSat missions have also been analyzed with payloads using the RF domain – similar to the concept behind the spot beam mapping mission to be analyzed through this research.

An example of a CubeSat mission with an RF payload is the Space Autonomous Mission for Swarming and Geolocation with Nano-satellites (SAMSON) [10]. The SAMSON CubeSat mission seeks to fly a cluster of three nanosatellites to geolocate a cooperative RF transmitter to within 100m – using RF information from ground transmitters.

Much like these mission examples, a spot beam mapping mission should also be possible, likely facing similar challenges and design considerations.

1.3 Scope / Application

The primary intent of this work is to complete a feasibility assessment of the general spot beam mapping mission with CubeSats. To be useful, the spot beam mapper in the most applied sense should be able to allow end users to identify regions of poor or

interfering spot beam coverage with the final product. Thus the scope of this work will focus on the capabilities and utilities needed to obtain that key desired final mission product: the ground-based spot beam coverage map. This work will also focus on the mission level concerns regarding mission design and analysis, scoped by CubeSats acting as black box systems with expected typical or state-of-the-art CubeSat capabilities.

It must be noted that, although some governing assumptions and requirements used for modeling the spot beam mapper are purely for academic reasons (see Chapter II), the models developed are created to be robust, should the mission assumptions or requirements change. As an example, should some future mission planner wish to identify how a given spot beam mapping constellation at some arbitrary altitude and inclination performs at producing a spot beam map, the simulations and tools created for this thesis are customizable enough to do that analysis.

Additionally, because there are a near infinite number of possible combinations of variables that change the performance factors and capabilities of the spot beam mapping mission [11], it must be noted that to further scope the research presented here, finding the “optimum” solution set for the spot beam mapping mission’s constellations and orbits is not the goal of this work. The various experimental parameters were varied within this work to complete the goal of determining mission feasibility, which means finding constellations that **would work** in the most practical engineering sense for completing the spot beam mapping mission.

1.4 Assumptions

The assumptions used within this work are intended to give boundaries to the problem such that a reasonable assessment of CubeSat spot beam mapping feasibility can be completed.

- All spot beams simulated are Ku- and Ka-band transponders, as lower bands, (which create larger beam patterns), are assumed to be easier to map than smaller beams --- this was a judgment call [12].
- No specific Ku- and Ka- band antennas were simulated due to specific antenna information being proprietary; antenna sizes for spot beams have been generalized within this research, and are simulated as near to typical spacelink Ku- and Ka-band antenna sizing as reported by Horak [13].
- Spot beam model assumes conical spot beam patterns formed by each beam's Half-Power Beam Width (HPBW) [14]. A real-world CubeSat payload must track received power to make a decision itself as to where the beam "edge" is.
- No atmospheric attenuation is simulated in this research for potential effect on ground-based beam patterns.
- The GEO Transmitter's position in space is assumed to be known, or otherwise determined on board the CubeSat. The accuracy of the transmitter position knowledge can significantly affect ground beam map accuracy, and is discussed in Ch. 4.
- The CubeSat receives standard NMEA GPS updates in the GGA format at 1Hz – hardware accurate to within 10m [15], with Doppler effects assumed insignificant.

- No launch insertion constraints are placed on the orbit designs. It is assumed that the CubeSats are able to be injected into constellation positions for all tested altitudes.
- Ground – based (i.e. space-pointing) signal sources acting as potential interference sources are not considered.

1.5 Methodology

In attempt to determine mission feasibility of completing the spot beam mapping with CubeSats, the methodology behind this research is to simulate the spot beam mapping CubeSat constellations with mission simulation and orbit propagation software (STK), then use custom scripts/programs to analyze the relevant and appropriate data generated by the simulation with calculation and computing software (MATLAB). The most important output of the simulation and data gathering process for the spot beam mapping mission, in terms of the notional end-user desire, is the final ground-based spot beam map, generated from the space-based data collects of the spot beam mapping CubeSats. The quality of the final ground spot beam maps is the primary indicator of a “good” constellation set up, and assist with determining “feasibility” of a selected spot beam mapping constellation.

1.6 Research Merit

The benefits of the product of this work, through analysis of the spot beam mapping CubeSat mission, apply to a variety of situations. In the case of primary goal establishment, this mission gives merit to sensibly managing the RF spectrum use for

space to ground links. By verifying regional RF domain use, the spot beam mapping mission has the potential to assist with decongestion, RF interference mitigation, and the possibility to help re-align possible space/ground link misalignments. Additionally, the CubeSat Spot Beam Mapper (SBM), in mapping global spot beams of a chosen frequency, can also determine spot beam coverage areas, allowing users to determine locations receiving weak or no signal from the space segment.

Along with the direct mission goal benefits, there are also secondary merits to this research, including the development of additional relevance for the continuously emerging small satellite community. The spot beam mapping CubeSat mission simulations and data outputs can also act as a reference or baseline project for other, perhaps similar, mission types. In addition, there are also educational benefits that stem from mission analysis and simulation. The spot beam mapping simulations developed within this work can act as the start of an optimization problem, which could in turn help with the optimization of other CubeSat-scale missions.

1.7 Thesis Overview

Chapter I gave an introduction to the spot beam mapping mission in relation to CubeSats. Chapter II covers background information applied to the spot beam mapping mission and the current technological state of CubeSats and their related technologies. Chapter III covers the methodology used to model the CubeSat Spot Beam Mapping mission and the mission's optimized data outputs. Chapter IV compiles and details the results of the simulation runs, which are also analyzed for effectiveness. Finally, Chapter

V gives the primary conclusions regarding the output of the research, and gives recommendations for future work with this mission.

II. Background

This chapter covers relevant background information related to CubeSats and the spot beam mapping mission concept. An overview of related historic CubeSat missions and spot beam generation processes are covered, including the first successful mission types, recent “modern” CubeSat missions, as well as CubeSat missions and proposals that have direct applications to the concept of spot beam mapping. Historic applications of mission analysis are presented, along with some historic research into the operations of maintaining awareness of the GEO belt, topics involving RF geolocation from various sources, and other research projects that have similar features to the spot beam mapping mission concept.

In addition, mission requirements are also presented here to define the basic properties of the spot beam mapping mission, along with performance measures to define what is desirable for mission success. Sources for error are presented with possible mitigation strategies. Finally, CubeSat general specifications are discussed, along with current state of the art and emerging capability of the CubeSat form factor as identified through the small satellite community.

2.1 Spot Beam Mapping Mission Context

The processes by which ground-based spot beam maps are traditionally or historically generated give the spot beam mapping mission appropriate context. Observing the data sources for publically available spot beam maps shows that global spot beam maps are typically generated and derived from manufacturer ground antenna

tests in a lab [16]. Referencing a technical document by Michael Schneider, Ka-band antennas used for generating GEO spot beam patterns are shown to be measured and tuned for beam pattern directivity and gain in scaled lab tests [17]. Although ground laboratory tests can be useful for tuning and modeling a transmitter's beam patterns before launching the system, and useful for generating commercial ground beam pattern maps once in GEO, the in-lab antenna measurement and characterization processes for beam map generation fall short in that the processes do not allow for on-orbit and active beam pattern recognition, observation, and verification.

Another approach to generating data for spot beam map verification comes from the utilization of wideband spectrum analyzers at a fixed ground station terminal. The International Telecommunications Union (ITU) is particularly interested in this method in order to monitor and verify global RF signal use, especially in terms of spot beams from the GEO belt [18]. Various sources have measured satellite signals in conjunction with ITU satellite monitoring (GEO spot beams included) using fixed ground stations. Although measuring signals in this manner provides data on transponder information, the ground map location data is for a single region ground point, and can only form a full beam map when combined with other ground stations. Even then, the beam map will not be of high resolution due to the (relatively) limited number and uneven distribution of ground stations around the globe. The single-station signal measurement method can provide correct “active” data samples needed for spot beam map generation, however has a major pitfall of low resolution, needing one ground terminal per data point, making global beam mapping impossible.

The shortcomings of the above processes, which are currently used to generate and check beam patterns of GEO comm-satellites, call for a more active and robust global-coverage GEO spot beam signal monitoring process. It is thought that by mapping GEO spot beams from LEO, it may be possible to generate and maintain a higher resolution beam pattern database when compared to lab measurements of hardware capability or fixed ground site measurements of GEO signals. Thus, the capabilities and effects of the LEO CubeSat mission for spot beam mapping will be identified, observed, and analyzed in comparison with the historic spot beam map generation techniques.

2.2 The CubeSat Standard

The CubeSat standard for small satellites was introduced to the public by Bob Twiggs and Jordi Puig-Suari just prior to the year 2000. The standard baseline size scaling for a CubeSat is 10cm x 10cm x 11 cm, referred to as 1U [19]. This 1U form factor can be scaled up to larger sizes by, for lack of better terms, stacking 1U cubes on top of or next to each other to create 2U and 3U CubeSats. These CubeSat sizes are designed to be deployed by the standard Poly-Picosatellite Orbital Deployer (PPOD) [19]. The 6U form factor, identified with this research is thus merely the simple geometry of two 3U CubeSats blended together to form a roughly 10 cm x 20 cm x 30 cm “shoebox”-sized spacecraft that can be stuffed with capabilities. The 6U form factor assumed for this research is assumed to be compatible with Planetary Systems Corp’s 6U Canisterized Satellite Dispenser (PSC/CSD) [20].

2.3 CubeSat Missions and Concepts

2.3.1 Early CubeSat Missions

The first missions flown by CubeSats after their initial proposal at the onset of the new millennium were test beds that opened the doors for space missions with potentially cheap access to space. The first CubeSat(s) launched and deployed following the CubeSat standard was in late 2002, known as the “MEPSI” mission, or Micro-Electro-mechanical Pico-Sat Inspector [21]. MEPSI specifically used two tethered 1U CubeSats to help with ground radar small spacecraft detection and observation. Figure 2 shows the un-tethered MEPSI components with their space shuttle deployment mechanism.

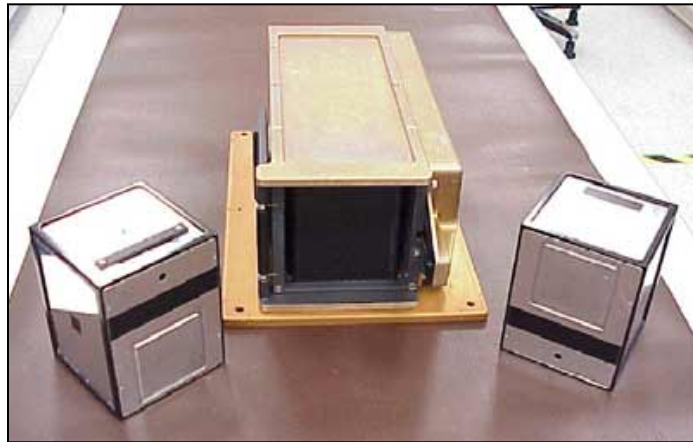


Figure 2: MEPSI, 2U CubeSat [USAF]

Although early CubeSat missions, MEPSI included, had significant reliability issues, according to M. Swartwout’s compiled CubeSat mission data, the first largely successful missions following the CubeSat standard were QUAKESAT-1 (2003) developed by Stanford University and CUBESAT XI-V (CO-58) from the University of Tokyo (2005) [21]. Although CubeSat standard missions following QUAKESAT and XI-V were often held to a coin toss whether or not they would operate correctly when

launched (and assuming the rocket carrying the CubeSats also didn't explode), as technology and experience improves within the small satellite community, reliability with the CubeSat scale becomes improved [21].

CubeSats have also been historically used as lower-cost test platforms for future capabilities and hardware for aerospace and defense.

Examples of CubeSat Testbeds for future capabilities:

- AEROCUBE 3, (2009), by the aerospace corporation, used for technology development [21].
- Boeing CubeSat TestBed-1 (CSTB-1), displayed in Figure 3, was developed to test design elements and ADCS approaches for nanosatellite-scale spacecraft [21].



Figure 3: CSTB-1 [Boeing]

Although there are certainly more, these early CubeSat testbed examples were important missions for improving small scale hardware and processes for use in future CubeSat missions.

2.3.2 *Modern CubeSats (2014+)*

Compared to the earlier CubeSat missions, modern CubeSats have trended towards higher reliability and more robust missions [21]. Additionally, constellations and formations/proximity operations have also entered into mission planning for certain CubeSat missions in more recent times.

Examples of recent CubeSat missions

AeroCube 6A and 6B (June 2014): A 1U CubeSat that divides in half and separates once on orbit flying near prox-ops measurements with micro-dosimeters.

Flock – 1 CubeSats: The “Flock” CubeSats, owned and flown by Planet Labs, are Earth Observation missions with ground resolution of 3 to 5 meters, operating in moderate to high inclination orbits. According to NASA, the Flock mission will be the largest constellation of CubeSats flown to date.

TacSat-6 and AFIT LEO iMESA CNT Experiment (ALICE): The Department of Defense has also sponsored several CubeSat missions. In recent times TacSat-6 was launched as a US Army CubeSat to test nanosatellite communications, and ALICE was an AFIT mission to test a carbon nanotube array, in an effort to better small satellite propulsion capabilities.

In addition to recent missions, additional technology developments for small satellites have become more apparent with time. An example of this comes from research that is being conducted at AFIT with the 6U form factor for CubeSats. Figure 4, below, shows an example of a 6U CubeSat form factor.

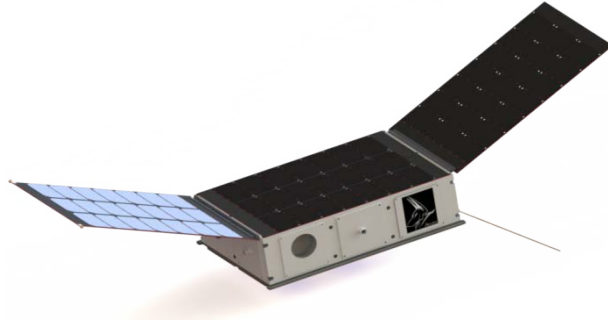


Figure 4: 6U CubeSat form factor example [AFIT]

With the additional SWAP capabilities and benefits offered by 6U CubeSats, it is hypothesized that 6U CubeSats may be able to carry more hardware and thus perform certain missions that were not traditionally possible with smaller 1U-3U CubeSats, all while maintaining similar affordability when referenced against large space missions. Dispensers, like the P-POD for the 3U form factor, for the 6U CubeSat form factor are sitting as “proposed” although none have actually flown any 6U CubeSat missions yet. Planned 6U CubeSat launches are on the near horizon, with missions such as ORS-Squared, for example, are scheduled for flight as presently as spring of this year (2015) [22].

2.3.3 CubeSat Missions related to Spot Beam Mapping

There also exist several CubeSat missions that have direct relation to the spot beam mapping mission concept presented in this research. The most closely related CubeSat missions include RF signal collection missions, RF signal geolocation missions, and atmospheric or surface mapping missions.

The Biarri CubeSat is a joint US, Australian, Canadian, and UK defense-related mission example of an RF signal collection mission that can be related to the spot beam

mapping mission through mutual use of GPS signals [9]. The Biarri mission seeks to use a formation of 3 Colony-II CubeSats, each employing a Field-Programmable Gate Array (FPGA) GPS receiver payload. The Biarri project, using GPS, offers a configuration architecture not unlike the spot beam mapping mission.

Capt. Small, in his thesis, researched the concepts behind conducting ground-based radio frequency emitter geolocation through a CubeSat mission. Capt Small's work simulated 6U CubeSat formations and methods to locate source transmitters on the ground through Time Difference Of Arrival (TDOA), Angle of Arrival (AOA), Direct Position Determination (DPD), and Instantaneous Received Frequency (IRF) geolocation methods, finding that the AOA method performs better than the others for single- or two-ball CubeSat based geolocation. When additional three or more CubeSats were used, Capt. Small found that the DPD geolocation method became the better option [23]. Ground-based transmitter geolocation gives additional merit to CubeSat missions focused on situational awareness and domain verification.

There are also scientific CubeSat missions that have direct application to the spot beam mapping CubeSats. The Dynamic Ionosphere CubeSat Experiment (DICE) mission, Launched in 2011 was tasked with "mapping geomagnetic storm enhanced density plasma bulge and plume formations in the Earth's ionosphere." DICE's measurements of atmospheric properties over an orbit duration with position data input is in direct relation to spot beam mapping, only with atmospheric properties as the desired samples instead of RF signals from GEO [24]. NASA is also investigating a rather sporting lunar mapping project using CubeSats, known as the Lunar Flashlight mission, in an effort to locate lunar ice for future use, should humans ever decide to actually explore the moon

again [25]. Although less directly relevant for Earth-based spot beam mapping than the above examples, the proposed Lunar Flashlight mission is researching the use of a 6U CubeSat form factor in a Lunar orbit to accomplish its mapping objective.

2.4 Mission Simulations for Optimization and Modeling

The concepts of simulating orbit/constellation design, conducting feasibility assessments, and performing optimization on small satellite missions has been an inherent necessity since the advent of small satellites. The research presented in this thesis centered on the development of simulations to conduct a spot beam mapping mission with CubeSats. The results of these spot beam mapping simulations are developed in such a form that they may be optimized to find the best solution in terms of cost and capability. AFIT conducts, and has conducted in the past, several research projects that optimize orbits, constellations, and mission configurations [5],[26],[27],[28],[23],[29]. Therefore, the spot beam mapping mission simulations developed through this research are intended to allow for mission optimization, using methods similar to the optimization methods presented below:

Through AFIT study, Maj. Robert Thomson has researched a conceptual architecture optimization for Defense Weather Systems and constellations. Using the concept of disaggregation of space missions as a foundation for cost reduction, Maj. Thompson sought to identify the methods by which to conduct trades between large aggregated missions versus smaller disaggregated platforms related to space based defense weather systems. Cost optimizing of the spot beam mapping mission scenarios was outside the scope of the research presented here, however will nonetheless benefit

from appropriate cost modeling techniques and optimization that Maj. Thompson discusses [29]. As a follow on to Maj. Thompson's work, 2d Lt. Evelyn Abbate used a genetic algorithm method to analyze and find optimum solutions for a disaggregated imaging spacecraft constellation given a specific target deck [5].

Mission modeling research with CubeSats has also been conducted in the past and presently at AFIT. Capt. Angie Hatch [30] conducted research into a Mission Modeling Tool (MMT) for a CubeSat mission. Capt. Hatch's specific mission for analysis sought to upgrade a previous AFIT work, a Colony-II Bus Mission Modeling Tool (C2BMMT) [31], in order model the power use for Electrospray Propulsion on board CubeSats. The MMT architecture takes advantage of the MATLAB and STK link capabilities, not unlike the spot beam mapping simulation tool presented within this research. Although Capt. Hatch's work was specific to power scenarios with one particular mission concept, the governing methodology and software tool development driving the MMT is applied to the spot beam mapping mission simulation tool development in this research, in order to model the spot beam mapping mission's payload capability in a useful manner.

2.5 Domain Verification at GEO

Due to the interest and demand for slots within the GEO belt, there are several research projects that have been done in the past that have been conducted in order to analyze RF signals or other concepts related to mission operations and verification of objects and features of spacecraft in GEO. On maintaining awareness of objects and events in GEO, Brian Spanbauer and Jesse Yates studied the challenges of deploying near-GEO observation satellites to increase observation and characterization capabilities

out near the GEO belt. Spanbauer and Yates studied orbit feasibility and constellation types effective for GEO observer satellites. Their analysis of orbits and constellations for GEO observation satellites utilized similar analysis and approaches relevant for research behind a spot beam mapping mission for mapping GEO spot beams from LEO [32].

The concept of using RF signals from GEO for interference and location estimation is also nothing new. As a good example, Ronald Bentley with the Southwest Research Institute conducted a study of RF signal geolocation techniques applied to geostationary satellites using known Time Difference of Arrival and Frequency Difference of Arrival position estimating techniques. The goal behind the project was to identify the ground-based location of interference signals with GEO communications satellites [33]. The goal of Bentley's work, finding the position of sources of ground-based interference for GEO comm-sats, gives additional merit to the similar objectives of the spot beam mapping mission's capability to detect areas of signals interfering with other spot beam signals. Although no empirical data for comparison was presented in Bentley's report, the equations and processes to test hardware's capability to geo-locate a ground-based interference source were listed.

2.6 Spot Beam Mapping Mission Requirements

The mission statement for this proposed CubeSat mission is to "Detect and map the boundaries of geostationary (GEO) communication satellites' spot beams at a given frequency by flying a CubeSat(s) through the spot beams at a low earth orbit (LEO) altitude." Stemming from this mission statement, a series of mission-level requirements, with minimum success criteria thresholds, were developed to give the CubeSat SBM

project its scope [34]. If this mission were to actually be pursued, some of these requirements would change depending on customer needs. However, for academic purposes, feasible requirements and constraints have been added to help lay the foundation for the spot beam mapping mission. Threshold requirements for the SBM mission were created to define minimum mission success. Optimism and/or ambition dictate the establishment of objective requirements as well, to define reasonable goals for the SBM mission. Thus, Table 1 displays the mission requirements, along with their threshold and objective (i.e. goal) values.

Table 1: Mission Level requirements, listed with threshold and objective values for the spot beam mapping CubeSat mission.

Requirement	Description	Threshold	Objective
Signal Detection	The CubeSat SBM shall be capable of collecting spot beam signals originating from comm-sats in GEO.	C/X/Ku-band 4-18 GHz collection	K/Ka-band added: 4-40 GHz collection
Signal Mapping	The CubeSat SBM shall record and download GPS information within detected GEO spot beams	Record LLA and Time of Spot Beam Edge location and download to ground station	Record at least 30 seconds of LLA and time in beams and download to ground station
Mapping Accuracy	The CubeSat SBM shall produce a ground map accurately	1 km ground map error	0.5 km ground map error
Robustness	For target frequency: find spot beams from comm-satellites	5 spot beams per comm-sat at target frequency	All spot beams per comm-sat at target frequency
Coverage	GEO Spot beam potential coverage area	Regional Beams of Target Frequency	Global Beams of Target Frequency
Mission Data	The CubeSat SBM must collect useful information	GPS position at beam edges , time, frequency	GPS position per time step in beam, time, gain, frequency
Timeliness	Target frequency spot beam map available in a reasonable amount of time	Beam map of target frequency completed after 3 days	Beam map of target frequency completed after 24 hours

These mission requirements were used as general assumptions for the required performance of a CubeSat spot beam mapping mission throughout this research. It must be duly noted that should these requirements change, the capability assessments made within this research may also need to be re-evaluated. For example, if the spot beam

mapping timeliness requirement becomes more demanding, then the simulations would need to be revisited to find feasible orbits and constellations for the new requirement. The mission requirements also listed the desirable frequencies to be mapped. The Ku- and Ka- band beam frequencies were focused on in the simulations presented in this research since they were at the higher end of the spectrum, and have been shown to be useful in space applications [35],[36],[37],[38],[39]. Lower frequency beams, such as the C- or X-band spot beams tend to cover much larger areas of the globe, and thus should be “easier” to find by the spot beam mapping constellations [12].

Constraints to give the CubeSat SBM mission its bounds were also established. These constraints were derived through existing regulations, or made through reasonable assumption for academic purposes. Note that since this is an academic study for feasibility and simulation of the spot beam mapping mission, cost and schedule would be purely fictional at this time, and thus have not been considered. Table 2 outlines the basic constraints applied to the CubeSat SBM mission.

Table 2: Constraints applied to the CubeSat spot beam mapping mission.

Constraint	Explanation
Payload	IEEE C/X/K-Band Receiver (various possible)
Operational Lifetime	At least 1 year for each CubeSat
Maximum Lifetime	25 years, if no de-orbit capability on-board
Form Factor	6U CubeSat standard volume assumed for this research

The payload constraint remains rather open, as the payload designer should select an RF payload that collects on the desired target spot beam or comm-satellite frequency range. The most important of these mission-level constraints related to mission design are the lifetime limits. The lifetime constraints significantly influence the workable orbit altitudes that the mission can use, and are discussed in Chapter III.

2.7 Orbit & Constellation Propagation

The CubeSats and GEO transmitters studied within the spot beam mapping mission use SGP4 orbital propagation methods within the simulation, which include two-body motion and perturbations effects in an attempt to simulate real-world orbital environments [40]. The equations of motion for the orbiting satellites are fundamentally governed by Kepler’s two-body equation, which Vallado [40] details as:

$$\ddot{\vec{r}} = -\frac{\mu}{r^2} \frac{\vec{r}}{r} \quad (1)$$

The two-body equation lists μ as the Earth’s gravitational parameter, and r as the satellite position in both vector and scalar form. The two-body problem forms the basis on which the features, shape, and position of an orbit can be determined – either in LEO or out at the GEO belt for my scenarios. The orbital period that a spot beam mapping CubeSat will be subjected to within its given circular orbit was also useful within mission design and was also derived fundamentally by Vallado [40] as:

$$P = 2\pi \sqrt{\frac{a^3}{\mu}} \quad (2)$$

The orbital period equation uses μ as the earth’s gravitational constant and a as the semi-major axis of the orbit (or radius of the orbit since circular orbits have been assumed).

In addition to basic two-body physics, there are also other perturbing forces present in the real-world space orbit environment that need to be accounted for in simulation. Significantly, since the earth isn’t in reality a perfect sphere, the gravitational effects of what is actually an oblate spheroid cause orbital plane precession about the

pole, in what has been called the J2 effect [41]. This J2 effect is also called “Regression of Nodes,” which can be modeled by the following equation [41], [40]:

$$\dot{\Omega} = \frac{3nJ_2R_e^2}{2a^2(1-e^2)^2} \cos i \quad (3)$$

The regression of nodes equation uses a , e , and i as the orbital elements “semi-major axis,” “eccentricity,” and “inclination,” respectively. R_e is used as the mean Earth radius, n as the mean motion, and J_2 as the perturbation constant ($J_2 = 0.00108263$).

Additional perturbing forces such as aerodynamic drag and solar radiation pressure act on low-earth orbiting spacecraft as well, however these will be analyzed later in Chapter III in conjunction with spacecraft lifetime concerns [34].

The nodal regression combined with the Earth’s rotation create an interesting effect on LEO satellite ground traces, which is relevant for the spot beam mapping mission, since the gaps in between the ground traces of the spot beam mapping CubeSat’s passes effectively govern how successful the constellation and orbit setup was. Although formally discussed in the results and conclusions of this research, it goes without saying that for maximum coverage gap reduction and to maximize beam detection capability, the spot beam mapping constellations and orbits should avoid harmonic “exact” repeating ground tracks. The equation to find the ground trace shift ($\Delta\lambda_{rev}$) for successive orbital revolutions/passes at the equator is shown as follows [40]:

$$\Delta\lambda_{rev} = (\omega_{earth} - \dot{\Omega})P_{\Omega} = \frac{2\pi R_e k_{day2rep}}{k_{rev2rep}} \quad (4)$$

The ground trace shift equation has ω_{earth} as the rotation rate of the Earth, $\dot{\Omega}$ as the nodal regression rate from the J2 effect, and P_{Ω} as the nodal period. R_e in the

equation is the equatorial Earth radius, k_{day2rep} is the number of days the satellite should take before repeating its ground track, and k_{rev2rep} is the “revolutions to repeat,” (a.k.a. the equatorial crossing points).

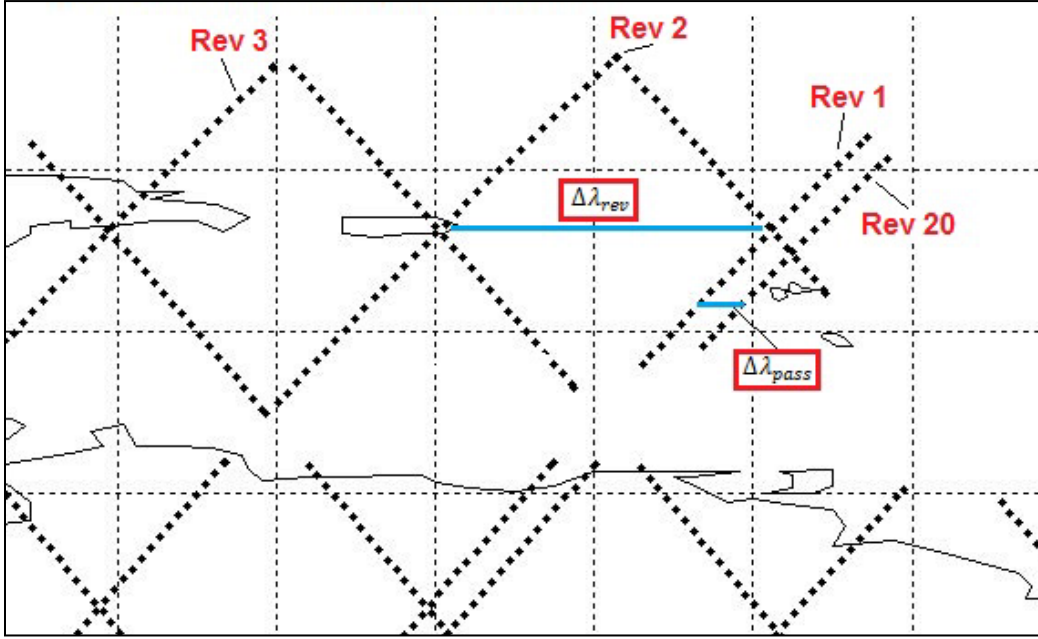


Figure 5: Spot beam mapping orbit traces showing a visual representation of the difference between “revolution” gap distances and orbit “pass” gap distances.

In order to reduce the size of the coverage gaps left by the ground trace of each revolution, ground track orbits that don’t immediately repeat themselves are desirable for the spot beam mapping mission. The above figure demonstrates that a repeating ground track orbit would have $\Delta\lambda_{\text{pass}} = 0$, which would not, given a single satellite, reduce the observed coverage gap size with spot beam mapping after any duration with successive passes. Although Vallado [40] does not seem to directly give an equation for $\Delta\lambda_{\text{pass}}$, the following equation gives the offset pass angle $\Delta\lambda_{\text{pass}}$ relative to the previous equatorial orbital pass for ground tracks that don’t repeat themselves immediately:

$$\Delta\lambda_{pass} = \left(\left\lfloor \frac{360^\circ}{\Delta\lambda_{rev}} \right\rfloor + 1 \right) \Delta\lambda_{rev} - 360^\circ \quad (5)$$

Note: the brackets inside of the equation are a “floor” operator (i.e. the number within the brackets must be rounded down to the nearest integer). A different form of the $\Delta\lambda_{pass}$ equation can also be shown for cases where $\Delta\lambda_{rev}$ has not been directly solved for, with the variables described above:

$$\Delta\lambda_{pass} = \left(\left\lfloor \frac{360^\circ}{(\omega_{earth} - \dot{\Omega})P_\Omega} \right\rfloor + 1 \right) (\omega_{earth} - \dot{\Omega})P_\Omega - 360^\circ \quad (6)$$

This new equation for $\Delta\lambda_{pass}$ becomes useful for finding desirable orbits for the spot beam mapping mission, since by changing the orbit $\Delta\lambda_{pass}$ for relative orbit passes can be tailored for best coverage gap reduction within the output spot beam maps. As will be thoroughly discussed, reducing the size of the spot beam map’s coverage gaps after successive passes reduces the risk of completely missing spot beams during data collection.

In addition to tailoring specific orbits, there are also specific constellation types that can be designed to take advantage of orbits to maximize Earth coverage. The “Walker Delta Pattern” [34] was simulated within this research to see how well the pattern could perform the spot beam mapping mission in comparison to other constellations. The equations governing the formation of Walker Delta Patterns are given by the following equations [34]:

First, the “Pattern Unit” upon which most features of the Walker constellation are derived from should be defined as:

$$Pattern\ Unit\ (PU) = \frac{360^\circ}{t} \quad (7)$$

Where t = the total number of satellites in the entire constellation. After determining the pattern unit, the geometry features of the Walker Constellation can be determined by the following series of simple equations [34]:

$$Plane\ Spacing = s * PU \quad (8)$$

$$Satellite\ Spacing = p * PU \quad (9)$$

$$Phase\ Offset = f * PU \quad (10)$$

Where: “ s ” = the number of satellites per plane, “ p ” = the number of orbit planes evenly spaced in node, “ f ” = the relative spacing in between satellites in adjacent planes (integer from 0 to $(p-1)$), and “ PU ” = the pattern unit of the Walker Constellation.

2.8 Spot Beam use at GEO

The GEO belt provides space missions with an orbit that allows continuous ground coverage over a hemispherical region of the Earth. Demand for slots within the GEO belt is extremely high due to the obvious practical uses of constant coverage over regions. The GEO belt is defined by the circular orbit at which the orbital period equals the length of a sidereal day, and thus satellites in GEO revolve around the earth at the same angular rate the earth revolves [41].

Spot beams coming from GEO can use a variety of frequency bands, including the Ku/Ka-bands focused on within this research (Detailed in Chapter III). Typical spot beams emitted from the GEO belt can have a large range of shapes and sizes [12]. GEO

spot beams can cover continents, or with high frequencies and/or large dish antennas, can be focused down to the size of perhaps a small island. GEO satellite uses range from typical telecommunications to radio traffic, data streaming, and even television and video services. Spot beam use in the future may even provide internet services globally at reasonable speeds [39].

An additional feature of GEO spot beams that may assist with the spot beam mapping concept is signal polarity. Numerous spot beams emitted from GEO are combined to form beam patterns, typically with vertically or horizontally polarized beams, relative to Earth-fixed coordinates. It may therefore be possible, as an additional feature, to complete the spot beam mapping mission of individual beams within a larger beam pattern network by measuring the polarization of the signals when flying through them. The beam edges within the larger beam pattern may therefore be identifiable when the CubeSat system measures a difference in polarity at the same target frequency.

2.9 Sources of Error / Mitigation

The spot beam mapping mission, like any other small satellite project, will almost certainly be exposed to sources of error. Potential sources of error for the spot beam mapping mission analysis are discussed within this section, including potential mitigation strategies. Although every possible source of error is not covered, a list of the major sources of error for the spot beam mapping mission analysis is shown.

- GPS coordinate error: Reported as 10m error for most CubeSat-scale GPS receiver packages [42]. Mitigation: Since 10m is reported to be state of the art for the

CubeSat scale, reducing this potential source of error would be best accomplished by collecting as much data as possible to allow for statistical filtering of the data.

- Atmospheric signal attenuation: It exists heavily for certain frequency bands, and may affect the actual ground location of spot beam RF signals. This is especially true for water vapor attenuation with weak transmitters in the upper K-bands [14]. Mitigation: Calibrate spot beam map translation algorithms with initial calibrating spot beam passes. Measure received orbit signals and compare with signals measured on the ground.

- CubeSat orientation affecting signal reception: If the CubeSat's payload signal receiving antennas aren't pointing towards the spot beam source, or if the CubeSat is tumbling, the risk is present of detecting the signal too late for edge detection reasons. Mitigation: Attitude knowledge and control hardware selection based on the payload receiver's capability.

- Imperfect CubeSat constellation spacing, constellation maintenance: Diminishing of ideal CubeSat spacing over time will cause performance degradation in terms of coverage gap reduction ability of the constellation [34]. Mitigation: Constellation degradation must be analyzed and on-board thrust mechanisms considered, if necessary.

- Transmitter position knowledge. If the position of the transmitter is largely unknown, the ground based spot beam map runs the risk of being inaccurate, or completely incorrect. Mitigation: Collect more data to allow for statistical filtering of ground-based spot beam map points. On-board transmitter referencing can also be considered, as can other possible position determination sources to improve accuracy [23].

- Space environment concerns (e.g. bit flipping / SEU's): Common with any space mission, space environmental effects are something that must be accounted for within on-board hardware and software [14]. Mitigation: Robust Hardware Design to account for the vehicle's environment.

- Drag estimation for lifetime concerns: Error with the satellite drag estimates for the spot beam mapping mission could change the usable orbit window [34]. Mitigation: Additional research and observations of on-orbit missions.

- Terrain effects on map accuracy: This research assumed Earth as an Oblate Spheroid (WGS84). Terrain changes will also move the ground beam intersection point – lowering map accuracy. Mitigation: Future models can incorporate terrain data onto the WGS84 assumption to increase terrain accuracy with respect to the spot beam map.

2.10 Performance Metrics

Following expectations from the mission requirements, the spot beam mapping CubeSat must output GPS information including Latitude, Longitude, Altitude (LLA), and Time while the CubeSat is within a desired spot beam. This information alone can produce a space-based spot beam map. When the space-based spot beam map is combined with the known position of the GEO Transmitter, a ground based (i.e. with zero altitude) spot beam map can be derived through trigonometry and vector analysis between the mapped points and the GEO transmitter's position (see Ch. 3).

To characterize the performance of the spot beam mapping CubeSat mission, five performance indicators were identified based on the developed mission requirements, namely: Beam Map Accuracy, Map Resolution, Beam Detection Capability,

Responsiveness, and Mission Lifetime. Each of these performance factors significantly drive the mission feasibility, constellation design, and orbit selection.

2.10.1 Beam Map Accuracy

The most important measure of performance relates to the desired output of the spot beam mapping mission – the accuracy of the final ground spot beam map. If the spot beam mapper cannot accurately find the edges and internal GPS coordinates of the target spot beams, it will be difficult to assist with the goals of RF domain verification and interference mitigation. The inability to accomplish those goals would significantly hamper the feasibility of the mission. Measured as a distance error (actual vs. measured), it is most desirable to have a spot beam map created as accurately as possible, with special attention given to each beam’s edges and location of maximum gain. The accuracy error of the beam map is determined by comparing measured / calculated beam edge locations (point collects) and comparing them with the beam edge points within the model, by the following equation:

$$\text{Pt. Error (deg)} = |\text{Measurement (Lat, Lon)} - \text{Model "Truth" (Lat, Lon)}| \quad (11)$$

2.10.2 Map Resolution

The final “resolution” of the spot beam map is also a key measure of performance since it is reasonably quantifiable by measuring the average size of the gaps in the spot beam mapper’s orbital coverage. The size of these coverage gaps is important to note – for example, if the spot beam mapper’s coverage gap size is larger than the average size of a spot beam, there is a chance that over the given collection duration, certain spot beams may be missed completely. In the simulations conducted, the coverage gaps were measured in degrees latitude and longitude at the earth’s surface. The total characteristic

solid angle for a selected coverage gap, Ω_{gap} measured in square degrees (or steradians) will be approximated with the following solid angle equation:

$$\Omega_{\text{gap}} = \frac{\lambda\psi}{2} \quad (12)$$

Where λ is the longitude difference (deg) between two successive orbital passes, and ψ is the latitude difference (deg) between two successive orbital passes.

2.10.3 Beam Detection Capability

Coverage gaps aside, a second method to assess the performance of the spot beam mapping constellations was to note how well the simulated CubeSat constellations were able to find each of the modeled spot beams in the STK scenario. Spot beam maps that are not appropriately characterized and mapped by the selected constellation are not as desirable as constellations that can create spot beam maps which can appropriately define all target beams. Determining detection capability using the known beams in the model was a qualitative analysis metric, after counting the number of beams the mapping constellation detected.

2.10.4 Responsiveness

The “responsiveness” performance measure refers to the ability of the spot beam mapping CubeSats to respond to a changing scenario. The simulations conducted contained beams that moved, disappeared, or were in constant motion. Although more difficult to quantitatively measure, the responsiveness of a given CubeSat constellation will be observed qualitatively by observing the beam map outputs from the simulation, and noting how many times, how often, and (subjectively) how well the CubeSats detected the mobile/disappearing beams.

2.10.5 Mission Lifetime

The lifetime of the spot beam mapping mission is a secondary consideration as an easy to quantify performance indicator. According to the mission requirements, it is desired that the mission must last at least one year, however due to legal constraints cannot stay in LEO longer than 25 years unless the CubeSat includes de-orbit capability. As performance is concerned, the longer a spot beam mapper can remain functional in orbit past the one year minimum, the lower the upkeep cost to replace the formation becomes for the end user. The equations governing mission lifetime are discussed in chapter IV.

The above five performance metrics together, combined with an extra parameter for “monetary cost,” form a unique mission analysis optimization problem. Although finding an optimum solution for spot beam mapping is not definable without end user input, it is nonetheless useful to note that the best theoretically possible spot beam mapper would meet the following performance measurements:

- *Beam Map Accuracy:* The distance error of measured spot beam locations (ECEF coordinates) shall be minimized.
- *Beam Map Resolution:* The latitude and longitude coverage gap size between all orbits over the collection duration shall be minimized.
- *Beam Detection Capability:* The number of beams detected and characterized within the spot beam mapping simulation must be maximized.
- *Responsiveness:* The number of times the spot beam mapping constellation passes through a given “active” spot beam shall be maximized and the time in between successive fly-throughs of a given “active” spot beam shall be minimized.

- *Lifetime:* The mission duration of the spot beam mapping constellation shall be maximized, applied under the mission lifetime constraints of “no shorter than 1 year, and no longer than 25 years.”

2.11 CubeSat Capability

The capability of nanosatellites such as CubeSats in recent times has trended towards miniaturized systems with increased capability and greater ability to integrate small systems and payloads [42]. The state of the art related CubeSat subsystem capability, as reported by NASA’s small satellite technology state of the art report for 2014 are as follows, with Technology Readiness Levels (TRL) listed where appropriate:

Power systems

- Triple-Junction Solar Cells with reported 29% efficiency. TRL 9.
- Lithium ion batteries (200 watt/hr per kg average) TRL 6.

Attitude Determination and Control Systems

- CubeSat Pointing Accuracy is typically around 2 degrees, expected to drop below 1 degree with miniature star trackers. Attitude knowledge for CubeSats is reported to be on the order of 0.1 degrees.
- Control typically accomplished with reaction wheels for slewing (avg. torque from 0.02mNm to 0.1Nm) TRL 7-9, and magnetic coils or rods for momentum dumping. TRL 9. CMG’s and Aerodynamic surfaces are also being studied. TRL 7-8.
- Propulsion can be done with cold gas, electric, or chemical thrusters with thrust on the order of >1N being possible for CubeSats. TRL 6-9 for gas and

chemical thrusters. Electric propulsion devices (<0.01 mN) with higher ISP's are also in the works, with TRL 2-5 on average.

- Gyroscopes typical for rate determination: 0.01 – 100 deg/hr range of bias instability. TRL 5-9.
- GPS receivers for small satellites listed as good to 10m position accuracy. TRL 9.

Structures and Mechanisms

- Aluminum alloys are the typical structural metals used for small-sats,
- Additive manufacturing is a technique being studied for use with small satellite production.
- Solar Panel hinges, antenna pointing devices in use, TRL 9.

Command and Data Handling

- Higher processing trends with reduced SWAP requirement trends. Large variety of data rate and data storage capabilities reported, along with variety of form factors. TRL 7-9.

Communications

- UHF/VHF/Microwave/IR/Visible spectra are current comm. bands for small satellites. Depending on mission needs, an appropriate band should be selected for SWAP, data rate, and licensing concerns.
- UHF/VHF at TRL9. Typical CubeSat data rates from 9600 bps to 38.4kbps.
- S-Band for CubeSats typically around 2 Mbps TRL 6-9.

- K-band transceivers were listed as heavier (~2-3kg) with larger form factors reported in the state of the art document, and as such may not be supported by CubeSats. Reported data rates ranged from 0.1-3 Gbps. TRL 3-9.

2.12 Spot Beam Mapping Applications

The primary applications for the spot beam mapping mission concept are identified as the following:

GEO RF Domain Verification --- It is desirable to know the locations where spot beams from GEO comm-sats are pointing at a given frequency to verify the accuracy of spot beam patterns and frequency use. Verifying spot beam patterns may allow GEO satellite operators to tune spacelink communications for greater efficiency.

Spacelink Interference Reduction --- According to Roddy [14], interference between telecommunications services can appear in a significant manner and in numerous ways. For GEO satellites, the interference modes of ground-to-GEO communications and GEO-to-ground communications drive the limits of spacing in between GEO slots. (For example, the FCC set spacing to 2 degrees for the 6/4-GHz frequencies, as reported by Roddy [14]). Although controlling GEO satellite spacing may limit interference, signal interference nonetheless still occurs, especially in less-resilient space-link systems.

Poor or Unnecessary Coverage Identification --- It is also desirable to identify, for a given commercial carrier, areas on the ground of poor or unnecessary spot beam coverage. As a rather extreme example, assume that a GEO commercial carrier's intent is to broadcast television services to the entire state of Michigan, and only the state of

Michigan. If the GEO transmitter's Michigan spot beam becomes misaligned in a southerly direction: A) the upper peninsula of Michigan might not be covered anymore, and; B) the spot beam would potentially be interfering with another carrier's Ohio spot beam! It is the intent of the spot beam mapping mission to identify ground areas of poor and/or unnecessary coverage.

2.13 Summary

In summary, a background of related topics tied closely with the spot beam mapping mission simulations analyzed for this research was given. Notable past CubeSat missions were discussed, in conjunction with a few modern CubeSat operations. A background behind mission analysis and feasibility assessments was discussed in Section 2.2. The RF domain and its use within the GEO belt was established, as well as the use of spot beams in geostationary orbit. Mission requirements and constraints for a spot beam mapping mission were given, as well as the governing equations and physics behind a spot beam mapping constellation.

On the methodology and analysis side of the spot beam mapping mission, sources of error and their mitigation strategies were introduced, along with the list of performance measures that were used to help characterize the final desired output of the mission: the ground-based spot beam map. Physical capabilities were also discussed, with CubeSat characteristics, specifications, and capabilities being introduced, along with how those CubeSat parameters related to a spot beam mapping mission. Finally, applications of the spot beam mapping mission were covered. The next chapter, Chapter III, covers the

methodology and the design of the simulations which were used to characterize and generate relevant data for analysis of the spot beam mapping mission.

III. Methodology, Design and Development

This chapter details spot beam mapping problem, as well as the creation and development of the CubeSat Spot Beam Mapping (SBM) mission, which was simulated using Systems Tool Kit® (STK), by Analytical Graphics, Inc. STK mission data from the simulation was collected and analyzed through an interface program created in MATLAB®, by The Mathworks, Inc. The simulation environment will be described in detail, specifically by describing the governing features of the STK scenario, including properties of the GEO transmitters, parameters assumed for the spot beam models, as well as the various CubeSat constellation configurations tested. For evaluation and analysis of mission feasibility, the performance metrics identified in the previous chapter will also be discussed and quantified.

3.1 Problem Overview

As discussed in the previous section, the problem for consideration is determining feasibility of completing the spot beam mission with CubeSat constellations in LEO, accurately, after a reasonable duration. To determine this feasibility, it was important to establish a methodology to allow for appropriate analysis to take place. Since the target output analysis of this work required ground-based spot beam maps created from CubeSat Lat/Lon/Alt/Time collects within spot beams, models needed to be created to simulate an expected scenario that a notional spot beam mapper could be expected to encounter.

The spot beam mapping CubeSat, during a notional orbit, was expected to physically fly through a large number of various size spot beams covering a wide band of frequencies. To collect on every possible frequency at the same time would add a significant amount of complexity and data aggregation to the system, thus it was decided that the spot beam mapping constellation should focus in on a selected frequency (Ka-band or lower) at the operator/user's discretion. Figure 6 demonstrates an example spot beam mapping fly-through of a spot beam. Once established on the target frequency, the spot beam mapper would collect GPS information whenever it measured signals at that frequency with enough power.

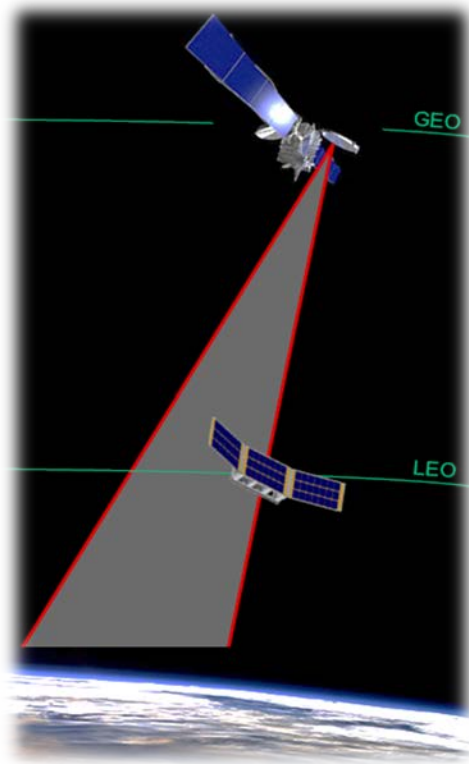
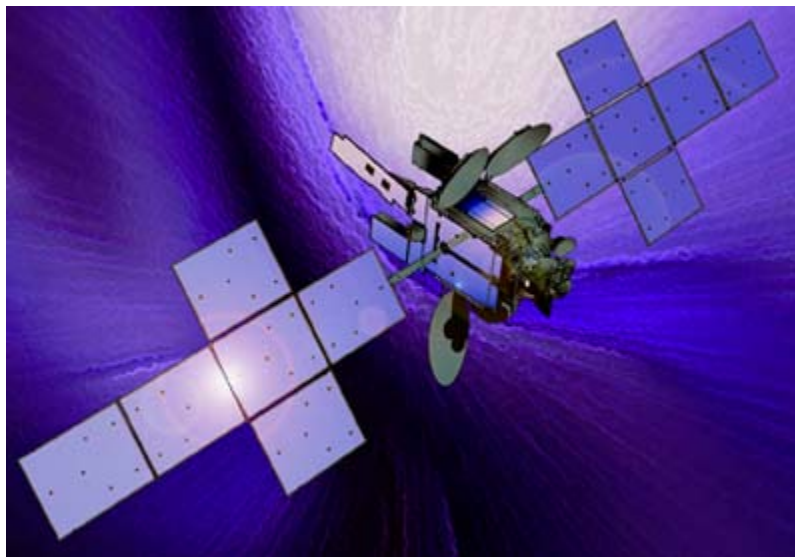


Figure 6: Collect Lat/Lon/Alt and Time information when within spot beams, and received power is high enough.

3.2 Model / Environment Simulation

The CubeSat SBM mission model was established within STK to analyze and map spot beams from two different GEO communication satellites. The first GEO satellite that was modeled was created with the intent to simulate a close approximation of what a spot beam pattern from an active and in-use GEO communications satellite would look like. The Intelsat Galaxy 28 (G-28) GEO satellite (Figure 7) located at 89 degrees west longitude was chosen to be modeled due to its relatively easy to see and model Ku-band beam patterns over North and South America [12]. The Galaxy 28 satellite also maintains spot beam transponders within the C-band; however these were not modeled since the Ku-band beams, which cover a smaller area, would provide a better means for a capability assessment. It was decided that if the CubeSat SBM could reliably map the relatively small Ku-band beams, then the larger C-band beams could also be mapped, assuming the hardware on board the CubeSat was capable of receiving in both bands.



**Figure 7: Intelsat Galaxy 28... Formerly known as Intelsat Americas 8...
Formerly known as Telstar 8... on SSL's LS-1300S bus. [SSL]**

The G-28 GEO transmitter’s true orbit was imported directly, which placed G-28 into its appropriate location at 89 deg west longitude, with slight variation. The G-28 Ku-Band spot beam patterns were then modeled using its known ground-based beam patterns [12]. To model the beams accurately, conic beam sensors were combined together over North and South America to notionally match the conic half-power beam width (HPBW) shape of the known beam patterns on the ground. Figure 8, below, shows the Ku-band ground beam pattern used within the model for G-28.

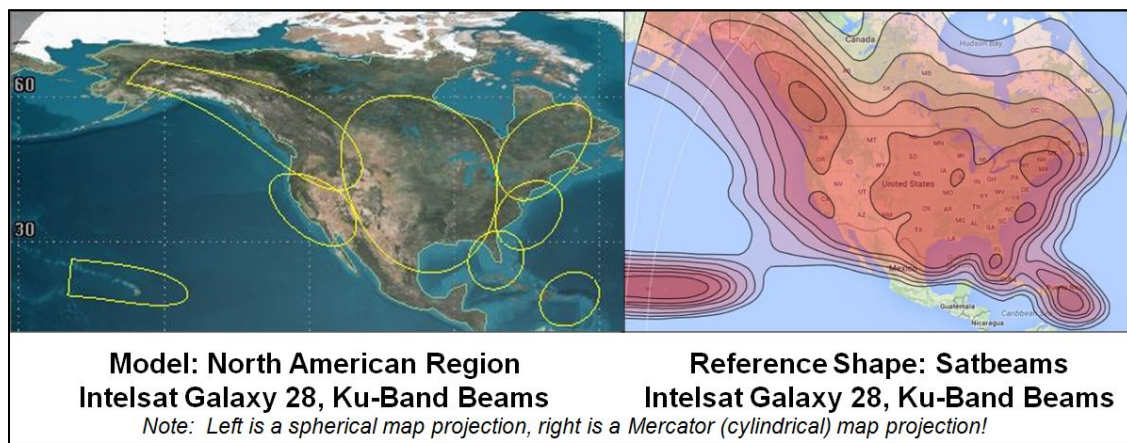


Figure 8: Spot beam model created for North America, using Galaxy 28's Ku-Band beam pattern.

The other GEO communications satellite, hereafter known as “G-II,” was created in a similar manner to G-28, except with simpler, more generic orbital parameters and spot beam pointing locations. The G-II orbital elements were set to be perfectly geostationary around Earth with zero inclination and drift, at -151 deg longitude. Three Ku-Band beams were then added, one pointing directly down to the equator, and two more pointing to the maximum north latitude and south latitudes visible to the satellite. All three of these fixed beams were given the same transmission properties, including frequency and antenna size. Additional beams coming from the G-II transmitter were later added to the scenario to act as test cases for spot beams that were not necessarily

static or immobile. Specifically, there are four additional “special case beams” added to the G-II satellite, and are detailed in the next section.

3.3 Spot Beam Models

As introduced in the previous section, the spot beams simulated for analysis of the spot beam mapping mission were based off of both notional spot beams as well as a model of a real-world Ku-band spot beam pattern. Modeling the spot beams according to expected actual sizes requires a known transmitter antenna size. Since most companies don’t publish exact antenna and transmit power levels due to their proprietary nature, typical and/or average antenna sizes for the simulated K-band beams is assumed [13], [43],[44]. According to R. Horak in his Telecommunications and Data Communications Handbook [13], typical spot beam antenna sizes for Ku- and Ka-band transponders at GEO are reported as follows:

Table 3: Typical satellite antenna sizes for Ku- and Ka- band transponders [13].

Freq. Band	Frequency, Downlink (GHz)	Antenna Diameter (m)
Ku-band	11.7-12.2	1.07
Ka-band	17.7-21.2	0.61

For this research, the simulated Ku- and Ka- band antennas were assumed to be 1m diameter within the simulation, using a small selection of frequencies within the bands. The simulated Ku-band beams were set at approximately 12 GHz, which is approximately the downlink frequency used by the Galaxy-28 transponders [12]. The simulated Ka-band beams used by the G-II satellite used 30 GHz and 40 GHz as its simulated frequencies, or rather, the highest frequency portion of the Ka-band [14].

These selected frequencies and antenna sizes are therefore deemed reasonable for estimating K-band beam sizes for simulation.

Several assumptions were made relating to the physical behavior of power and gain of the modeled spot beams. The governing RF equations used or exhibited by the model have been listed below. Specifically, the Equivalent Isotropic Radiated Power (EIRP) of the transmitter is needed for calculation of Free Space Loss (FSL). FSL is the loss that occurs for any radiated signal over a given spatial distance. The equations used have been detailed below [14].

EIRP of the transmitter:

$$EIRP = P_s (W) + G (dBW) \quad (13)$$

Free Space Loss (in dB):

$$FSL (dB) = 10 * \log \left(\frac{4\pi r}{c/f} \right)^2 \quad (14)$$

r is the range between the transmitter and receiver, c is the speed of light in vacuum, and f is the transmit frequency. Applying free space loss, the received power from a given distance (in Watts) is determined by:

$$P_R (Watts) = EIRP * G_R * \left(\frac{c/f}{4\pi r} \right)^2 \quad (15)$$

$EIRP$ is the Equivalent Isotropic Radiated Power of the transmitter, G_R is the receiver gain, and the right part of the equation is the free space loss, described above.

The same equation can also be written with dB as the base metric:

$$P_R (dBW) = EIRP (dB) + G_R (dB) - 10 \log \left(\frac{4\pi r}{c/f} \right)^2 \quad (16)$$

Since frequency and the speed of light in vacuum are usually known, the free space loss equation can be simplified to:

$$FSL (dB) = 32.4 + 20 \log r(km) + 20 \log f (MHz) \quad (17)$$

The free space loss equation can therefore be used to check losses for a GEO transmitter. Since Galaxy 28 broadcasts at about 12 GHz in the models presented here, the free space loss for G-28's spot beams from GEO to a LEO orbit at 450km is shown to be:

$$FSL (dB) = 32.4 + 20 \log(35786 - 450) + 20 \log(12000) \quad (18)$$

$$FSL (dB), GEO to 450km = 204.95 dB$$

The Galaxy 28 beams were then modeled in STK using available ground Ku-band beam pattern references at 11.9 GHz, as detailed in the previous section. These beams were modeled using conic spot beams within STK, which were placed together in such a configuration to roughly model the spot beam patterns of the real-world Galaxy 28 satellite. These spot beams cover the continental United States, Lower Canada & Alaska, South America, with one additional beam towards Hawaii and another towards Puerto Rico. Figure 9 shows an Earth view of the modeled Galaxy 28 Ku-band spot beams.

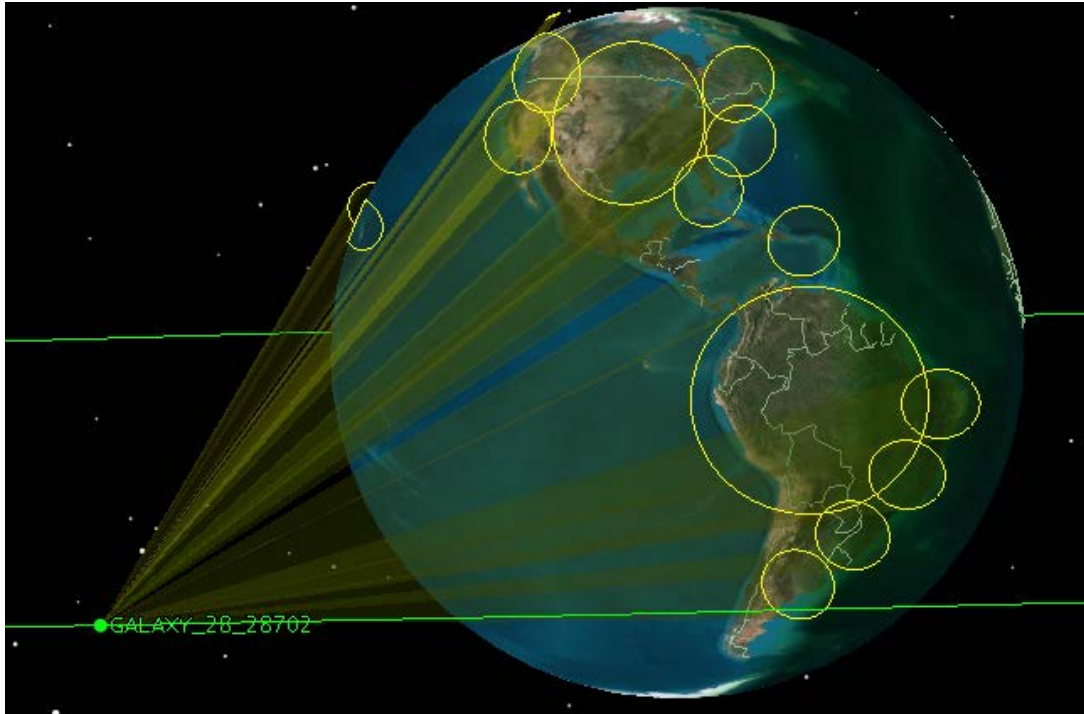


Figure 9: Intelsat Galaxy 28 Ku-band spot beams as modeled in STK.

The G-II beams were modeled differently, as arbitrary conic spot beams placed in reference locations. The arbitrary Ku-band (12 GHz) spot beams were pointed at the maximum Earth-pointing latitudes and directly towards the equator. The Ka-band (30/40 GHz) beams were pointed at various pacific islands for location variety. The Ka-band beams were added as test beams for beams that were not always static and/or fixed. Figure 10 shows an Earth view of the modeled G-II Ku- and Ka-band spot beams.

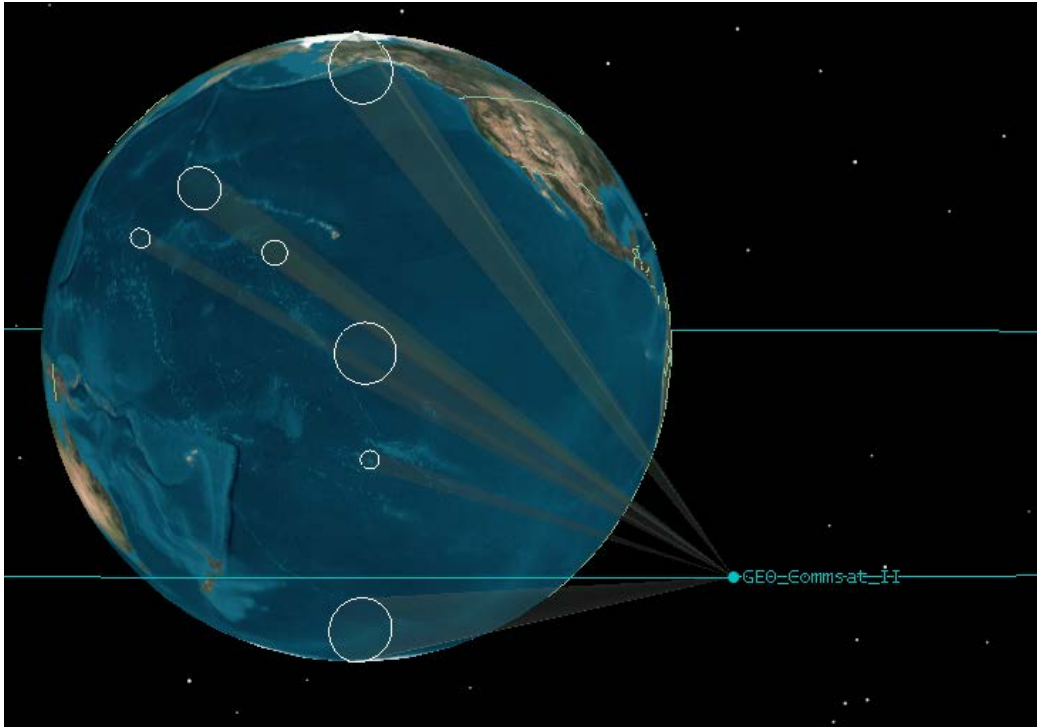


Figure 10: Geo-CommSat-II (notional) Ku- and Ka-band spot beams as modeled in STK.

The first special case beam used the same size antenna as the Ku-band beams, but the frequency was increased from the base Ku-band (12 GHz) up to the Ka-Band (40 GHz). Increasing the transmit frequency reduced the HPBW, and thus reduced the size of the beam's coverage area [14]. The increased-frequency beam thus became harder to detect and track since it covered a much smaller swath of the earth's surface versus the lower frequency beam. The higher frequency beam was implemented as a stationary and fixed beam, pointing just below the equator at the same longitude as the G-II comm-sat.

The second special case beam was also implemented as a high frequency upper Ka-band beam (40 GHz); however this beam vanished after 36 hours within the scenario. The goal behind implementing the vanishing beam was to see if/how the beam mapper could figure out that the beam was no longer there.

The third special case beam was implemented in the Ku-band. This beam was designed to shift itself from its initial ground pointing location to a new pointing area after 36 hours passed in the scenario. Similar to the vanishing beam case, the goal behind this beam was to see if/how the spot beam mapper could figure out that the beam over the initial area had disappeared, and reappeared over a new ground target.

Finally, the last special case beam was implemented as an upper Ka-band (40 GHz) beam that followed a transiting ground target, in this case a ship was simulated, travelling at a constant speed southwest starting from Honolulu, HI with a course towards Guadalcanal, northeast of Australia. This beam was implemented to see if the spot beam mapping mission could find a constant-rate transiting beam.

3.4 Algorithms / Software Tools

The software tools developed to create and analyze the spot beam mapping constellations and orbits were developed in MATLAB. To populate the scenario with user-desired constellation and orbit configurations, a script was written to run the simulations through the link through MATLAB with STK. Figure 11 is a flowchart depicting the spot beam mapping software tool's use of MATLAB for simulation commands, STK for orbit propagation and data generation, and Microsoft's Disc Operating System (MSDOS) for merging access reports and data handling/directory management.

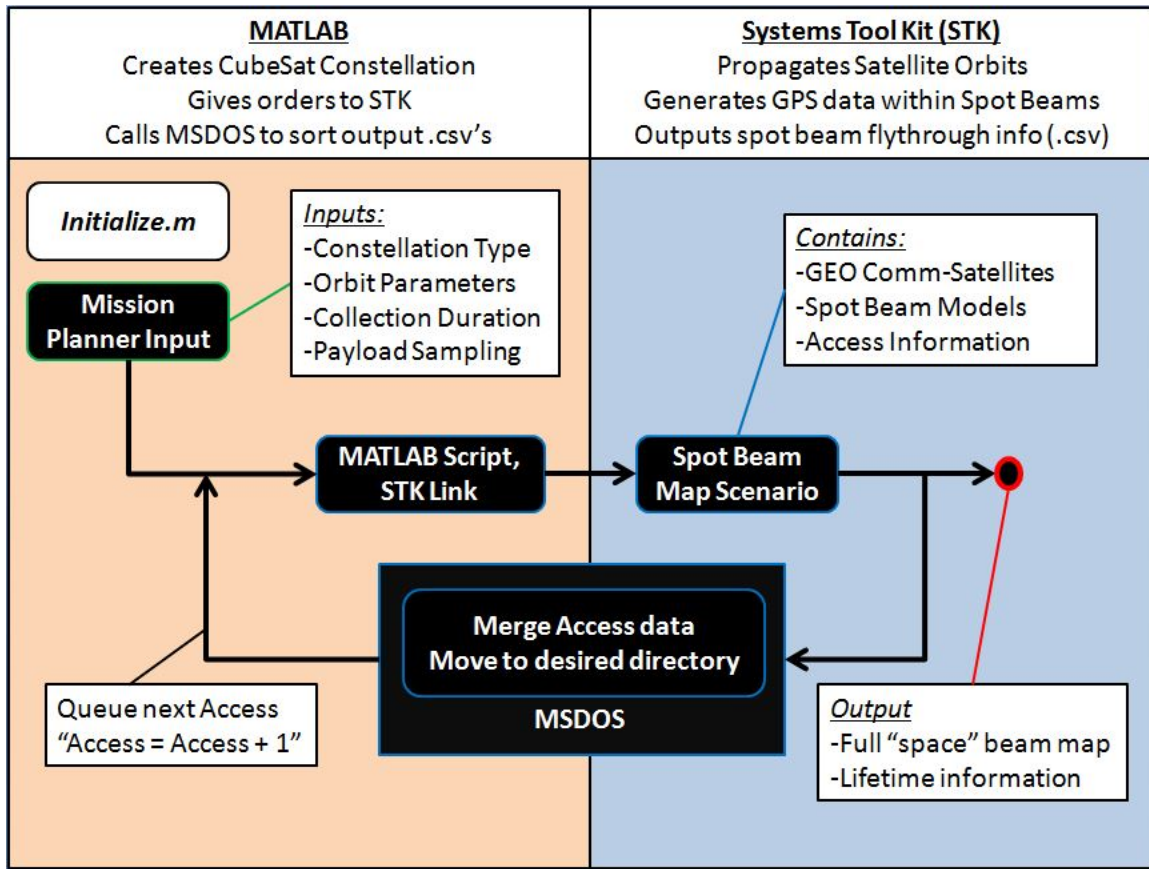


Figure 11: Flowchart depicting the simulation side of the spot beam map generation process.

In summary, the software tool within MATLAB took the desired user inputs and constellation parameters and converted them into usable STK commands [5], [45]. The base STK scenario, with the pre-modeled spot beams, was then called by the MATLAB software, and the user-desired CubeSat constellation was automatically added to the scenario with the specified orbit. The constellation's orbit was then propagated forward in time through STK, as commanded by MATLAB. Once the propagation of the entire constellation was completed, STK generated an access report containing collected GPS collects including Latitude, Longitude, Altitude, and Time information for each spot beam pass, for each CubeSat.

The next pieces of the spot beam map generation tools were the scripts that created the ground-based spot beam map. These two scripts took the output of the initialize.m script described above, (i.e. the space-based orbital beam map made from compiled GPS points), and mapped the points to the ground, based on a known GEO transmitter position. The program could also simulate variance in the transmitter position for ground map error estimation based on lack of transmitter position knowledge. The ground-based spot beam map generation scripts produced four output beam maps for analysis: a spot beam edge map, a merged space/ground beam map, a merged space/ground beam map in 3D, and (most importantly), the ground-based spot beam map. Figure 12 is a flowchart depicting the spot beam map generation scripts.

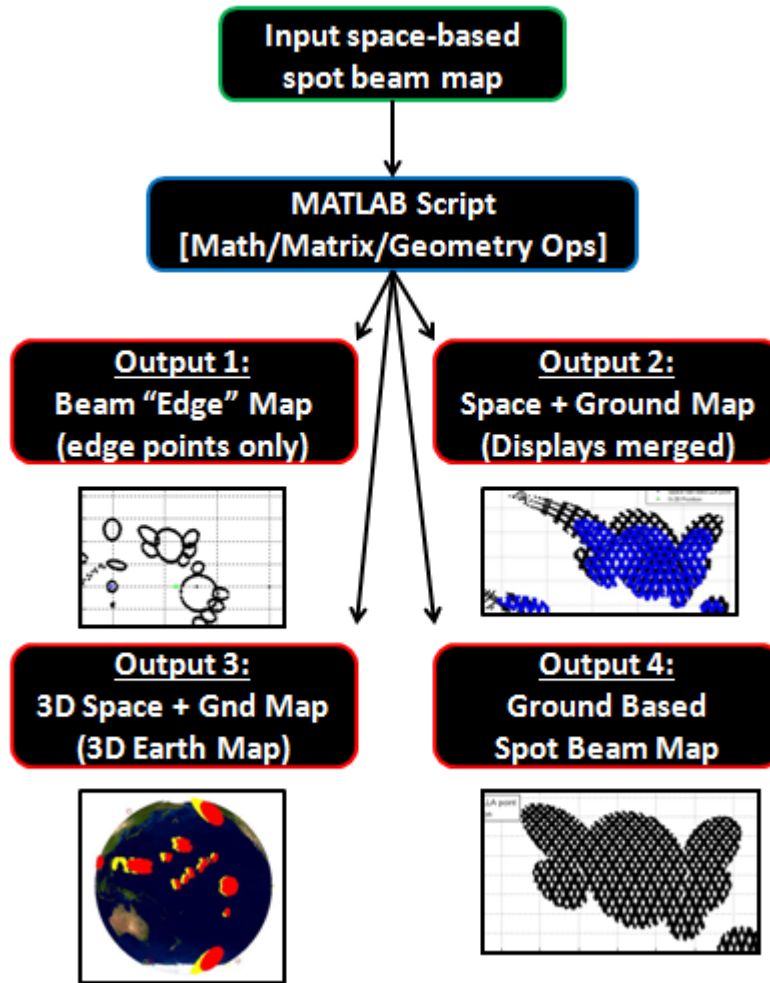


Figure 12: Flowchart showing the process used to obtain the final spot beam maps for analysis.

The inputs for the ground beam map generation script were the LLA points collected by the CubeSat GPS subsystem (or by CubeSat simulation as discussed previously). To perform the space-based beam map to ground-based beam map translation, the 3-dimensional position vectors of the GEO transmitter and the space-based map points were converted to the direct Earth-Centered, Earth-Fixed (ECEF) Cartesian coordinates, with the 1-axis pointing through the prime meridian/equator intersection point at zero degrees latitude and longitude. The 3-axis was set as pointing through the Earth's rotationally fixed North Pole, and the 2-axis followed the right-hand

rule, perpendicular to both the 3-axis and the 1-axis. Figure 13 shows the coordinate system used for the space to ground map calculations.

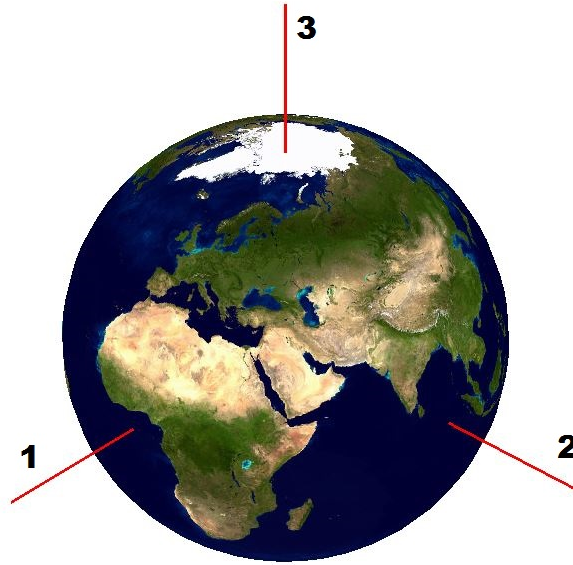


Figure 13: Earth-Centered, Earth-Fixed coordinate axes used for beam map point translation.

The “known” variables for this space to ground point translation were the LLA position of the GEO comm-satellites, as well as the necessary earth properties. In the Matlab beam generation script, the values for the position of each tested GEO comm-sat were stored as 3 dimensional LLA position vectors, as shown in Table 4.

Table 4: LLA position vectors of Galaxy 28 and G-II

	Galaxy 28 (LLA)	G-II (LLA)
Latitude (deg)	0	0
Longitude (deg)	-89	-151
Altitude (km)	35786	35786

These GEO position vectors were then converted by the script from LLA coordinates into Cartesian coordinates, along with the GPS LLA data points collected for

the space beam map. At this point, *if* the script was told by the operator to do so, the script added in scaled “noise” to the position vectors. The noise was simulated as GPS position error when desired, as well as transmitter position knowledge error.

After importing the necessary position vectors of the GEO transmitters and space beam map points, the coordinate frame of the Earth was rotated to the west about the Earth-fixed 3-axis to the transmitter longitude (λ_T) such that a vertical plane was formed along the Earth-fixed 1 and 3 axes which included the center of the earth and the GEO transmitter’s position. To form this new plane, the following R3 rotation matrix was used and applied to the position vectors [41]:

$$R3(\lambda_T) = \begin{bmatrix} \cos \lambda_T & -\sin \lambda_T & 0 \\ \sin \lambda_T & \cos \lambda_T & 0 \\ 0 & 0 & 1 \end{bmatrix} \quad (19)$$

In order to map the space point to the ground, a second rotation matrix about the Earth-fixed 1-axis was applied in order to rotate the vertical (1,3) Earth plane counterclockwise until the plane intersected the space point to be mapped to the ground. This new plane therefore contained three key points: The center of the earth, the GEO transmitter, and the space point to be mapped to the ground. To rotate the vertical plane to the space point, the following R1 rotation matrix was used and applied to the position vectors, where ψ_S was the counter-clockwise rotation angle from the vertical plane to the new plane including the space point, obtained by computing the cross product of the vertical “3” vector with the normal vector of the plane containing the analysis point [41].

$$R1(\psi_S) = \begin{bmatrix} 1 & 0 & 0 \\ 0 & \cos \psi_S & -\sin \psi_S \\ 0 & \sin \psi_S & \cos \psi_S \end{bmatrix} \quad (20)$$

The geometric relations within this new plane were then used to find the ground intersection location of the space point as defined by the line through the transmitter's position. Figure 14 displays the new geometry within the now twice rotated plane used to map the space point measured at altitude to the ground.

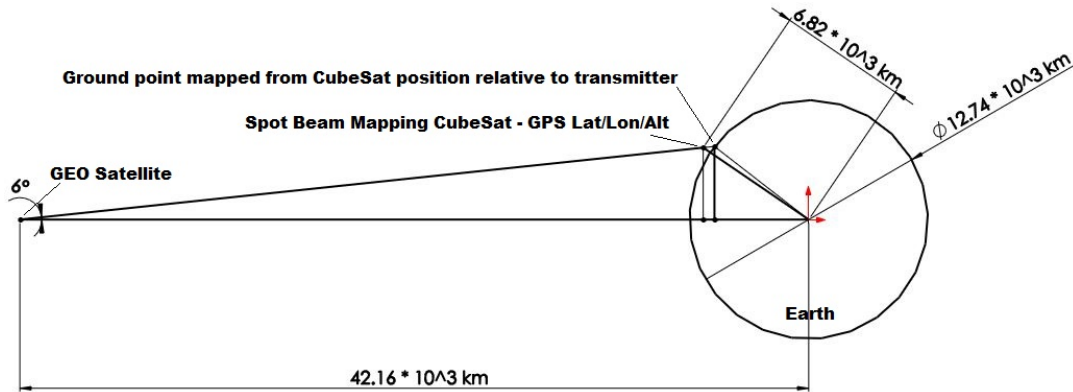


Figure 14: "In plane" geometry used for mapping space-based LLA data points to the ground.

Once the ground point was obtained with in-plane coordinates, it was then necessary to convert the point from its current state back to the non-rotated standard ECEF Cartesian or Lat/Lon/Alt coordinates. This was done by multiplying the transposed R1 and R3 rotation matrices, (in opposite order), by the obtained ground point --- then converting to LLA if desired. It is also worth mentioning that at this point the data was error-checked within the MATLAB script. If at any time STK (for whatever reason) passed MATLAB any erroneous (read: ridiculous) GPS data points, the MATLAB script was programmed to find it and throw it out.

Finally, the last step required to generate a ground-based spot beam map was to compile the data points in one place and plot them. The plots were created in both 2D

and 3D, with and without the space points as an overlay. Further, since beam “edges” were also considered important features, another beam map output was also created showing only the beam edges, for analysis. The combined direct applications used to solve for the ground points given the space location points can be found in the MATLAB beam map generation scripts (e.g. “G28_beam_maps.m”) which are shown in Appendix A.

After collecting Lat/Lon/Altitude and time information from the CubeSat, a beam map at altitude could be created showing the 3D location where the CubeSat flew through each of the beams from the transmitters. However, in order to convert that “space map” into a “ground map,” the approximate location of the transmitting GEO satellite had to be known [23]. There are two ways to do this that have been considered in this research. The first was to simply assume that position of the GEO transmitter would be known from external sources, thus creating the ground beam map assuming good knowledge of the transmitting satellite’s position in GEO. The effects of transmitter position knowledge on the anticipated accuracy of the ground-based spot beam map are analyzed in Chapter IV.

A second, more active and complex on-board method to conduct position determination of the GEO transmitter has been cleverly dubbed “GEO-location,” in which the CubeSat SBM’s receiver includes hardware and software on board that can generate lines of bearing to the transmitting GEO satellite while flying through one of its spot beams. Due to the relatively great distance between LEO and GEO, the on board accuracy of the CubeSat’s attitude determination and control system will significantly drive the overall accuracy of the line of bearing estimation. An analysis of required

CubeSat attitude accuracy was conducted within MATLAB comparing the attitude accuracy required at a given orbital altitude to produce an error ellipse of desired size for the position of a GEO comm-sat. The error ellipse size, in turn affected the accuracy of the ground-based spot beam map (See Chapter IV).

3.5 Performance Measurements and Variables.

Using G-28 and G-II as the basis GEO comm-satellites for the spot beam mapping scenario, various CubeSat constellations were added to the scenario taking advantage of link capability between MATLAB and STK. To determine which CubeSat constellations and orbits could feasibly meet the requirements of a spot beam mapping mission, several orbit and payload parameters were adjusted to find the best mapping resolution. Note: Only circular orbits were analyzed. Table 5, below, shows the parameters that were varied, as well as what simulation results those parameters could influence.

Table 5: CubeSat constellation variables used within the spot beam mapping mission scenarios

Parameter	<u>Orbit Altitude</u>	<u>Orbit Inclination</u>	<u># of Orbit Planes</u>	<u># of CubeSats per Plane</u>	<u>Payload Sampling Rate</u>	<u>Duration</u>	<u>Spacing between CubeSats in Plane</u>
Range Simulated	200-500 km	68,75,82, 90,98 deg	1-6 Planes	1-6,8	1,5,10 sec/sample	1 day, 3 days	Fixed Angle, Walker, or Even Spacing

The reasoning and analysis conducted behind the simulated ranges for each variable will be discussed in the following subsections.

3.6.1 Altitude

The altitude test parameter range selected for spot beam mapping mission analysis was 200 – 550km, where lifetime concerns of a fully loaded or light (i.e. 12kg or 6kg) 6U CubeSat [20], and the altitude effects on the mission output were the principal drivers behind the mission altitude selection range. The altitude effects on the generation of the ground-based spot beam map are discussed in Chapter IV. Related to lifetime concerns, using the lifetime tool within STK, the altitude bounds for the spot beam mapping mission are discussed here and compared with similar work done for CubeSats, namely the 6U results observed by Qiao et al. [46].

The acceleration on an orbiting object due to aerodynamic drag can be modeled with the following equation [40]:

$$\vec{a}_{drag} = -\frac{1}{2} \frac{c_d A}{m} \rho v_{rel}^2 \frac{\vec{v}_{rel}}{|\vec{v}_{rel}|} \quad (21)$$

Which, when solved for as a force equation in more general form as [46]:

$$F_d = \frac{1}{2} \frac{c_d A}{m} \rho v_{rel}^2 \quad (22)$$

The above equations for aerodynamic drag estimation use c_d as the object's coefficient of drag, A as the object's cross sectional area facing towards the velocity vector, m as the object's mass, and v_{rel} as the velocity of the object with respect to the field of air molecules causing the drag force. The lifetime tool within STK applies these equations to lifetime estimation, applying atmospheric and solar radiation pressure models for additional accuracy.

To compute the lifetime of a spot beam mapping 6U CubeSat within STK, the properties of the 6U CubeSat needed to be procured. Estimates of constants were

selected for the drag coefficient and the solar reflection coefficient, and the NRLMSIS-00 atmospheric density model was selected to model the atmosphere within STK. The variables used for this research were effective drag area and the mass of the satellite. These were varied based on their effects on the expected lifetime, and set such that the long and short cases for each variable would be simulated. Table 6 shows the constants and variables used within the lifetime analysis using STK lifetime tool.

Table 6: Constants / Variables used within STK's lifetime tool to compute expected lifetime of the Spot Beam Mapping 6U CubeSats.

Constant or Variable	Set Value
Drag Coefficient	2.2, models a “flat plate”
Solar Reflection Coefficient	1.0
Drag Area	0.06 square meters (short case) 0.03 square meters (intermed. case) 0.02 square meters (long case)
Satellite mass	12 kg (Fully loaded 6U) – long case 6 kg (“Light” 6U) – short case
Atmospheric Density Model	NRLMSIS-00 (Mass Spectrometer Incoherent Scatter) [40]

Varying the mission altitude of the spot beam mapping CubeSat would have significant impact on lifetime and mission duration considerations. STK’s lifetime tool yielded workable results that allowed the appropriate orbit range for the spot beam mapping CubeSat mission to be determined. Table 7, below shows the various CubeSat altitudes analyzed, along with notes regarding lifetime information for a 6U CubeSat in that tested orbit. The “Long Case” column was dictated by a 12 kg, 6U CubeSat that was flying with its minor axis (i.e. least surface area) pointing towards the orbital velocity vector. The “Intermediate Case” column displays the lifetime dictated by a 12kg, 6U CubeSat flying with its intermediate (i.e. in gravity gradient stable attitude) axis pointed towards the orbital velocity vector. The “Short Case” column displays the lifetime results

assuming the 12kg, 6U CubeSat was flying with its major (i.e. max surface area) axis pointed towards the orbital velocity vector.

Table 7: Results of lifetime simulations for various orbits. Assumed fully loaded (12kg) 6U CubeSat.

Orbit Altitude	Long Case Lifetime (days / years)	Intermediate Case Lifetime (days / years)	Short Case Lifetime (days / years)	Meets Mission Requirements?
200 km	9d / 0.025y	6d / 0.016y	3d / 0.008y	No
300km	167d / 0.45y	108d / 0.29y	51d / .14y	No
350km	584d / 1.6y	365d / 1y	177d / .48y	Possible
400km	2519d / 6.9y	1351d / 3.7y	548d / 1.5y	Yes
450km	5402d / 14.8y	4088d / 11.2y	2263d / 6.2y	Yes
500km	>9125d / 25y	8870d / 24.3y	4672d / 12.8y	Possible

At 200km, the mission lifetime was found to be rather short (3-9 days), and at 500km, the on-orbit lifetime of the fully loaded 6U CubeSat was found to be rather long, (12 – 25 years), which at worst case reached the limit 25 year maximum orbital lifetime requirement. Thus, with the present assumptions, the most practical orbit range that was found to be acceptable to perform the spot beam mapping mission, with the current requirements, was in the range of 350km to 500km. Other altitudes could be considered, however trades with the mission duration requirement, i.e. shorter or longer mission would need to be considered. Applying these lifetime results, the simulations completed in the next chapter test CubeSat constellations within this 350km to 500km altitude window.

The effects of reducing the mass of the CubeSat were also checked. By lowering the mass of the fully loaded 6U CubeSat (12 kg) to a significantly lighter 6 kg, the lifetime duration of the CubeSat for the tested altitudes and orientations was shown to decrease. Table 8 shows the lifetime results obtained for a “lightly loaded” (6kg) CubeSat case.

Table 8: Results of lifetime simulations for mission orbit altitudes. Assumed “lightly” loaded (6kg) 6U CubeSat

Orbit Altitude	Long Case Lifetime (days / years)	Intermediate Case Lifetime (days / years)	Short Case Lifetime (days / years)	Meets Mission Requirements?
200 km	5d / 0.014y	3d / 0.008y	2d / 0.006y	No
300km	79d / 0.216y	51d / 0.14y	27d / 0.074y	No
350km	274d / 0.75y	177d / 0.485y	83d / 0.23y	No
400km	912d / 2.5y	548d / 1.5y	256d / 0.7y	Possible
450km	3468d / 9.5y	2263d / 6.2y	803d / 2.2y	Yes
500km	7373d / 20.2y	4672d / 12.8y	3176d / 8.7y	Yes
550km	>9125d / 25y	>9125d / 25y	5366d / 14.7y	Possible

Comparing Table 7 with Table 8, it has been observed that the mass decrease in the “lightly loaded” case decreased the expected orbital lifetime for the tested orbits. The light case lifetimes reported for the 6kg, 6U intermediate case above compares roughly with the 6kg, 6U findings of Qiao, et al [46], except for the 450km orbit, where Qiao reports an expected 6kg, 6U lifetime of 3.7 years, and this research reports 6.2 years. This difference in results at 450km could be present due to a number of factors: solar cycle timing difference (Late 2014 simulation vs. 2011 simulation), test orbit inclination difference (Qiao tested sun-synch), atmosphere model used, or reporting error.

In summary, the usable altitude window for the spot beam mapping CubeSat mission has been profiled for the 6U CubeSat as 350km to 500km, so long as the CubeSat maintains a mass greater than 6 kg. For the 350 km orbit, it is desirable to have a heavier CubeSat in order to meet the mission requirements. Extra hardware or mass blanks ballast will need to be considered for a 350 km orbit to work. On the higher side, 500km was the worst case upper bound for the heavier 6U CubeSat, extending to 550km under certain attitude profiles for the lighter mass case.

3.6.2 Inclination limits

Since the spot beam mapping mission has the intent to cover all points on the earth where spot beams from the GEO belt could be pointing, the inclination of the CubeSat SBM would likely need to be rather high, if not polar. The limiting bounds on the inclination variable are therefore defined by coverage capability of the spot beam mapping CubeSat. Since an equatorial orbit wouldn't be able to find spot beams pointing towards higher latitudes, higher inclinations are desirable. Since a polar orbit is the highest possible inclination that includes total global coverage capability, 90 degrees was chosen as the maximum prograde inclination bound for the simulations. This 90 degrees maximum inclination bound *does not* exclude retrograde orbits, for example sun-synch orbits at ~98 degrees so long as the retrograde orbits do not drop lower than the minimum design inclination looking in the retrograde direction. To determine the minimum inclination limit for the spot beam mapping mission, the minimum angle through which every Earth pointing spot beam from GEO could be fully flown through at a LEO altitude had to be determined.

Starting with the assumption that this CubeSat mission would fly no lower than 200km, trigonometric relations were used to figure out the minimum inclination angle where all earth-pointing spot beams from GEO could be flown through completely. Figure 15, below shows the geometry used to find the lowest practical inclination for the spot beam mapping mission, assuming an absolutely minimum possible mission altitude of 200km.

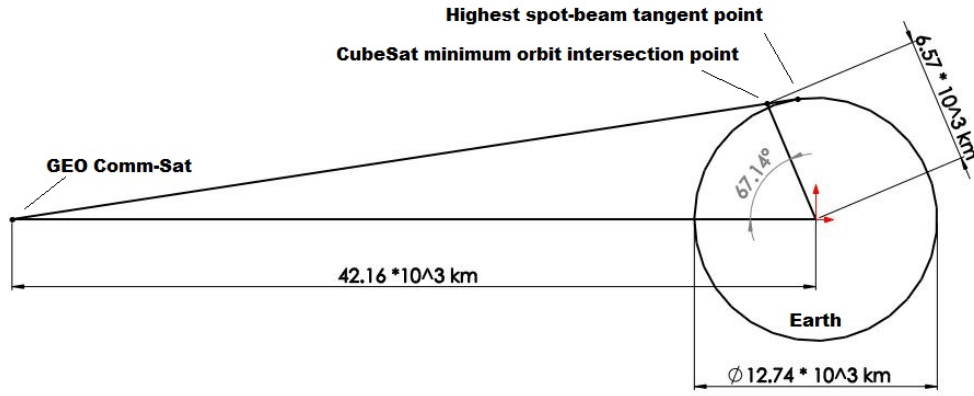


Figure 15: Geometry used for inclination limit calculation.

Following this Earth geometry, the minimum inclination for the CubeSat spot beam mapping mission to fly through all fully earth-pointing spot beams emitted from the GEO belt was determined using conservative altitude values, along with the known radius of earth and its known geostationary orbit altitude.

Highest look angle expected for a spot beam:

$$Max\ look\ angle = \sin^{-1} \left(\frac{6371\ km}{42157\ km} \right) = 8.69\ deg \quad (23)$$

Applying Pythagorean's theorem to the newly-formed right triangle gives the tangent slant range distance as 40,064 km. Following this, the Law of Sines was applied to find the desired angle for the inclination boundary.

$$\frac{\sin 8.69^\circ}{6571\ km} = \frac{\sin i_{limit}}{40064\ km} \quad (24)$$

The result yields: $i_{limit} = 67.136^\circ$, which is the (conservative) minimum inclination the spot beam mapping mission can have in order to fly through all earth-pointing spot beams.

3.6.3 # of Planes and # of CubeSats

Another set of variables changed for the spot beam mapping scenario were the discrete number of CubeSats used within a constellation, and the discrete number of planes that the CubeSats were spread out into. The range of testing for number of CubeSats was 1 to 8. More CubeSats are certainly possible, however were limited to 8 to apply scope to this problem. Each CubeSat could also be evenly spread into a number of different planes as well. The number of planes was tested for various orbit configurations from 1 to 6. Multiple plane testing also carried over into a different constellation type, the Walker Delta constellation, which is discussed below.

3.6.4 Data Rate

Another variable that could be easily checked for effects through the simulations was the sampling rate of the CubeSat collectors. The sampling rate of the CubeSat's payloads affected how many data points could be collected within a spot beam of certain size. Under the strictly academic assumption that it is desired to have at least 3 data points within an average spot beam pass for the smallest simulated Ka-band spot beam, minimum payload sampling rates were determined using the following process:

Variables:

$\theta_{res} = \text{Angular distance between collects (deg)}$

$R_{\oplus} = \text{Earth Radius (km)}$

$Alt = \text{Orbit Altitude (km)}$

$$L_{arc} = \text{Arc Distance Between Collects (km) @ Orbit Alt}$$

Figure 16 shows the geometry with the variables necessary for calculation of the minimum data rate with respect to the Earth and the orbit of the CubeSat SBM. It has been assumed that a minimum of 3 GPS collects need to be obtained within the smallest simulated spot beam.

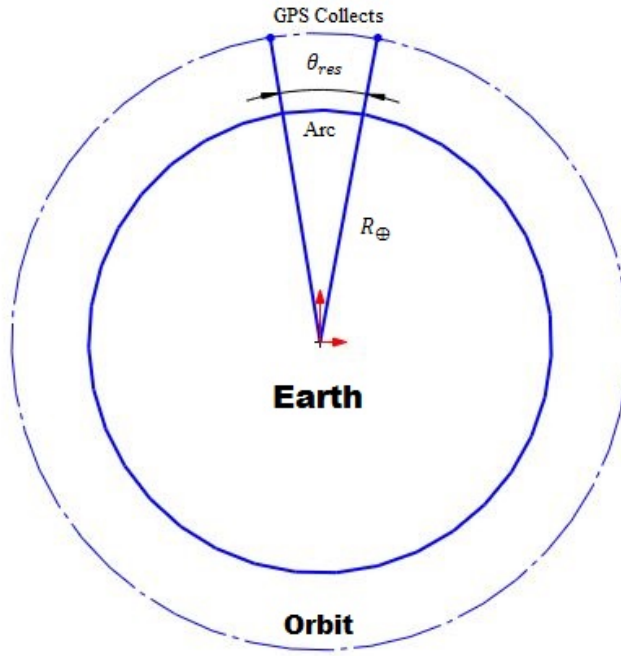


Figure 16: Geometry driving angular measurement resolution and the payload sampling rate

The equations governed by the given geometry are defined as:

$$\theta_{res} = \frac{\text{Sample Rate} \left[\frac{\text{sec}}{\text{sample}} \right]}{\text{Orbital Period} [\text{sec}]} * 360^\circ \quad (25)$$

$$L_{arc} (\text{km}) = \frac{\pi}{180^\circ} * \theta_{res} * R_{\oplus} + \text{Alt} \quad (26)$$

The above equations were sampled for beam widths from 0.1 deg to 15 degrees, assuming that the HPBW of the beam was set equal to $\frac{\theta_{res}}{2}$. The in-beam fraction, or the

percentage of the orbit spent within the minimum expected spot beam size was calculated by dividing L_{arc} by 360 degrees. The total time spent within the minimum expected beam size was then found by multiplying the orbital period by the in-beam fraction. The fact that not all beam passes would be optimum (e.g. right through the middle of the beam) was accounted for at this point in the script. Finally, the sampling rate needed for the spot beam mapping CubeSat's receiver for the given expected beam width was obtained by dividing the time spent in beam by the number of desired points within the beam (e.g. assumed 3 points for this work).

3.6.5 Collection Duration

The selected collection durations simulated for the spot beam mapping mission were directly selected based upon the mission requirements. Since it was desired that a full ground-based spot beam map be obtained within 24 hours of collection start but no later than 72 hours, it was decided to test both objective and threshold collection durations within the scenarios. In doing so, it was expected that the longer duration case would generate more data and produce a higher resolution ground-based spot beam map when compared to the shorter duration 24-hour case. Observing whether or not 24 hours was enough time to obtain a “resolved enough” spot beam map will be discussed in Chapter IV.

3.6.6 Constellation Type / Spacing

Although there are an infinite number of technically possible constellation variations, there were four significant circular-orbit constellation “classes” that were used for analysis within the simulations presented within this research. The four classes of constellations simulated were: Single plane constellations, Walker constellations

(formulation explained in Chapter II), Multiple plane non-walker constellations, and constellation formations with fixed spacing angles [34]. It must be noted that the term “formations” is used roughly here, as the spot beam mapping CubeSats are not inter-linked, nor do they need to communicate with each other. The “formation” case, presented in Chapter IV, simply sets a fixed spacing angle between in-plane CubeSats, which does not evenly spread the group throughout the orbit.

3.6.7 Simulation Performance Measurements

After identifying the necessary the variable ranges of the CubeSat SBM mission simulations, the variables to be tested (Constellation Type, Orbital Elements, Collection Duration, and Payload Sampling Rate) were entered into the model. The model software then formed the requested CubeSat constellations and gathered access information whenever a CubeSat flew through a spot beam of a GEO comm-sat. The access information consisted of information relevant for what would be required to complete the Spot Beam Mapping mission: GPS location, Altitude, Time, and Gain of the signal collection received.

Once the access information was obtained for a given CubeSat constellation, space and ground layer maps were formed and analyzed. Analysis of the output spot beam maps related mostly to the performance measures of beam map resolution, beam detection capability, and responsiveness, as indicated above. These three simulation performance measures were checked in the simulation outputs by answering the following quantitative and qualitative metrics for each data set collected:

- 1) **How many beams from G28** (out of 13 total) were detected by the SBM constellation?

- 2) **How many beam features from G-II** (out of 8 total) were detected by the SBM constellation?
- 3) How many of the **small (Ka-band) beams** (out of 2 total) were detected by the SBM constellation?
- 4) Was the SBM constellation able **to readily find/track the dynamic beams**?
- 5) **How large were the major coverage gaps** in the full beam map after the simulation duration (deg Lat x deg Lon)?

Of these, coverage gap reduction played the most important role in finding the “best” scenarios, since the constellations with the smallest coverage gaps were able to best identify beam shapes and clearly define their features/edges. Figure 17 shows an example of orbital coverage gaps which were measured for each simulation (circled in red).

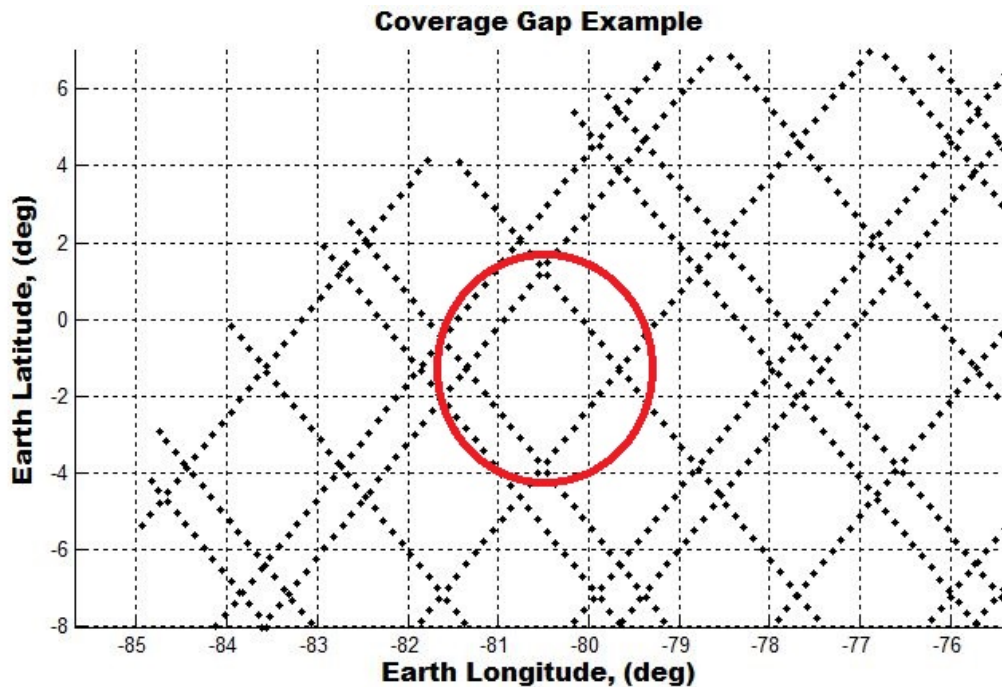


Figure 17: Example of orbital coverage gaps in compiled beam map. (Circled in red)

The orbital coverage gaps, in the form of an angular “diamond” on the surface of the Earth, as taken from a spherical section, were measured based on their latitude and longitudinal sizes. Combining these into a solid angle gave an effective spherical area missed through the coverage gap. The “best” spot beam mapping simulations were the simulations that could minimize the effective size of the latitude and longitudinal gaps between successive passes over the globe.

3.6 CubeSat System Metrics

A basic Concept of Operations (CONOPS) was developed for the spot beam mapping CubeSat mission. It must be noted that the actors and users at this point have been established as generic. The primary mission area of this CONOPS involves flying CubeSats through spot beams of a targeted frequency from GEO comm-satellites and then reporting the Lat/Lon/Alt/Time information of spot beam fly-throughs to the ground station by storing and, once over ground stations, forwarding that data down to the end user. Should the technology become mature enough, “real-time” data relaying methods through GlobalStar, Iridium, or a similar service may also be a possibility for this mission, to increase responsiveness and reduce on-board data storage requirements [26], [47]. However, the real-time methods would require higher technology readiness at the CubeSat scale.

Related to near-real-time orbital communications, Capt. Bastow, in his thesis [48], assumed data transfer and orbital communications using the Iridium network for his analysis of a “Payload Alert Communications System (PACS),” designed to act as a Resident Space Object (RSO) GPS position reporter [48]. AFIT is also conducting

research into real-time orbital communications as well, and is developing a prototype to carry the PACS payload. The AFIT proof-of-concept experiment to carry PACS is known as the Space Object Self-tracker (SOS). Real-time communications using the Iridium network were assumed to work as long as PACS and/or SOS maintained their orbits below 750km [48]. These real-time methods can also be kept as an open option for the Spot Beam Mapping (SBM) CubeSat as well, since the SBM orbits cannot exceed 500km due to lifetime concerns of the 6U CubeSat.

Therefore, if the baseline “store and forward” methods for command, control, and mission data are not capable of dealing with the data requirements of the spot beam mapping mission due to not seeing ground stations enough, then the optional “real-time” cases must be studied further for the spot beam mapping case. To show the command, control, and data relaying options in a more visual fashion, Figure 18 displays an OV-1 for the CubeSat SBM mission.

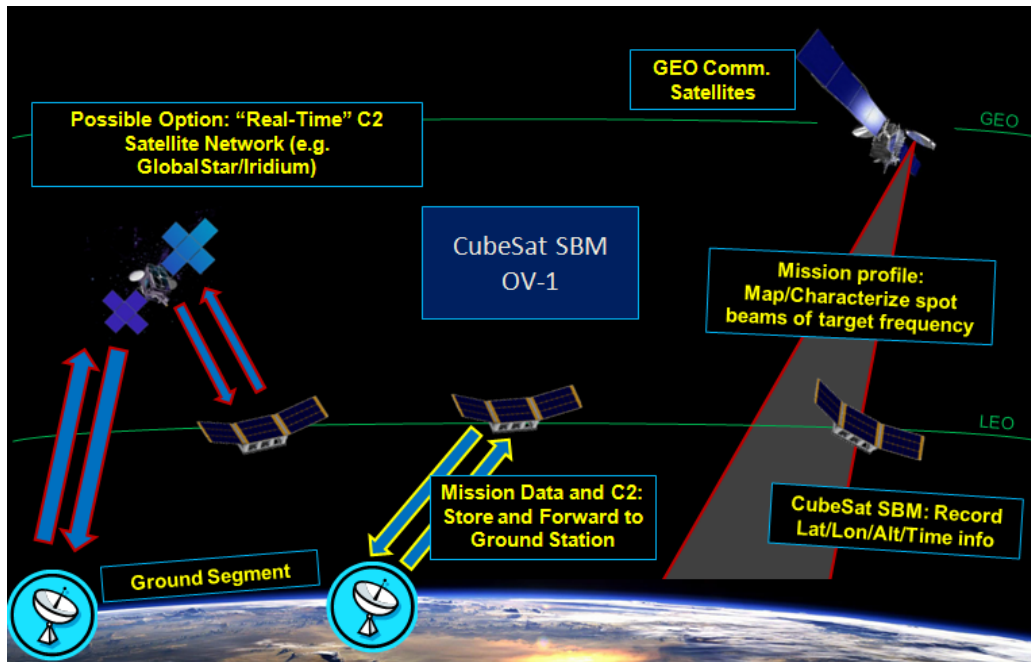


Figure 18: OV-1 for the CubeSat spot beam mapping mission.

Completing the spot beam mapping mission in this manner requires each CubeSat within the constellation to transition between several different modes of operation, since the CubeSat must complete several different tasks, including the collection of spot beam signals, as well as ground station passes, in conjunction with the CubeSat's own internal health and state monitoring routines. Figure 19 incorporates the key mission tasks the CubeSat must accomplish, in order to complete its mission, as a profile transition diagram.

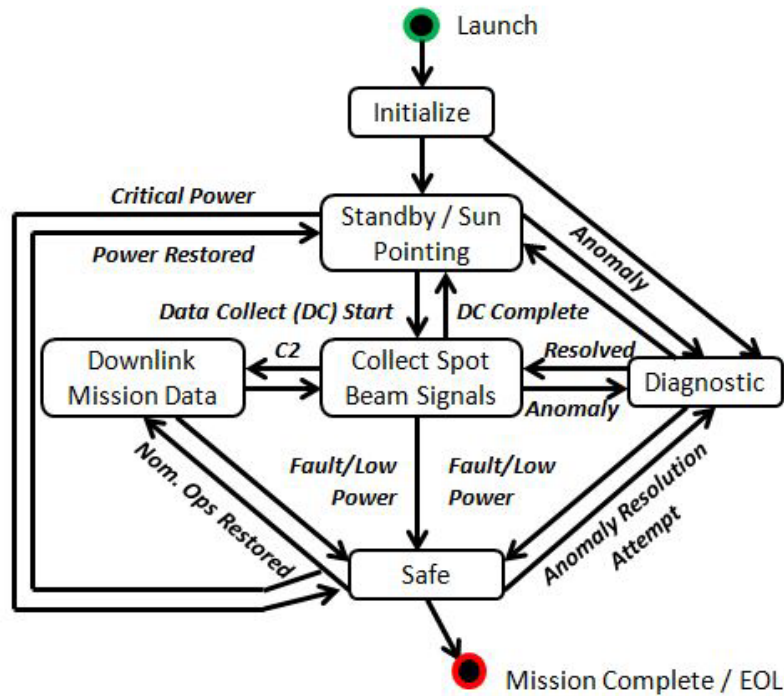


Figure 19: SBM mission profile transition diagram.

After launch and deployment, the spot beam mapping CubeSat would enter an initialization phase, where it would complete a checkout of its systems and payload. Assuming the on-board systems were initialized properly, the standby/sun pointing state would be entered in order to charge the batteries and prepare for mission operations. The

standby/sun pointing state was implemented as the “base” state for the spot beam mapping CubeSat to be in when it wasn’t performing the primary mission. When the ground operator desired the mission to begin, the CubeSat would enter the mission state, in order to both collect spot beam signals and proceed to download the collected information to the ground user, either through real-time methods or direct download to a ground station. If at any point a significant anomaly or error occurs in any of these states, a diagnostic state could be entered, for the purpose of figuring out what might be wrong. A safe state, where all critical subsystems would be powered off and maintained in that state until nominal conditions were restored, was added as an emergency state to save power should conditions merit such action.

Looking at the mission level requirements and constraints as they apply to a CubeSat itself, it has been assumed that the payload for the spot beam mapping CubeSat system in this particular scenario was a receiver capable of analyzing signals in the desired frequency band, this receiver fitting within a maximum payload form factor of the 6U CubeSat standard. Further assumptions made regarding the 6U CubeSats for the SBM mission follow standards according to the Planetary Systems Corp. Canisterized Satellite Dispenser’s (PSC/CSD) data sheet [20]. From that set of specifications, the 6U CubeSat’s mass must not exceed 12 kg, has volume approximately 10cm x 20cm x 30cm, with constrained moment of inertia properties [20]. Three-axis stabilization using reaction wheels and magnetic torquers must also be considered for sun-pointing and fixed attitude control profiles [49].

3.7 Summary

In summary, Chapter III detailed the methodology behind the simulations developed for the CubeSat Spot Beam Mapping (SBM) mission. The software operations were described, along with the necessary interfaces and governing assumptions. The simulation environment was also described, along with the properties of the GEO transmitters, spot beam models, and features of the various CubeSat constellation and orbit configurations that were tested. The process by which spot beam maps were obtained was covered, including base geometry and operations to convert payload data into usable maps. Finally, high level necessary system metrics for the spot beam mapper were discussed.

Chapter IV discusses the results obtained by the spot beam mapping simulations. The scenario results for single plane, multiple plane, Walker, and formation constellations are presented. The results also include effects of changing variables on the mission's output, the ground-based spot beam map. In addition to the beam map generation, the importance of transmitter position knowledge is discussed related to spot beam map generation, including necessary CubeSat attitude requirements for accurate map generation. Finally, an analysis of the results is conducted, with an analysis on desirable mission configurations.

IV. Results and Analysis

To properly assess feasibility and determine whether or not the spot beam mapping mission could meet requirements, it was deemed most desirable to know how well the CubeSat platform could detect and map the edges of spot beams. Figuring out how well the CubeSats could perform the spot beam mapping mission was done by comparing the simulation results to the metrics specified by the mission requirements for each constellation and orbit type. A ground beam map was ultimately desired as the principal output, which, to translate efficiently from the acquired space beam map, required position knowledge of the GEO transmitter satellite. Robustness and responsiveness of the spot beam mapping CubeSat mission was also compared based on how often a CubeSat would fly through each of the different beam types, which included fly-throughs of the special cases of relocating, mobile, and disappearing beams.

The spot beam mapping simulation was queued for a variety of the feasible mission orbit and constellation parameters. The results of each simulation run were then compiled and analyzed in comparison with each other to determine which spot beam mapping constellations performed best in light of the established requirements. This section covers the various solution types obtained from the spot beam mapping simulations. Although every obtained data run was different, for better or for worse, the results have been categorized into different types for analysis purposes.

4.1 Data Parameters and Trade-offs

The data output process for the CubeSat SBM simulation included the collection of GPS latitude, longitude, and altitude (LLA) points corresponding to the space-based LEO position of spot beams from the GEO transmitter. It was assumed that the CubeSat SBM payload and data reporting hardware/software would be in a configuration such that whenever the received target spot beam signal to the CubeSat was greater than a designated threshold power level; the CubeSat would record its position in space (LLA). After leaving the beam, when the received power levels declined below that designated threshold power level, the CubeSat would cease reporting its position. Collecting data over time, these LLA coordinates were merged and further analyzed to create a ground-based map of spot beam locations and edges.

The data on the ground-based spot beam map that was measured within the scenario for analysis was the largest latitude and longitude difference “gaps” left in the spot beam map. As previously discussed, the number of beam features detectable by the end user in the beam map was also observed, as was how well the spot beam mapping constellation could, in a qualitative sense, map the special case beams. Also of primary interest was how well the spot beam mapping CubeSats could complete the mission timeliness requirement of completing a beam map of all spot beams for a given target frequency after a period of 3 days versus the goal of 24 hours.

4.2 Scenario Results (Single-plane constellations)

This subsection details the typical results of the spot beam mapping mission when applying various orbits and number of CubeSats, when applied to a single-plane constellation type. Using different parameters for each run, the results varied. Shown as an example, a relatively “decent” resultant spot beam map for the 3-day threshold mission requirement duration was found from a 6-ship constellation, with even in-plane spacing at 350km altitude, with the variables detailed below in Table 9.

Table 9: Test variables for the Single Plane Constellation resultant beam maps shown.

Test Parameter	Set Value
<i>Constellation inclination</i>	68 Degrees
<i>Constellation altitude</i>	350 Kilometers
<i>Payload sampling rate</i>	5 seconds per sample
<i>Number of orbit planes</i>	1 plane
<i>Number of CubeSats in plane</i>	6 CubeSats
<i>CubeSat spacing within plane</i>	Evenly spaced
<i>Simulation data collection duration</i>	3 Days

Using the above table of variables as inputs to the simulation, the following space / ground beam map was obtained for the Galaxy 28 comm-sat, displayed below in Figure 20.

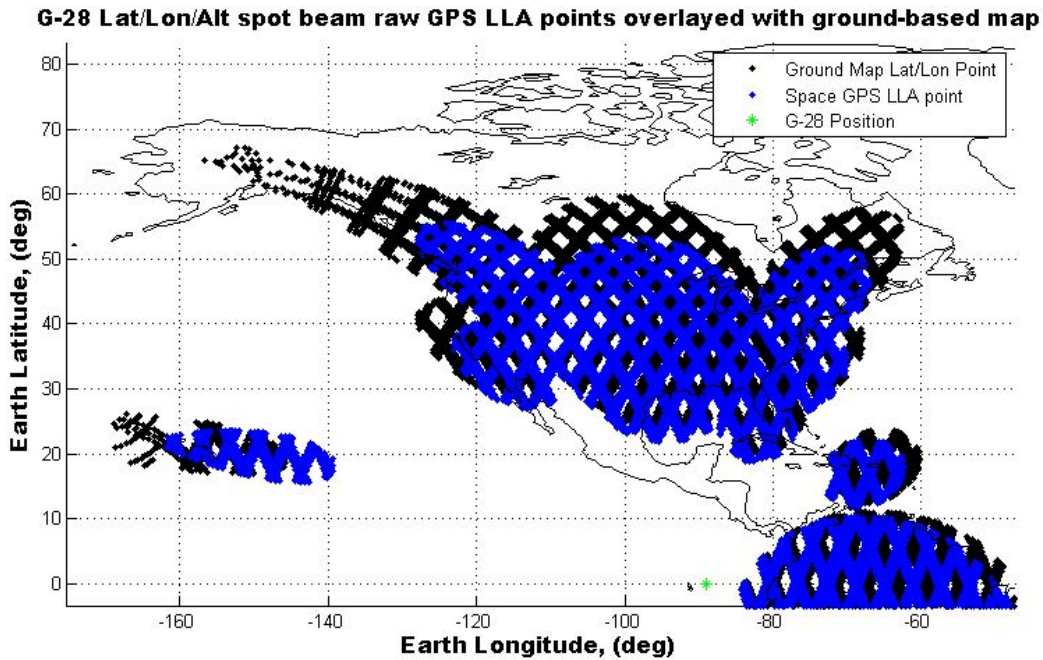


Figure 20: G-28 Space map data points as overlay (blue) with calculated ground map (black), coverage over North America and Hawaii.

In the above resultant spot beam map for Galaxy-28, The “blue” data points correspond to the measured space-based GPS points, and the “black” data points correspond to the translated ground-based coordinates for the space points. This spot beam map for the 68-deg/350-km/1-plane/6-CubeSat constellation mapped over three days still had noticeable coverage gaps, however was nonetheless able to find and map out all of the scenario’s spot beams. Although this solution was deemed “good,” better solutions were obtained later with different parameters.

Using the same CubeSat constellation parameters, the same space and ground map was generated for the G-II notional GEO comm-satellite’s beam patterns. These beam patterns included the extreme latitude beams, as well as the dynamic beam samples that moved, disappeared, or were otherwise relatively “small” Figure 21, below shows the obtained space and ground map for the G-II beams developed over 3 days with the

same single-plane, six-ship constellation detailed above. The special case beams, discussed in the previous chapter, have been annotated for reference.

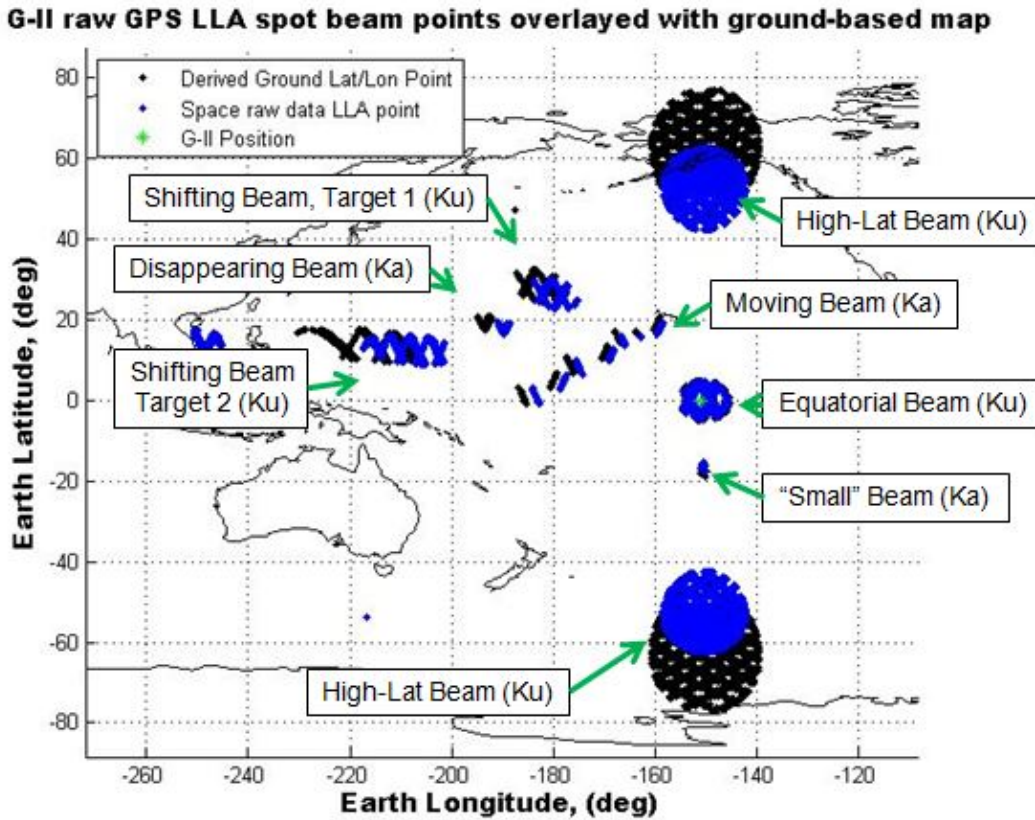


Figure 21: G-II Space map data points as overlay (blue) with calculated ground map (black), coverage over the pacific.

The single-plane, six-ship constellation found all of the G-II beams in the scenario, and demonstrated how the resultant beam map would appear based on the presence of dynamic beams. Again, as with the Galaxy-28 measurements, coverage gaps were still visible in this beam map.

For better visualization, and to observe what physical geographic regions were being covered, the same data set could be plotted in 3D, and superimposed onto a spherical globe. Figure 22 shows the 3D earth plot of the two space and ground spot

beam maps generated by the 6-ship constellation orbiting at 68 deg. inclination at 350 km altitude after 3 days. Figure 23 is the same 3-D plot as in Figure 22, except zoomed in on the North American region, for clarity.

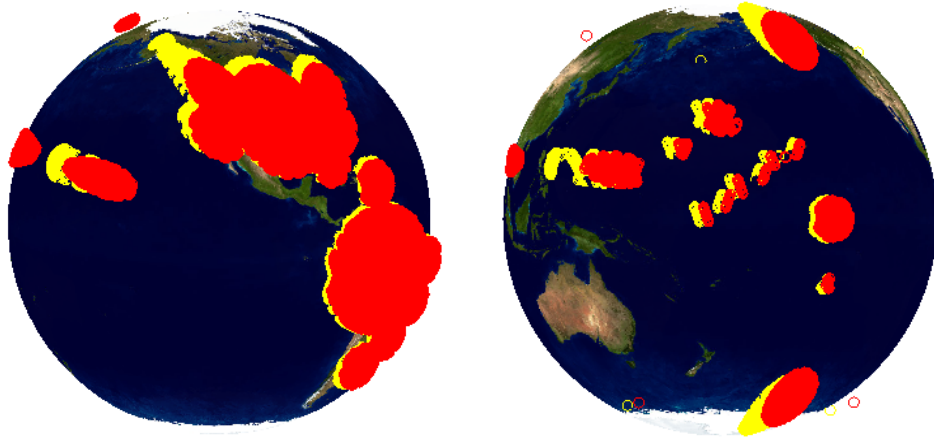


Figure 22: 3-D Space and ground beam data maps superimposed on the globe, as recorded by the CubeSat SBM constellation from G28 transmitter (left) and G-II transmitter (right).

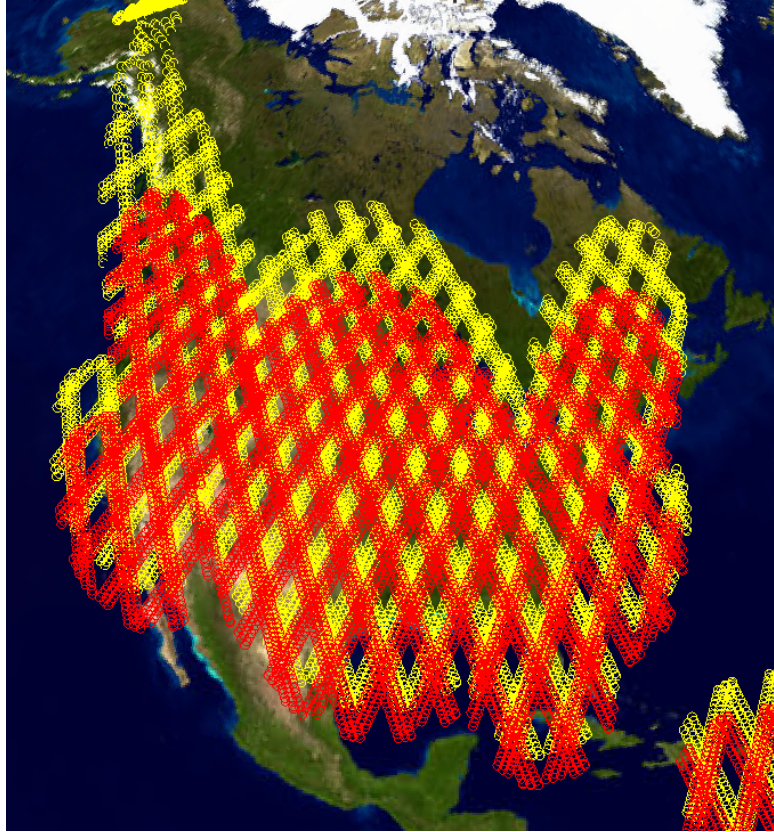


Figure 23: 3-D space and ground beam data maps superimposed on the globe, from G-28's North America beams, zoomed in.

This mapping procedure was followed for numerous configurations of different single-plane CubeSat constellations and payload behaviors. Table 10, below displays a sample set of results for single-plane constellations over the threshold three day (72 hour) collection durations.

Table 10: Selected sample of result information demonstrating single plane constellation capabilities for 3-day collection duration.

Number of CubeSats in Plane	Altitude (km)	G-28 Beams Found (of 13)	G-II Beams Found (of 8)	Number of accesses - mobile beam	Size of Major coverage gaps (sq. deg)
1	350	13	5	0	192
1	400	9	8	1	360
1	450	13	6	1	224
1	500	8	6	2	900
3	350	13	8	2	130
3	400	13	8	1	60.5
3	450	13	6	3	165
3	500	13	8	2	41.4
6	350	13	8	7	22
6	400	13	8	6	30
6	450	13	8	6	35
6	500	13	8	6	32.5

Although there are not enough data points collected here to characterize spot beam map performance for all orbit and constellation variables, mission feasibility and needs for CubeSats can be explored with this information. The results for various constellations and orbits with effects of changing each variable will be discussed later this chapter.

The three day scenarios for most constellations typically yielded useful and usable results for a variety of CubeSat constellations. However, an *objective* for the mission was established which set a goal to download the spot beam map within a significantly shorter duration of 24 hours. Thus, another series of data sets were collected to see if the same CubeSat constellations used in the 3-day case would still be capable of mapping global spot beams of the target frequency over just 24 hours. In short, a good, workable data result collected for the shorter duration seemed to again be apparent for the single plane constellation, at the lowest reasonable mission altitude – 350km. Figure 24 shows a

shorter duration 24 hour collection for a 350km orbit, single plane, 6 CubeSat constellation (compare to Figure 20, above).

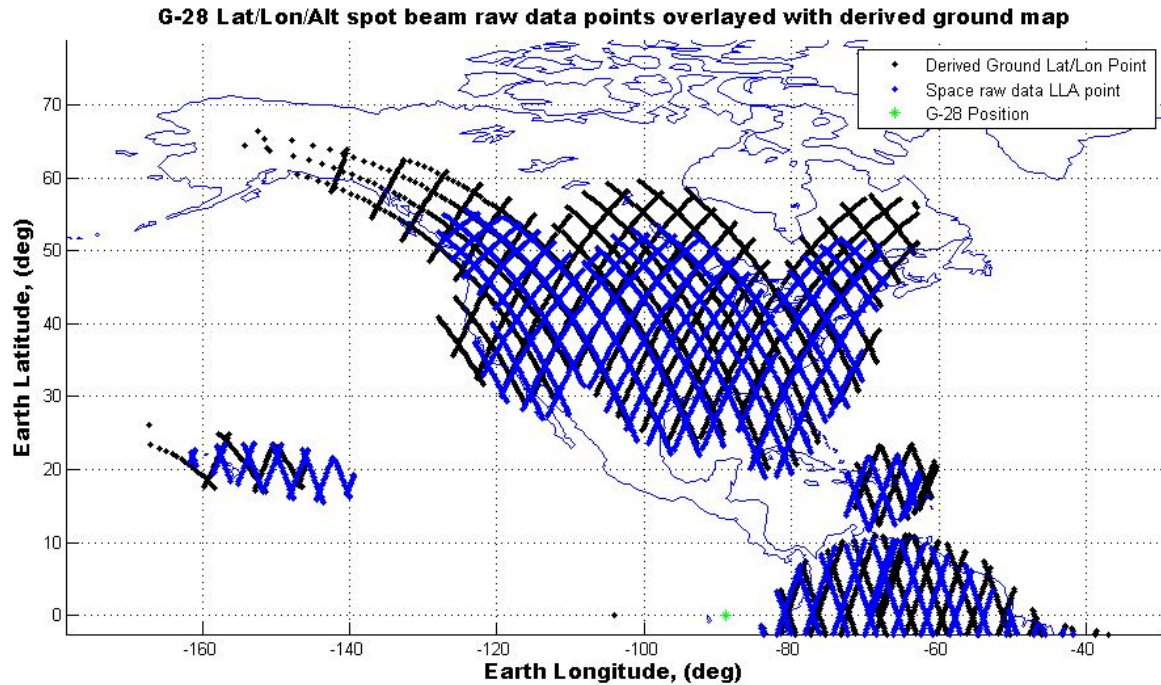


Figure 24: Shorter duration (24 hour) collect, using parameters: 350km 68 inc. 1 plane 6 satellites even spacing.

Although the 1 plane / 6 CubeSat constellation was able to complete the beam map in 24 hours, there was noticeable performance degradation in terms of coverage gap size. For the 24 hour / 1 plane / 6 CubeSat constellation to match the capability of the 3-day / 1 plane / 6 CubeSat case presented earlier, more CubeSats needed to be added to the plane. It was found that if two additional satellites were added to the 1 plane / 6 CubeSat constellation, the resulting coverage gap sizes could be comparable to the original 3-day duration constellation measured at 350km altitude. Table 11, shows how the single plane constellations compared with each other for various altitudes and number of in-plane CubeSats.

Table 11: Selected sample of results demonstrating single plane constellation capability for 24-hour collection duration.

Number of CubeSats in Plane	Altitude (km)	G-28 Beams Found (of 13)	G-II Beams Found (of 7)	Number of accesses - mobile beam	Size of Major coverage gaps (sq. deg)
1	350	5	4	0	660
1	400	3	4	0	1500
1	450	5	4	1	1600
1	500	6	4	1	1500
3	350	12	6	1	172.5
3	400	12	6	0	180
3	450	13	6	1	184
3	500	13	7	1	184
6	350	13	6	3	48
6	400	13	7	2	48
6	450	13	7	2	48
6	500	13	7	2	48

The table clearly shows that as the number of CubeSats in plane are increased, the ability of the spot beam mapping constellation to find all the beams from the simulation (Galaxy-28 and G-II) increases. The size of the coverage gaps become smaller as well, indicating that more satellites improve beam detection capability. For the test case presented here, altitude seemed to become a less dominant variable as well with increasing number of CubeSats.

It must be mentioned that not every constellation simulated yielded workable results. Some had gaps in coverage that were simply too pronounced to locate even the most obvious of beams. When the number of CubeSats in the constellation was too few, or when the data collection duration was too short, the coverage gaps tended to be large – which made the beam map’s resolution very low. Figure 25 shows one prime case of this where there was only one CubeSat tasked to map all of the spot beams from G-28 and G-II in the allotted duration of one day.

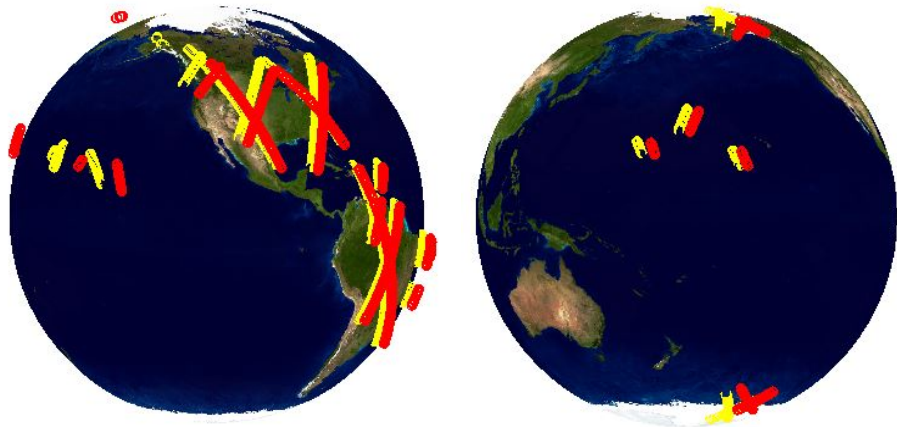


Figure 25: Space/Ground 3D Map with "less informative" data collects. Cfg: 450km, 68deg inc, 1 day, 5 sec data rate, 1 plane, 1 sat

This single CubeSat was able to identify the large areas covered by the multiple beams over North and South America; however the edges and pointing locations of the found beams are not easily identifiable. With such large gaps in coverage, it would be easy to completely miss or mischaracterize spot beam patterns. Every tested scenario experienced some form of coverage gaps, ranging from an effective missed coverage area approximation of 2 square degrees up to 2220 square degrees per single coverage gap on the surface of the Earth, using one full day of signal collection as a baseline.

4.3 Scenario Results (Walker Constellations and Multiple Planes)

The output results of Walker Delta constellations also tended to give favorable results for spot beam mapping. Of the simulations that were run, particular Walker constellations hold the record for “best” results measured through the simulation tool, although they cannot be deemed “optimum,” as this research did not measure and compare every single humanly possible constellation configuration in conjunction with monetary cost. The “best” Walker constellation that was simulated was a 6-3-2 Walker constellation at 350 km altitude. The designator 6-3-2 identifies that there were 6 total

satellites split into 3 planes with 2 satellites per plane. Figure 26 shows the resultant spot beam map obtained for the 350km, 6-3-2 Walker constellation of CubeSats.

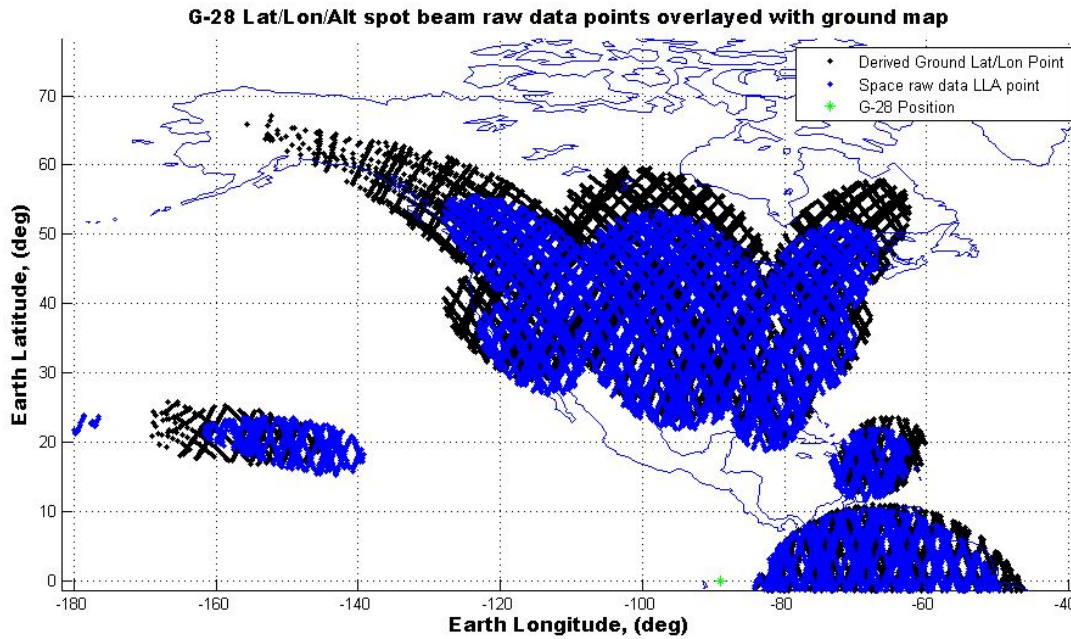


Figure 26: 350km 6/3/2 Walker Constellation Spot Beam Map -- Galaxy 28 North America Region.

The 6-3-2 Walker constellation at 350 was in a configuration such that a significant amount of coverage gap reduction took place --- meaning that the chance for the spot beam mapping CubeSats to miss a spot beam was very small. The ground-based spot beam map's features were also well identified and beam patterns were easily visible, for all spot beams mapped within the scenario.

Another set of noteworthy results were obtained by directly splitting one plane of CubeSats into two, with the same amount of CubeSats and not accounting for the walker constellation true anomaly offset for each plane. Rather than incorporate the walker offset, it was decided to see what would happen with two similarly synchronized planes with 3 CubeSats each. Figure 27 demonstrates a specific multiple plane constellation at 350km, using 2 planes with 3 satellites per plane with 3 days of collection time.

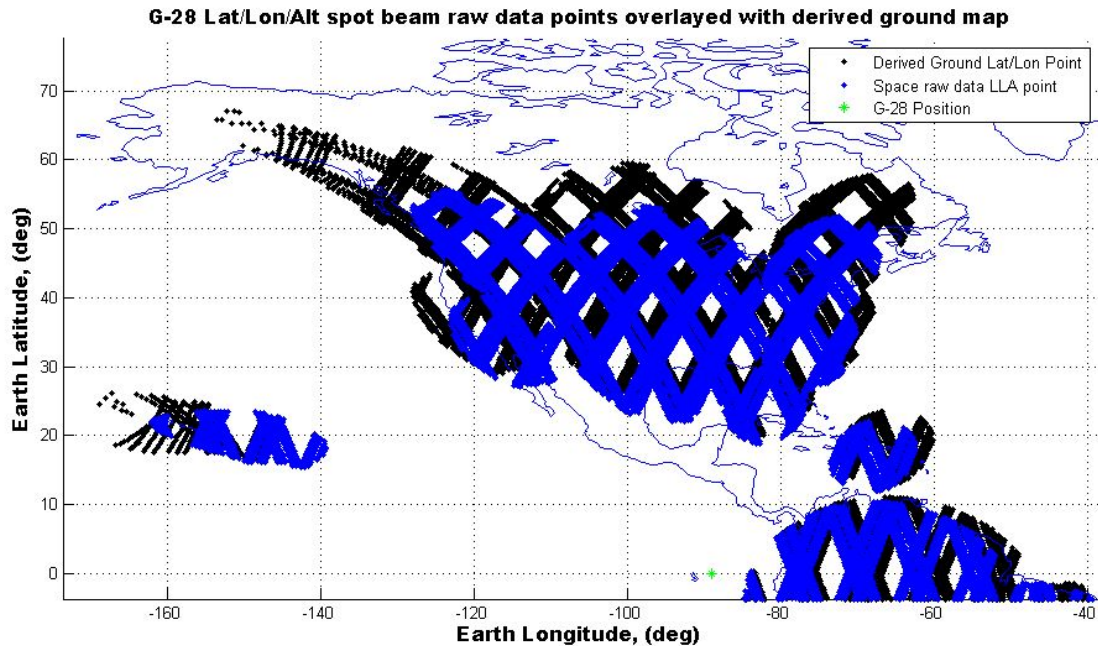
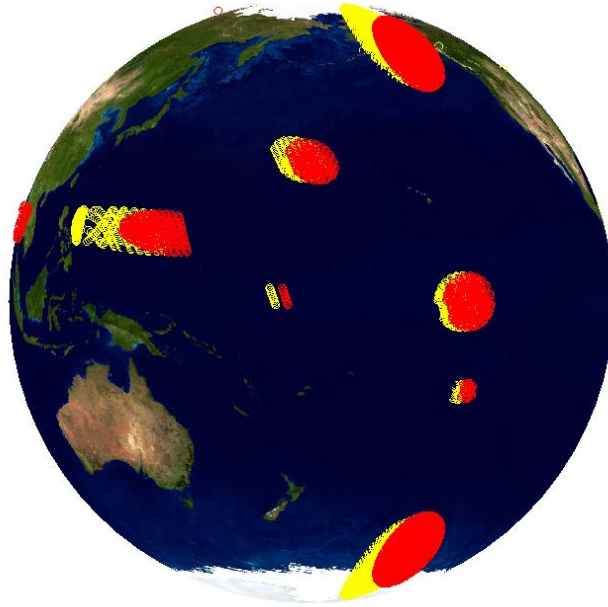


Figure 27: 350km, 68inc, 3day, 5sec, 2plane, 3sats/plane, even spacing

The test with 2 plane / 3 satellites per plane constellation at 350 km shown above does a “fair” job at completing the spot beam mapping mission, however left large gaps in coverage, due to being non-synched with the Earth’s rotation. This constellation was essentially the same as a Walker Delta pattern, however *did not* include the Walker feature that offsets the true anomaly for each different plane.

An additional constellation configuration using a single plane, but without even spacing through the entire orbit, was tested for its effects on spot beam mapping capability as well. This beam mapping “formation” was tailored such that a number of CubeSats all pass over a single area within minutes of each other, allowing the edge of any beams being flown through to be easily characterized, since each CubeSat would fly through them at slightly offset coordinates – essentially painting large swaths of the globe per pass. Over the long-case 3 day duration, this constellation configuration, when

tailored to take advantage of the Earth's rotation correctly, produced a very 'clean' spot beam map, shown in Figure 28.



**Figure 28: "Clean" spot beam map constellation result from mapping G-II beams.
Constellation: 68 deg, 350km, 3 days, 5 sec, 1 plane, 6 sats, 20 deg sep. Compare to
known G-II beams, note missing beams.**

The three day case using the set-spacing formation yielded beam maps with good resolution. However, for the short-case 1 day duration, most formations did not have enough time to complete a broad enough sweep to cover the globe, and thus there were large coverage gaps in the areas the formation had not visited yet.

It must also be noted that although this constellation type could produce a very nice-looking spot beam map after a few days, the constellation was typically unable to find the moving spot beam, and also did not at all find the "disappearing" beam that disappeared 1.5 days into the scenario. Comparing Figure 28 to the right half of Figure 22, it can be clearly seen that some features are missing; regardless that Figure 28's

flythroughs are cleaner with very small coverage gaps. Thus, the constellation with fixed separation tested within the scenario performed very well for mapping static beams over moderate duration, and did not perform very well at all for moving or for finding short-duration specialty beams.

4.4 Effects of Changing Altitude

With lifetime considerations addressed, the usable orbital altitudes from 350 km to 500 km were then compared against each other with the area of coverage gaps in the spot beam map for different constellation types. In doing so, it was found that varying the altitude from 350 km to 500km showed that the CubeSat SBM mission's design altitude was a significant factor in the final beam map's resolution. In other words, the beam mapping capability changes depended on altitude and constellation type. Single-plane constellations yielded interesting results for coverage gap size based on altitude. Figure 29, below, shows the coverage gap size for selected single plane constellations at the mission altitudes.

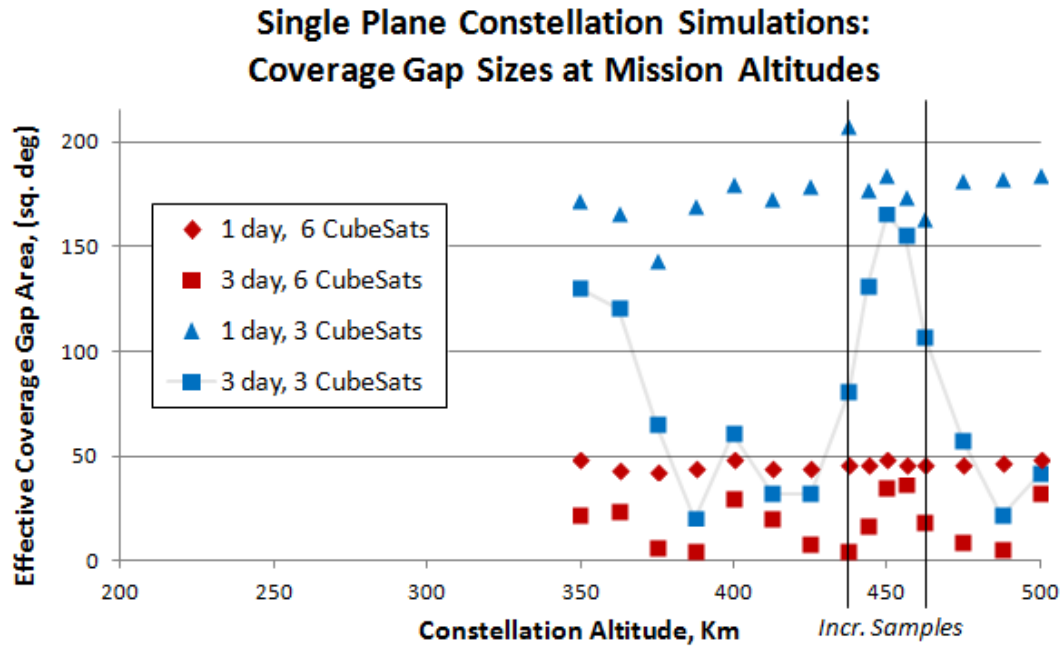


Figure 29: Coverage gap sizes at mission altitudes for single plane constellations using 3 or 6 CubeSats -- 1 day of collects compared to 3 days of collection.

The plot of coverage gap size per altitude for the selected formations proved interesting. The 1 day, 6 CubeSats in-plane case for the altitude range stayed mostly consistent with just under 50 sq. deg of solid angle between passes. Allowing this same constellation to work over three days increased the variance of the data, but decreased the mean coverage gap value, with some minimum (i.e. good) results less than 10 sq. degrees. The “3” CubeSat constellation varied much more significantly for the 3 day case, even appearing better than the 6 satellite tests at certain points in terms of coverage gap reduction! Given only 24 hours, the “3” CubeSat formation behaved less aggressively, with larger coverage gaps at all tested altitudes.

Altitude was also a significant driver for the other tested constellations. Figure 30 gives an altitude vs. coverage gap size result in similar fashion to the single plane altitude vs. coverage gap size plot. Recall that Walker Delta notation was listed as X-Y-Z, where

X was the total number of satellites, Y was the number of planes, and Z was the number of satellites per plane.

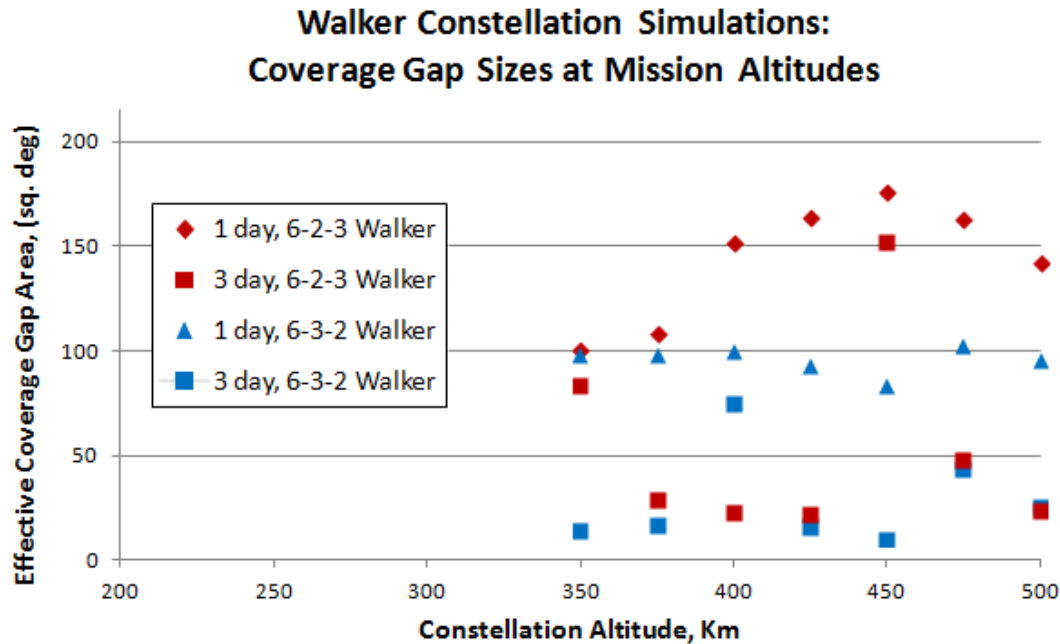


Figure 30: Coverage gap sizes at mission altitudes for 6-2-3 and 6-3-2 Walker constellations -- 1 day of collects compared to 3 days of collection.

As with the single plane results before, the Walker constellations also had coverage gap variance driven by altitude. On the whole, the 24-hour duration Walker constellations seemed to have limited data variance for the tested altitudes, whereas the 3 day duration constellations did not. It is worth mentioning that the plots here are not to be treated as trends, but rather as discrete data points consistent with the developed simulation tool's output --- more data would need to be collected to verify the non-existence of data aliasing.

4.5 Effects of Changing Number of CubeSats

Determining an appropriate number of CubeSats to use within a spot beam mapping constellation was necessary to complete the mission reasonably within the parameters dictated by the mission requirements. Technically, this spot beam mapping mission *could* be completed with even a single satellite; however the tradeoff for this would be a significant reduction in responsiveness to moving or changing spot beam patterns. Plus, it was found that the time it would take to obtain a fully defined spot beam pattern map using a single satellite would take greater than the threshold of 3 days, and usually greater than 5 days, regardless of mission altitude. The single CubeSat option also tended to show the most difficulty with locating the smaller spot beams in the scenario. The larger spot beams from Galaxy 28 were characterized easily enough, but the smaller spot beams emitted from the G-II comm-sat were harder to find.

Thus to increase responsiveness and shorten the necessary data collection duration of the mission, more CubeSats were added to the orbital plane. Table 12 shows a sample of the averaged effects of adding CubeSats to an orbital plane at the various altitudes tested in the scenario.

Table 12: Results for varying number of satellites within one plane, using collection durations of 1 and 3 days.

# of CubeSats in plane	Data Collect Time	Avg. G28 Beams Detected (of 13)	Avg. G-II Beam Features Detected (of 8)	Avg. G-II Small (Ka-Band) Beams Detected (of 2)	Avg. Size of Coverage Gaps lon x lat, (sq. deg)	Qualitative Outlook
1	1 day	5	4	0	25 x 60, (1500)	
1	3 days	10	6	1	12 x 30, (360)	
3	1 day	12	6	1	8 x 22.5, (180)	
3	3 days	13	8	2	5.5 x 11, (60.5)	
6	1 day	13	7	2	4 x 12, (48)	
6	3 days	13	8	2	3 x 10, (30)	
8	1 day	13	8	2	3 x 9, (27)	
8	3 days	13	8	2	2.25 x 7 (15.8)	

Thus, as more satellites were added to the scenario, the performance of the spot beam mapping process tended to increase for the single plane constellation type. Increasing the number of satellites also tended to increase the probability of detecting the harder-to-find small or dynamic beams. Figure 31 shows the relative coverage gap sizes for different amounts of CubeSats in a single plane at the tested mission altitudes.

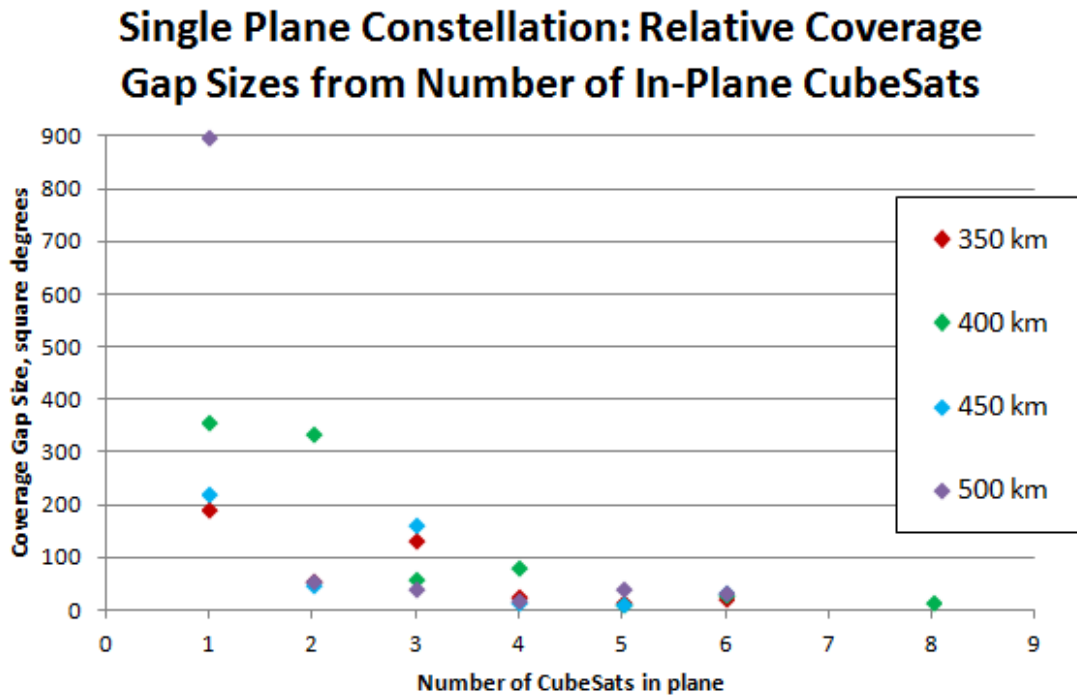


Figure 31: Relative coverage gap sizes obtained from changing the number of single plane CubeSats at tested mission altitudes.

The trend therefore was usually downward, as the number of satellites was increased, the coverage gap sizes in the final ground-based spot beam map decreased on average. Increasing the number of satellites also increases the cost and complexity of the whole constellation. Therefore it would be desirable that the case of “too many satellites” be avoided. After adding about 6 CubeSats in a constellation, the cost per benefit ratio seemed to begin following the law of diminishing returns. Adding in two

extra satellites to create the 8 CubeSat constellation does indeed continue to reduce the coverage gap size and improve responsiveness as expected over the 6 CubeSat constellation; however adding in more satellites beyond this wouldn't really give much in the way of cost per benefit for mapping K-band and lower frequency beams from GEO.

4.6 Effects of Changing # of Planes

Following the results of changing the number of CubeSats in-plane, the effects of keeping the number of satellites constant, but varying the number of planes within the spot beam mapping mission were also analyzed. Spreading the satellites out between different planes opened the possibility to reduce response times, and make spot beam passes more efficient: potentially reducing the necessary number of satellites while maintaining capability. Table 13 shows an example of the averaged effects of adding orbital planes with 6 CubeSats in LEO.

Table 13: Sample of results by adding CubeSat planes for constant 6 total satellites, with collection durations of 1 and 3 days, 400km alt.

# of CubeSat Planes	Data Collect Time	Avg. G28 Beams Detected (of 13)	Avg. G-II Beam Features Detected (of 8)	Number of Accesses - Mobile Beam	Avg. Size of Coverage Gaps (sq. deg)	Qualitative Outlook
1	1 day	13	7	2	48	
1	3 day	13	8	6	30	
2	1 day	13	6	0	108	
2	3 days	13	8	3	17.5	
3	1 day	13	7	2	172.5	
3	3 days	13	8	7	143.3	
6	1 day	13	6	0	188	
6	3 days	13	8	1	58.5	

The small sampling of simulation results shown above for separating the six CubeSats into separate planes demonstrate that improved capability was possible for the 68 deg, 400 km, circular orbit case. It can also be observed that for many of the cases, splitting the CubeSats into separate planes also reduced capability, in some instances

significantly. This was especially evident in the constellation’s capability at finding the mobile beam. It was more commonly detected by the single plane case, and varied wildly with the multiple plane case.

4.7 Effects of Changing Payload Data Rate

Changing the rate at which the payload reported its latitude, longitude, and altitude over time from a notional scenario value of a location report every five seconds did not seem to significantly alter the ability of the CubeSat SBM to produce a beam map as a whole, unless the data rate was significantly reduced. Increasing the data sampling rate of the receiver payload corresponded to an increase in spot beam map resolution in the orbit plane, making the output spot beam map appear to be in more of a “high definition” state. Figure 32 shows two different collection passes through one of Galaxy 28’s Ku-band spot beams over the Gulf of Mexico, comparing two different payload sampling rates.

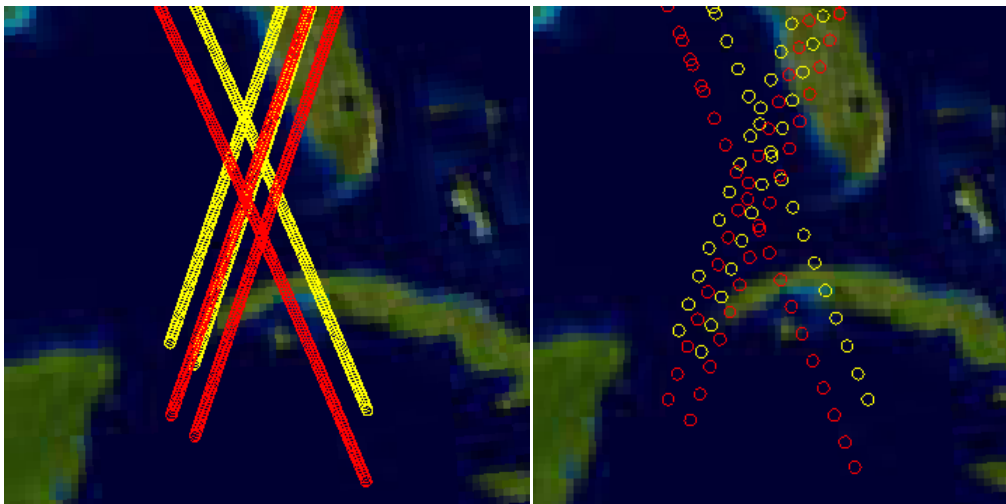


Figure 32: 400km altitude Ku-band spot beam collection passes over the Gulf of Mexico using different payload sampling rates. Left: 1 second per sample, Right: 10 seconds per sample.

Although changing the payload data rate doesn't necessarily reduce major coverage gap size significantly, it may otherwise be useful for the mission planner to know what the in-plane ground map resolution would be for the mission orbits and desired payload data sampling rate. The phrase: "in-plane ground map resolution" refers to the arc-length distance between collected location points as translated on the ground-based spot beam map. Figure 33 shows the calculated in-plane ground point resolution (in kilometers), for various payload sampling rates, at the mission altitudes.

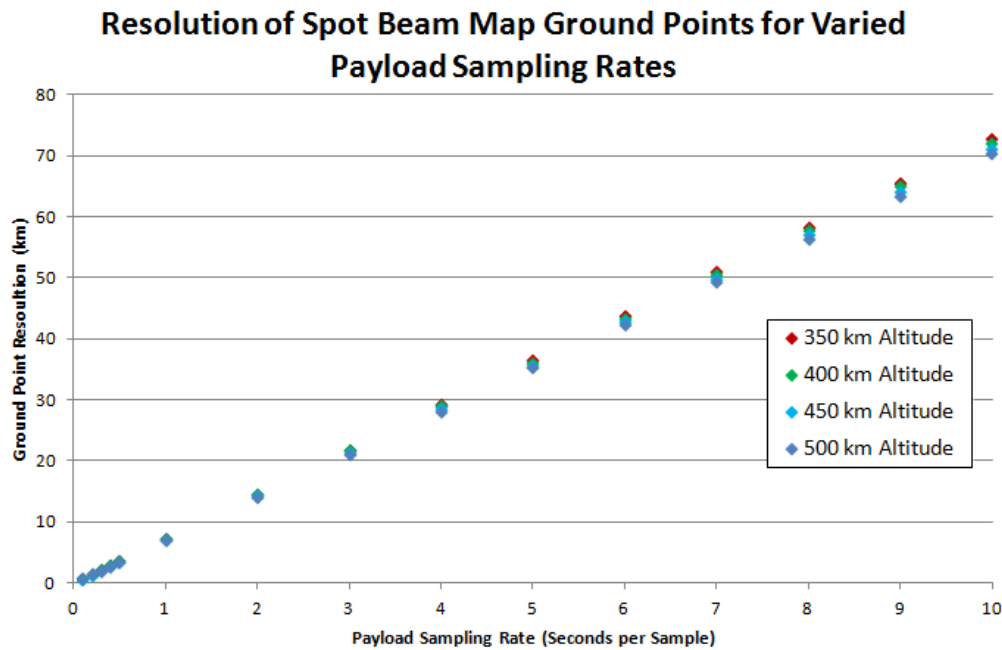


Figure 33: Ground-based spot beam map accuracy for changing payload data sampling rates, for the mission altitudes.

As expected, for lower sampling rates such as 10 seconds per sample, the distance between ground points for all mission altitudes was on the order of 70+ km. For higher sampling rates, at sampling frequencies greater than or equal to 10 Hz (0.1 seconds per

sample), the distance between ground points for all mission altitudes was reduced to less than a kilometer.

It does not come as a surprise, therefore, that when the data rate used for constellation analysis and data collection in the simulation was doubled from 5 seconds per data set to 10 seconds per data set, a decrease in overall resolution of the in-plane data points on the beam map was observed, meaning the distance in between each data point increased, as expected. However, more importantly, the location and edges of all K-band beams within the scenario were still clearly resolvable. These edge locations could be determined more accurately, if desired, by averaging the collected edge data points around the entire spot beam (*IF enough passes were made through the selected spot beam!*).

However this increased “high definition” data rate comes at the cost of generating more data, which must be stored on the spacecraft and forwarded to the mission ground station. The below Table 14 shows the required data storage size for one spot beam mapper’s collected GPS information. The information assumes NMEA GGA GPS strings --- 79 Characters with 8 bits/character, and 1 byte = 8 bits.

Table 14: GPS information: Necessary data storage size determined by *constant* collection durations and payload sampling rate.

	1 sec / sample	2 sec / sample	5 sec / sample	10 sec/sample
10 seconds	0.79 kb	0.395 kb	0.158 kb	0.079 kb
1 minute	4.74 kb	2.37 kb	0.948 kb	0.474 kb
1 hour	284.4 kb	142.2 kb	56.88 kb	28.44 kb
1 day	6.83 Mb	3.41 Mb	1.37 Mb	0.68 Mb
3 days	20.47 Mb	10.24 Mb	4.10 Mb	2.05 Mb

Thus as an example, to obtain the data for a full spot beam map on the ground after the threshold requirement of 3 days, with the CubeSat's on board memory storing GPS information at 5 sec / sample, the CubeSat would need to transmit a grand total of 4.1 Mb of information to the ground. This 4.1 Mb of total data assumes that the full 79 characters of the NMEA GGA GPS strings must be transmitted. Excluding additional telemetry and health data, 4.1Mb seems to be reasonable as a payload data storage requirement on board a 6U CubeSat.

The above mission data requirements apply for ground segment and on-board link capability for the spot beam mapping CubeSats. According to O'Brien, the Naval Postgraduate School site of the MC3 ground station network can handle data rates up to 57.6 kbps down, and 9.6 kbps up [50]. With CubeSat daily mission operations, the NPS ground station has demonstrated data handling of about 10MB per day, assuming 30 minutes of talk time is completed with the satellite per day. Comparing these reported values with the simulated spot beam mapping mission, a simple calculation shows that the NPS ground site of the MC3 network is capable of handling any of the cases presented in the table above, following similar assumptions and hardware capability. A possible limiting factor on these trades therefore falls to the hardware selection on-board the spot beam mapping CubeSats.

Choosing a sample rate to fit the mission parameters is a necessary trade for the spot beam mapping mission. An analysis was conducted to check the effects of different spot beam sizes and the payload sampling rates needed in order to effectively characterize them. Using the beam width of the spot beam compared to the angular

coverage of the spot beam within a CubeSat's orbit along with the orbital period at that altitude, reasonable minimum sampling rates were obtained.

An assumption governing the determination of the minimum required payload sample rates was that at least three (3) data points "collects" were desired for the spot beam pass to be considered. Spot beam geometry and orbital geometry were used to find the total time each CubeSat spent within spot beams of the different sizes for each of the mission altitudes. The "time spent within beam" number then had a safety factor applied to it, since not every pass through the spot beam would be perfect, as in "right through the middle." This was then divided by the minimum number of data points desired to obtain the minimum sampling rate needed (min. number of data points needed was decided as a judgment call, and is easily modifiable within the script). Figure 34, below, shows the calculated minimum sampling rates necessary to generate an appropriate spot beam map for different target spot beam sizes.

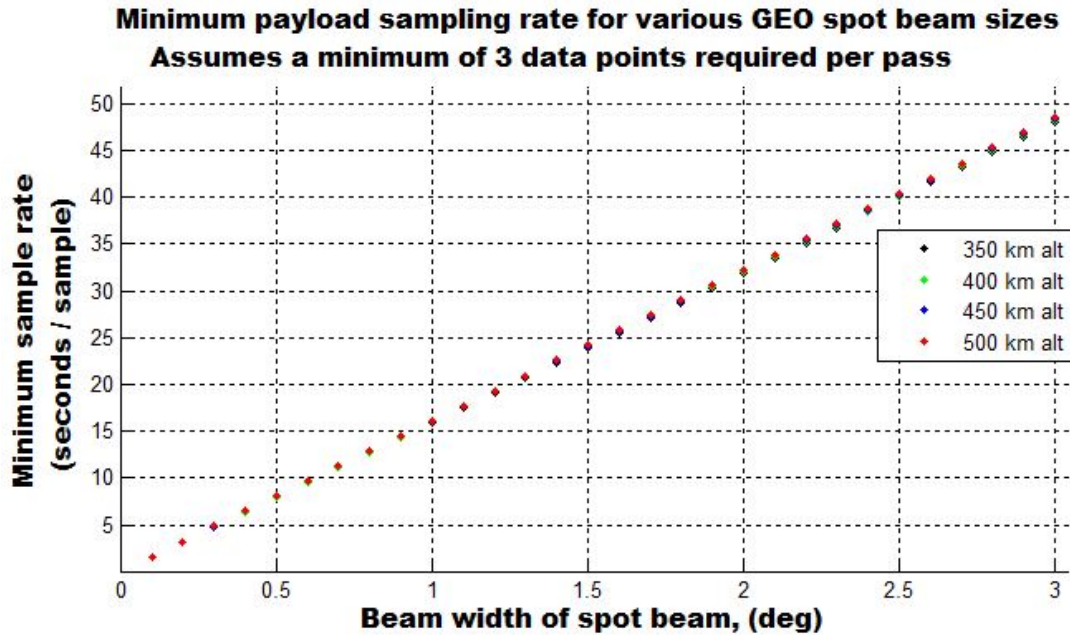


Figure 34: Minimum sampling rate needed for given spot beam sizes. Assumes 3 data points are required for each pass.

The simulation modeled Ku- and Ka-band spot beams used beam widths near 2 degrees and 0.5 degrees, respectively. Spot beams emitted from GEO with beam widths of ~2 degrees would therefore require a payload that could sample at a minimum of approximately 32 seconds per sample in order to properly locate the beam, assuming that three data points within the beam at LEO was desired at a minimum. For the smaller Ka-band beams modeled with 0.5 degrees beam width, a payload would need to have a sample rate of at least 8 seconds per sample in order to properly detect the beam with a minimum of 3 data points per pass.

4.8 Effects of Changing Inclination

Changing the mission inclination for the spot beam mapping constellations has significant effect upon the ground-based spot beam maps. To analyze the effects of designing the spot beam mapping mission with different inclinations, a stable mission

constellation configuration has been held constant. The inclination analysis constellations simulated were 6-3-2 Walker Delta patterns at 400 km altitude, with 5 sec/sample payload sampling, simulated for 24 hours. To set a base for comparison, Figure 35 shows the ground-based spot beam map for the standard scenario with inclination set to 68 degrees (Chapter III details reasoning behind 68 deg. inclination).

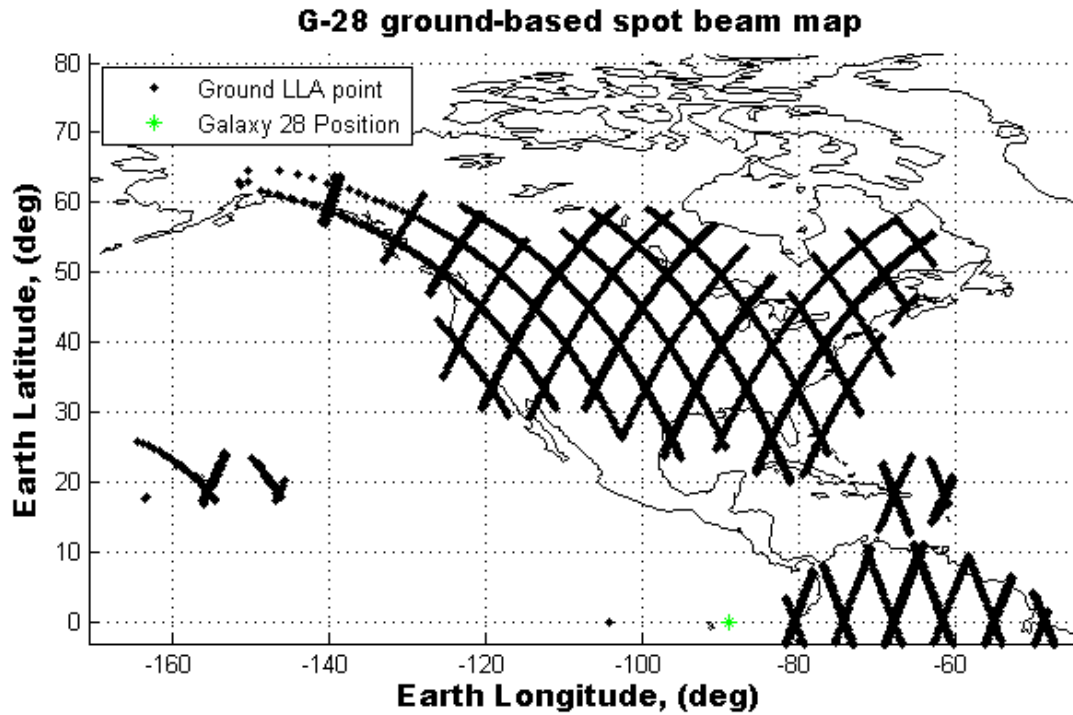


Figure 35: Inclination: 68 deg. Walker 6-3-2 Constellation at 400km, simulated for 24 hours.

This ground-based spot beam map with inclination set at 68 degrees has relatively large coverage gaps. For the Galaxy-28 Ku-band beams, the coverage gaps within this particular simulation run are small enough such that the gaps do not interfere with total beam coverage determination. The 68 degree inclination test shown was successful in providing coverage through all beams depicted in the scenario, as expected according to the inclination range determination completed in Chapter III. In an effort to demonstrate

orbit flexibility for the spot beam mapping mission, the inclination was then tested at 75 degrees. Figure 36 shows the ground-based spot beam map result with inclination increased to 75 degrees.

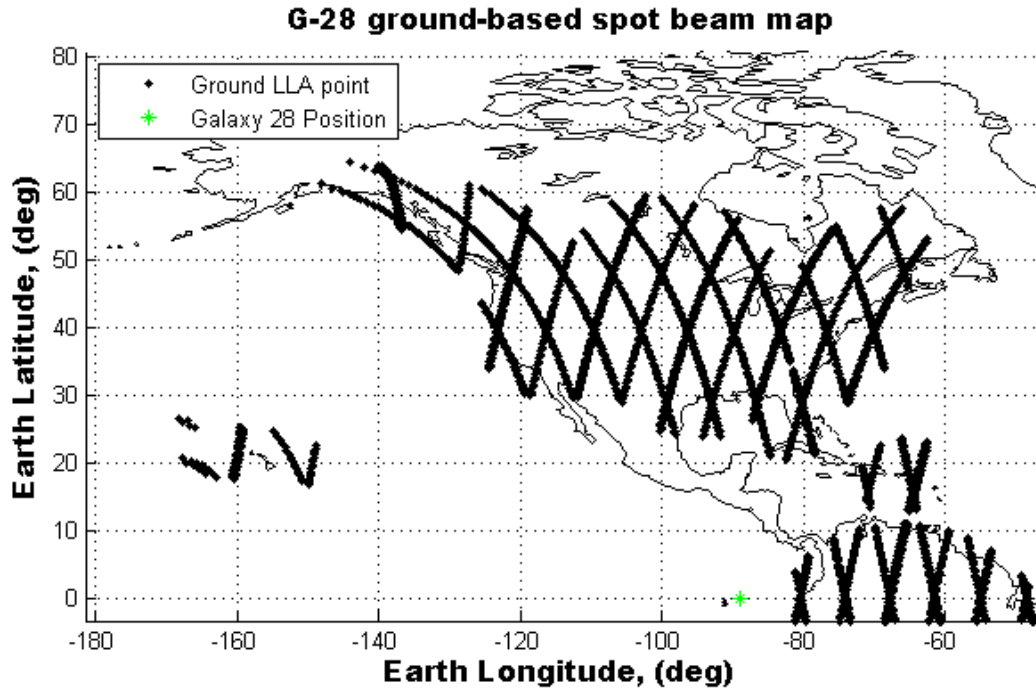


Figure 36: Inclination: 75 deg. Walker 6-3-2 Constellation at 400km, simulated for 24 hours.

The 75 deg. inclination test compared to the previous 68 deg. inclination test shows that for the higher inclination, the coverage gaps become more elongated in latitude while, (since the orbital period remained constant), the longitude difference remained constant. Additionally, with higher inclination comes a reduced amount of time the spot beam mappers spend actually mapping Earth-pointing beams from GEO, since spacecraft in GEO cannot point their spot beams at extreme Earth latitudes. All things considered, the 75 deg. inclination test case was still not a “bad” case, and remains a feasible option for spot beam mapping. Similar to the 75 degree inclination, the 82

degree inclination case, shown in Figure 37, also demonstrates the “elongated coverage gap” effect, with more extension.

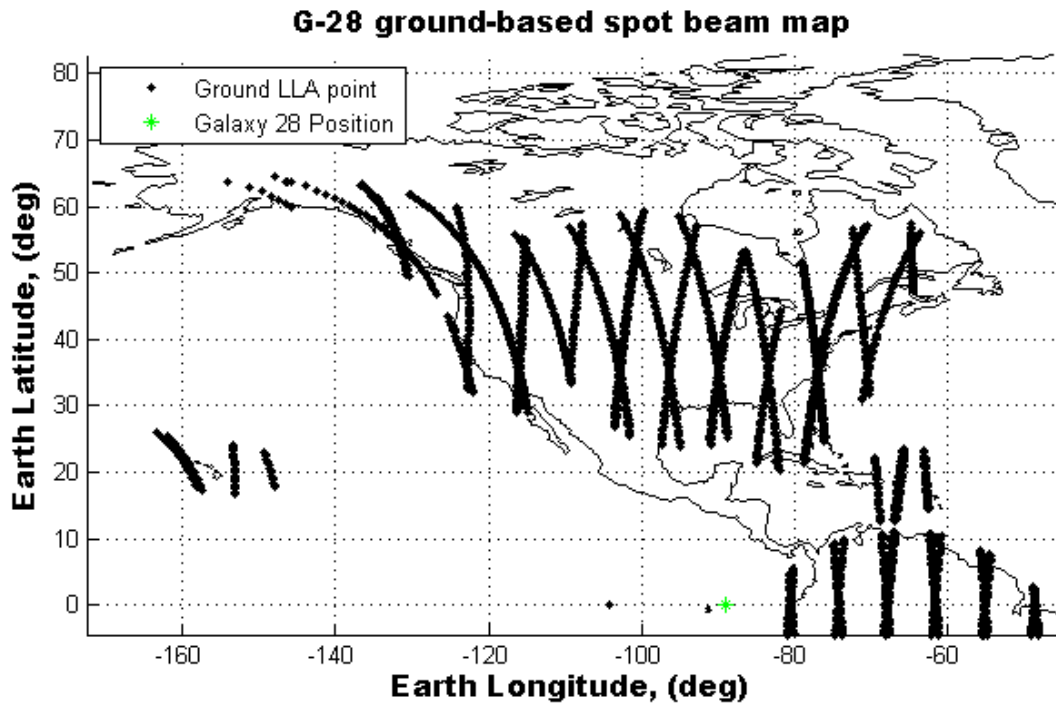


Figure 37: Inclination: 82 deg. Walker 6-3-2 Constellation at 400km, simulated for 24 hours.

The 82 deg inclination case still maps the edges of the spot beams from Galaxy-28; however the ability to determine longitude edges accurately begins to become noticeably deficient at higher inclinations, especially with this short 24 hour case. Making the orbit completely polar (90 deg.), in Figure 38, further adds to the effects demonstrated above.

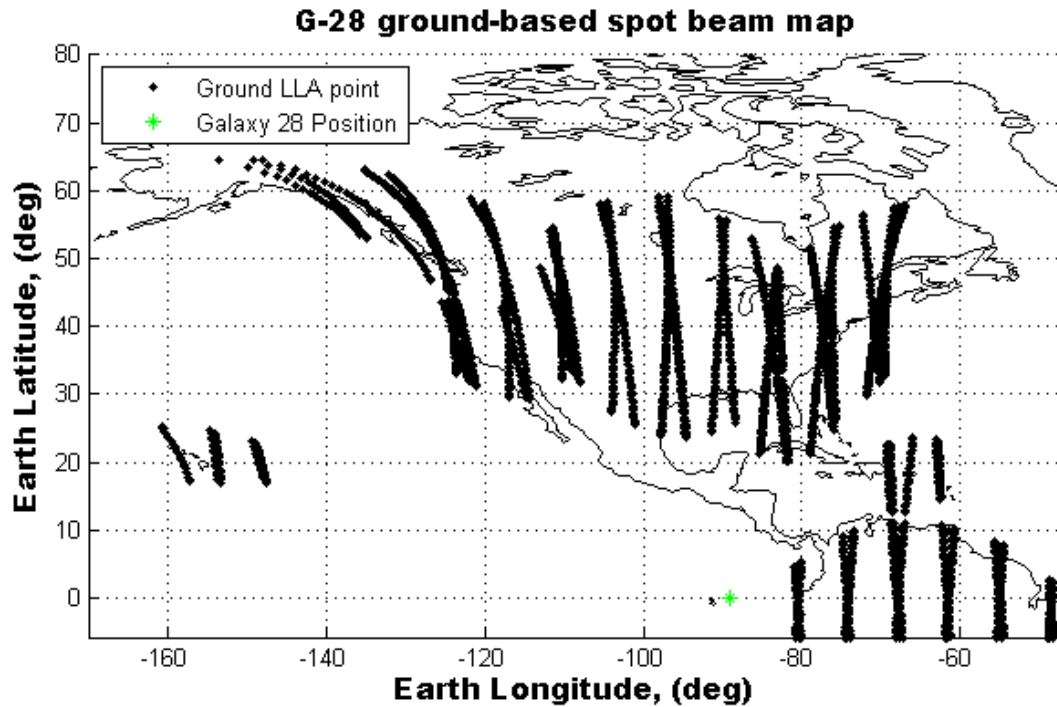


Figure 38: Inclination: 90 deg, polar. Walker 6-3-2 Constellation at 400km, simulated for 24 hours.

Again, increased inclination to maximum further spreads the latitude coverage gap difference. This was emphasized in the Hawaiian region shown in the above figure. Galaxy-28's Hawaiian beam was not mapped very well in the longitudinal sense. Given more collection time, the longitude gap can be significantly reduced, assuming the orbit does not have an immediately repeating ground track. In summary, polar orbits can be made to work for the spot beam mapping mission, however they are not likely to be considered the best choice for short duration global coverage scenarios, due to the longitudinal resolution issue.

Another commonly flown orbit that could be used for spot beam mapping was the sun-synchronous orbit. At 400 km, the sun-synch inclination was found to be approximately 97.1 degrees, with a corresponding ground-based spot beam map as shown in Figure 39.

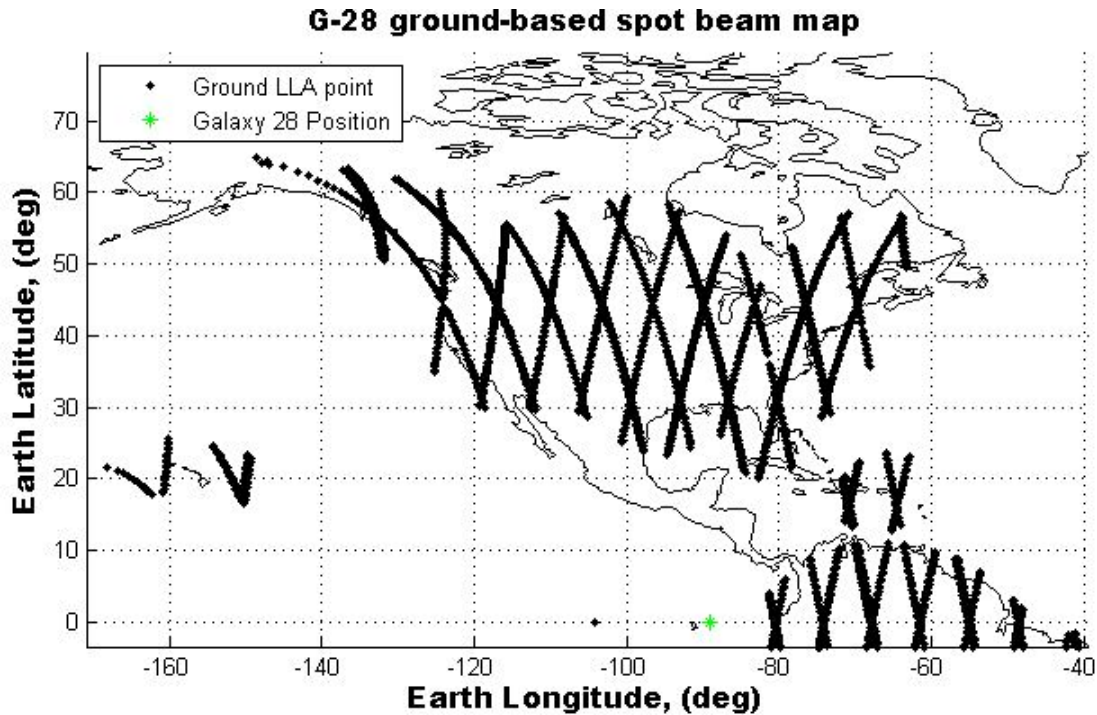


Figure 39: Inclination: 97.1 deg. Walker 6-3-2 Constellation at 400km, simulated for 24 hours.

The pro-grade sun synchronous orbit behaves, as expected, much like a similar highly inclined retrograde orbit. Sun synchronous orbits “can” be used for the spot beam mapping mission, however sun-synch comes with a noticeable negative side effect for spot beam mapping: since the orbit passes over the same ground location at the same time daily, spot beam map coverage gaps will not decrease in size significantly over time after the first set of passes are obtained.

In addition, the case for inclinations less than the global beam coverage inclination (68 degrees) were also looked at. Lower inclinations than 68 degrees have the benefit of very favorable coverage gap reduction, however with the high cost of losing coverage capability altogether above the orbit’s maximum latitude. The benefit of coverage gap reduction and cost of lost coverage capability has been demonstrated through the 28 deg. inclination case, shown below in Figure 40.

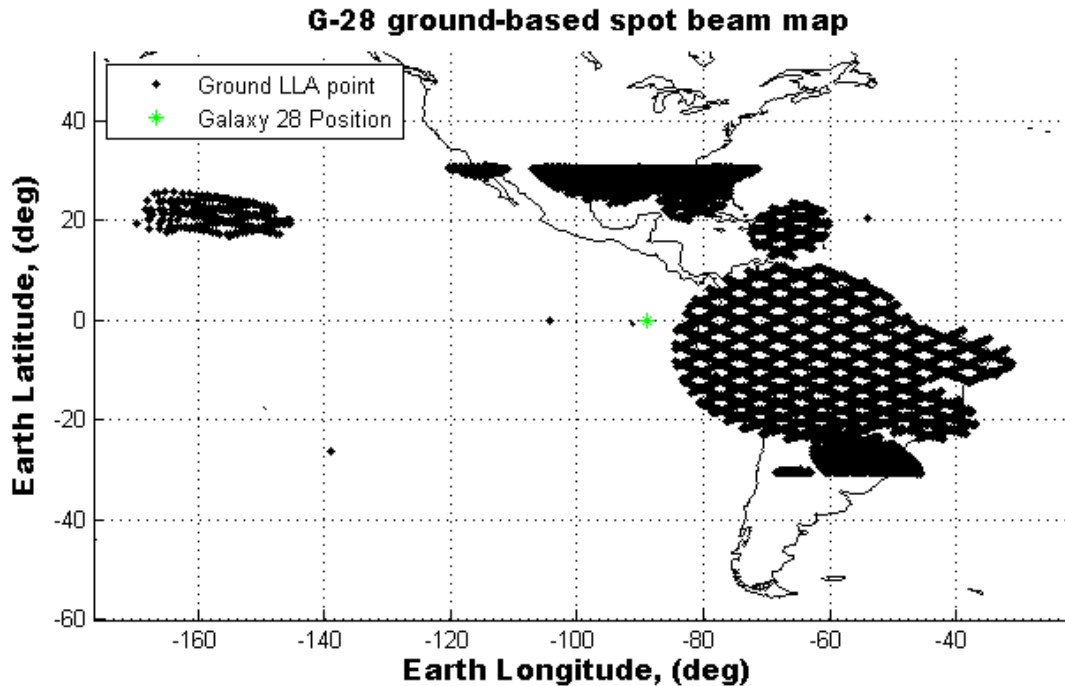


Figure 40: Inclination: 28 deg. Walker 6-3-2 Constellation at 400km, simulated for 24 hours.

Using an inclination of 28 degrees (Cape Canaveral latitude), greatly improves spot beam mapping capability around the equator up to 28 degrees latitude compared to the 68 degree inclination case. However, the 28 degree inclination completely removed beam detection coverage over most of the continental U.S. and Canada, which is unacceptable with the current set of mission requirements.

4.9 Effects of Changing Duration

For all data sets collected, changing the mission collection duration from the minimum requirement of 3 days up to the goal requirement of 24 hours showed that longer duration collections in most cases produced a better spot beam map. In simplest terms, since the CubeSats have more time to collect data when given three total days, more resolution and coverage gap reduction could occur. Figure 41 shows the ground

based spot beam map obtained from the single plane, 6 ship constellation, orbiting at 350km, after one day of collection.

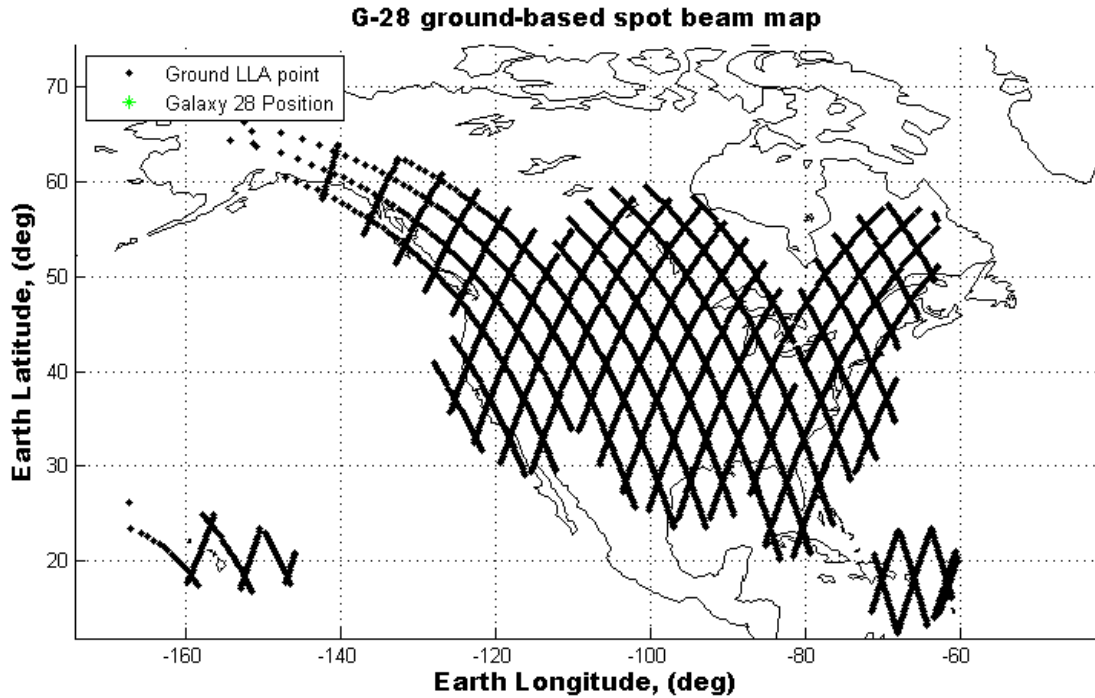


Figure 41: Obtained 24-Hour ground-based spot beam map over North America for a single plane of six CubeSats orbiting at 350 km, 68 deg. inclination, with 5 samples/sec sampling rate.

It can be observed in the above ground-based spot beam map that for the 24 hour period, the CubeSats made several ascending and descending passes over the North American region, where a portion of the Galaxy 28 beams were situated. Based on the size of the coverage gaps and definition of the beam edges, enough information appears to be present to determine the effective coverage pattern and shape of the Ku-band beams on the ground. That said, the nominal sizes of the coverage gaps in the above Figure 41 are still large enough to nearly fit the entire surface area of Lower Michigan within them. Thus, any “small” spot beam that could fit within this area runs the chance of being missed entirely within this 24 hour collection. Since a 72 hour (3 day) collection period

is still acceptable within the established mission requirements, Figure 42 below shows the final ground-based beam map obtained from Galaxy 28's Ku-band beams by the same single plane, 6-ship constellation orbiting at 350 km.

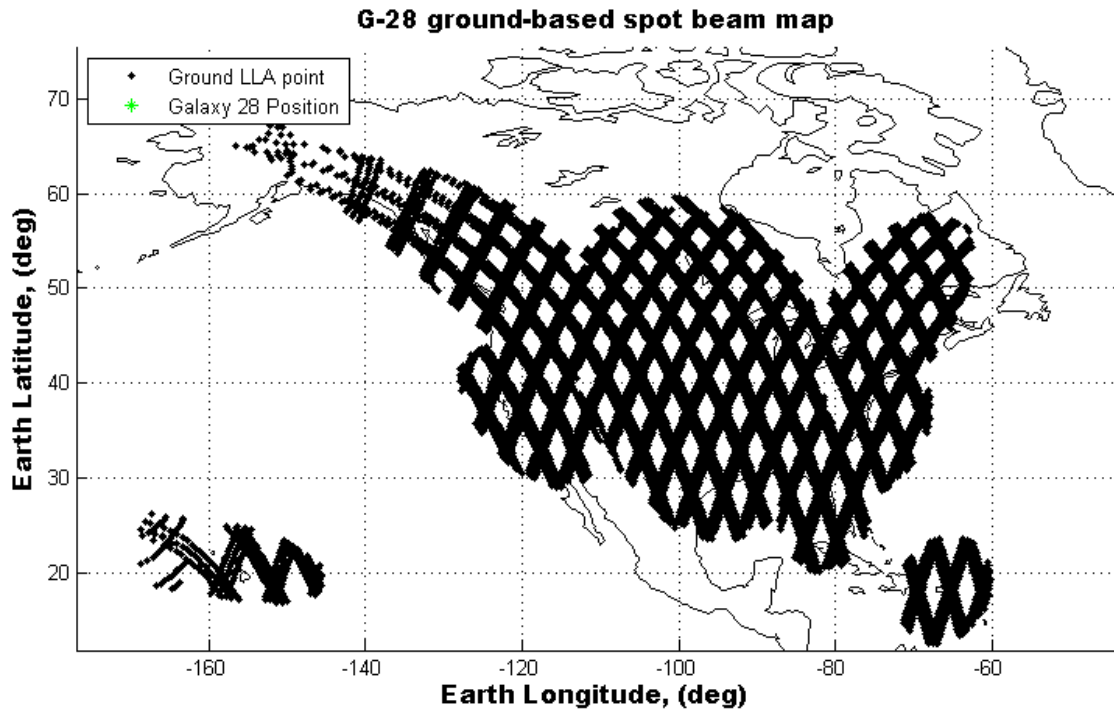


Figure 42: Obtained 72-hour ground-based spot beam map over North America for a single plane of six CubeSats orbiting at 350 km, 68 deg. inclination, with 5 samples/sec sampling rate.

Since more time passed within the scenario, the non-repeating ground track of the CubeSats reduced the size of the coverage gaps, as expected. So, as the gaps in coverage decrease over the extra duration allotted, the chance to completely miss previously unobserved spot beams also decreases. It must be noted, therefore, that if the constellation was to use a repeating ground track orbit type, the final ground coverage gaps would remain the same size, regardless of duration.

4.10 Transmitter Position Requirement

As previously discussed, the position of the GEO transmitter must be known for the ground based spot beam map to be appropriately generated. In the optimal case, position knowledge of a cooperative GEO transmitter would be known to within a reasonable accuracy, thus no location-determination would need to be performed on the spot beam mapping CubeSat. However, optimal scenarios are not always the case, and thus if location determining was performed on the spot beam mapping CubeSat, additional attitude determination and control requirements must be analyzed. Thus, a study of CubeSat attitude knowledge accuracy required in order to locate the GEO-transmitter was conducted for the various CubeSat SBM orbital altitudes. Figure 43 below shows an example set of unfiltered line-of-bearing estimates, obtained during a spot beam mapping pass, used for transmitter position determination.

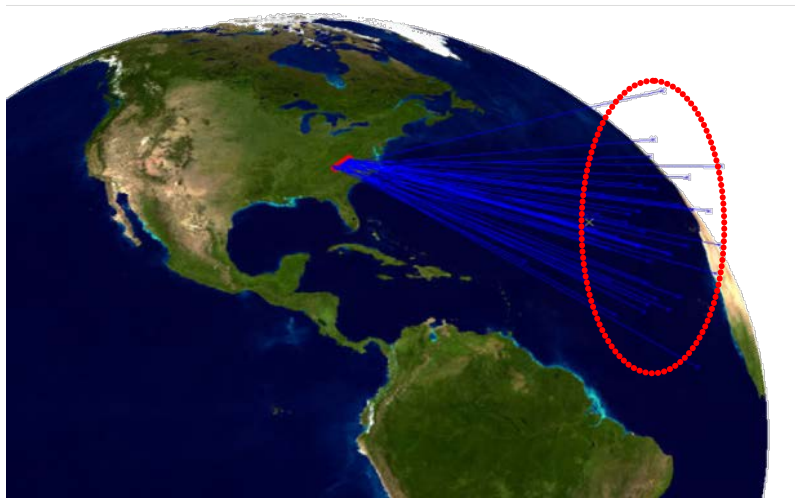


Figure 43: Attitude knowledge error effects on GEO position error covariance determination.

The required bearing estimate in conjunction with a position estimate for the GEO transmitter during spot beam collection passes was observed against the azimuth or elevation angle of the CubeSat with respect to the ECEF GEO transmitter vector. As the CubeSat orbits the earth, the CubeSat's distance from the GEO transmitter varies through a given pass. The distance from the CubeSat to the GEO transmitter is referred to as the CubeSat's "Slant Range." During a given pass, as the slant range increases with the changing Azimuth and Elevation angles on the globe, the required attitude knowledge on board the CubeSat becomes slightly more demanding to generate the position estimate. The increase in slant range becomes important to note since not all spot beams point conveniently towards the equator and the sub-satellite point of the GEO transmitter. Over the GEO transmitter's sub-satellite point, the attitude knowledge requirement for position determination is relaxed. Attitude knowledge capability of the CubeSats within the highly inclined spot beams then drive the overall attitude knowledge requirement, should the CubeSats need to determine the position of the GEO transmitter on their own in the first place.

Looking at the spot beam accuracy for additional error ellipse sizes shows the impact of GEO position knowledge in terms of how accurately the ground beam map can be obtained. Since the position estimate accuracy significantly affects the accuracy of the ground-based spot beam map mission output, the effects of the position estimate on the accuracy of collected spot beam location points was analyzed. The GEO position estimates, along with the position estimate's effects on the primary mission's ground based spot beam map point accuracies, have been shown in Table 15.

Table 15: Ground map geometric error and angular bearing error based on GEO position error estimate. 350km altitude results shown.

GEO Position Estimate, Error Ellipse Diameter	Angular Bearing Estimate	Ground Map Error (0 deg slant)	Ground Map Error (30 deg slant)	Max. Ground Map Error (60 deg slant)
1 km	0.0007 deg	8.5 m	13.4 m	160 m
10 km	0.007 deg	85.5 m	134 m	1.6 km
100 km	0.07 deg	0.86 km	1.3 km	16.0 km
1000 km	0.7 deg	8.5 km	13.4 km	162 km
1333 km	1 deg	12.2 km	19.2 km	235 km
2000 km	1.5 deg	18.3 km	28.7 km	366 km
2666 km	2 deg	24 km	38.3 km	518 km

There is therefore a clear trend that can be observed on the whole: as the position estimate accuracy of the GEO transmitter decreases, the ability of the spot beam mapper to translate measured GPS points from space to the ground also decreases, especially for beams with higher slant angles (i.e. higher elevation or azimuth). As an example, the information gathered demonstrates that if the position of the GEO transmitter is known to within 100km (0.07 deg), the ability of the spot beam mapping CubeSats to map GPS points from space to ground will be accurate to within 0.86km at the GEO sub-satellite point, within 1.3 km at 30 degrees of slant angle, and within 16 km at 60 degrees slant angle. For large spot beams covering hundreds or thousands of square kilometers, this accuracy on the order of a few kilometers for most beams does not seem too bad for determining coverage areas, especially if all measured data points were to be statistically filtered.

CubeSat attitude knowledge accuracy has historically been on the order of 1-2 degrees with standard CubeSat-caliber ADCS packages [42]. Using the least favorable case of the reported attitude accuracy (2 deg attitude knowledge error), a simple Kalman filter was applied to a set of observations (i.e. line of bearing estimates to the transmitter)

for a selected spot beam pass over North America, sampled at 5 seconds/sample. Figure 44 shows the collected observations for the spot beam pass, unfiltered, with 2 degrees of attitude knowledge capability on board the CubeSat, with a distance constraint applied to the geostationary orbit.

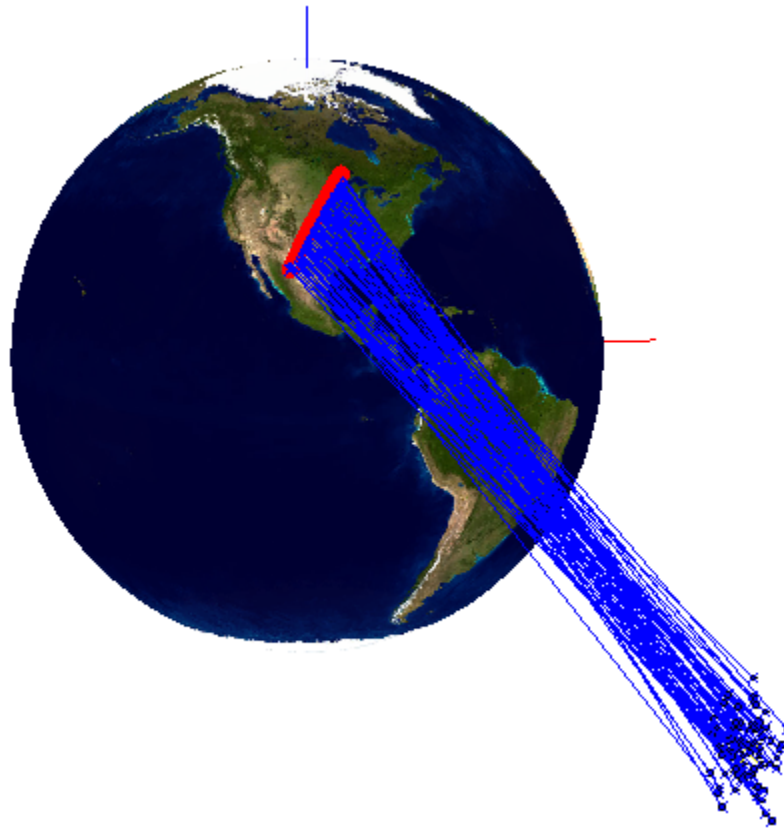


Figure 44: 3D View of bearing estimates from CubeSat to GEO Transmitter during a spot beam pass, unfiltered, with GEO orbit distance constraint. (75 samples @ 5 seconds/sample)

Applying the simple Kalman filter to the CubeSat spot beam mapper's line of bearing observations to the GEO comm-sat created a position covariance estimate. Figure 45 and Figure 46, below show an example of a CubeSat's filtered position estimate capability, based on the filtered North American beam pass observations

displayed in Figure 44 above for the X (perpendicular to G-28, red) and Z (north, blue) ECEF axes.

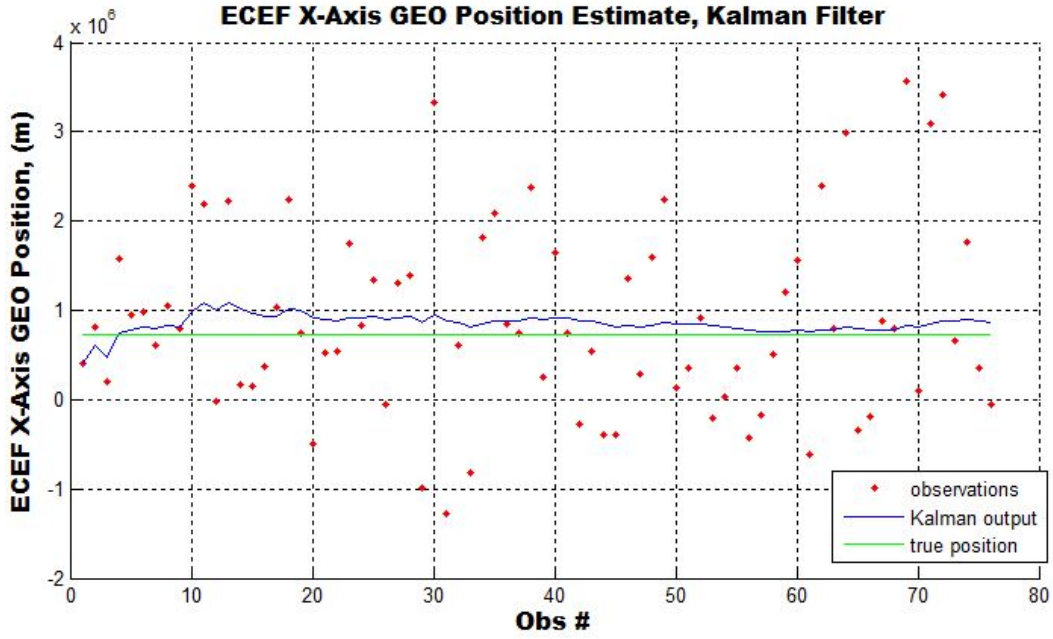


Figure 45: Filtered CubeSat position determination of Galaxy 28 along ECEF X-Axis. Data shown for single beam pass over North America, sampled at 5 seconds/sample, with 2 degrees of attitude knowledge error.

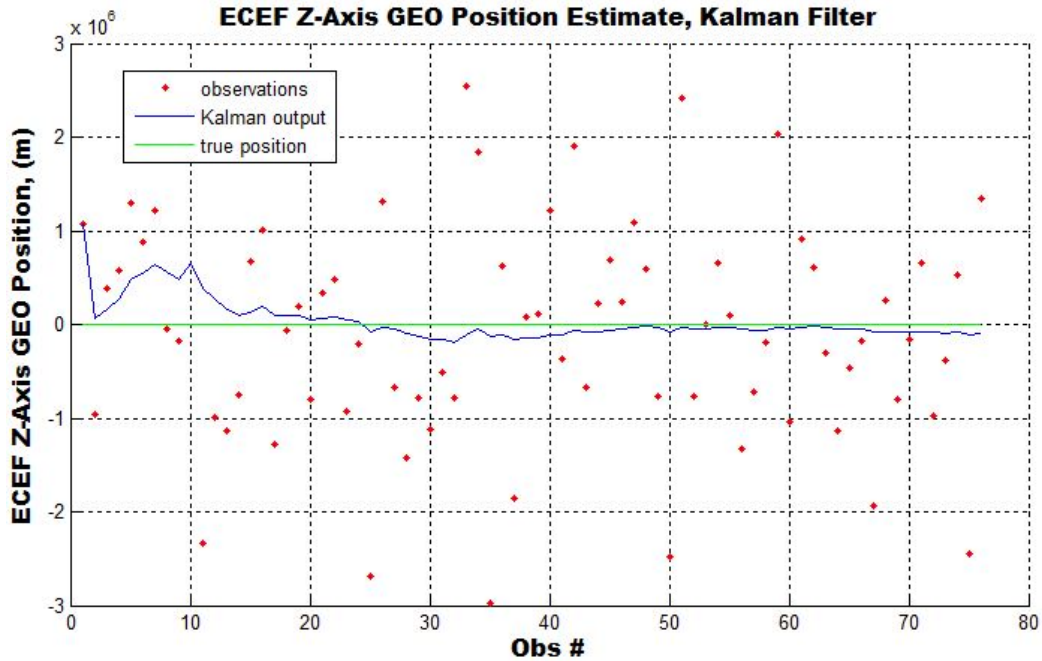


Figure 46: Filtered CubeSat position determination of Galaxy 28 along ECEF Z-Axis. Data shown for single beam pass over North America, sampled at 5 seconds/sample, with 2 degrees of attitude knowledge error.

The filtered data observations shown above yield a steady state GEO-location position estimate, constrained to the GEO orbit, on the order of 100 km error in the ECEF X direction, and a position estimate of approximately 80 km error in the ECEF Z direction. Considering that this estimate came from a single simulated LEO spot beam pass, using a simple, non-calibrated Kalman filter shows promise for completing position determination, and therefore spot beam mapping with reasonable accuracy, using a CubeSat – especially if the Kalman filter were to be tuned.

Given variously sized spot beams, the impact of the GEO position variance shown here works well for the cases studied, specifically mapping spot beams of Ku- and lower frequency bands typical of GEO comm-satellites. However, it is ultimately up to an end user to determine how accurate the edge locations need to be, and to define just what the

edge of a beam's gain pattern actually is. That said, if higher beam edge resolution accuracy is desired over the filtered results, the spot beam map data can take advantage of better statistical filtering to improve the beam edge position knowledge. Tuning and/or expanding the Kalman filter, in addition to adding in more observations from additional look angles will only improve the GEO position estimate. Should that not be enough, additional CubeSat hardware could also be introduced to the ADCS subsystem on board the spot beam mapper, likely in the form of higher accuracy star trackers [51], in order to improve bearing estimate resolution through additional attitude knowledge.

4.11 Summary

Chapter IV displayed the results obtained through the spot beam mapping mission simulation tools, the primary results being the mission goal of a usable ground-based spot beam map obtained within the thresholds set by the mission requirements. It was demonstrated that GPS coordinates obtained within spot beams can be translated to the ground and a ground beam map can be obtained with varying degrees of accuracy depending on how well the position of the source transmitter is known. Additional dependencies for the procurement of an accurate ground-based spot beam map included constellation type, altitude, inclination, payload sampling rate, number of satellites, and GPS accuracy, among others.

The results of selection of different constellation types were shown in comparison to each other, in addition to the effects of changing orbit and configuration parameters. On orbit selection, it was found that there are resonant orbit altitudes for constellations that can produce very unfavorable spot beam maps, and very good spot beam maps, given

the same number of satellites. For best ground-based spot beam map resolution, it was found that transmitter position knowledge must be minimized. If transmitter position determination were to be completed on-board the CubeSat, it was shown that the GEO transmitter position error could be determined on the order of 100km using a simple Kalman filter (un-tuned), under the assumption of 2 deg attitude knowledge on board the CubeSat, with a single LEO pass collecting 75 observation obtained at 5 sec/sample.

Regarding ground beam map accuracy, knowing the GEO satellite's position, for example with 100 km error, it was shown that the corresponding ground map error would be roughly 0.86 km at the sub-satellite point, 1.3 km with 30 degrees slant, and up to 16 km at 60 degrees slant angle. For larger Ku-band spot beams, 0.86 - 16 km on the ground is not bad for determination of beam feature location. For smaller spot beams, 16 km of beam edge accuracy on the ground may or may not be an issue, depending on end user requirements. The next chapter, (Chapter V), presents the conclusions of this work and areas for future work, drawn from the data presented above in Chapter IV.

V. Conclusion

In conclusion, a Spot Beam Mapping CubeSat mission was found to be a possible venture that, if pursued further, could be made to work with modern CubeSat standards. Spot beam mapping with CubeSats offers an active approach that includes global coverage for spot beam mapping when compared with generating spot beam maps from commercial/manufacturer's ground antenna characterization from in-lab measurements. A LEO CubeSat mission also improves upon static ground station spot beam measurements, by mapping entire beam patterns with a single mobile system versus compiling data from multiple static ground receivers. The CubeSat SBM mission allows for mapping global beam patterns at a target frequency, in a relatively quick and efficient manner.

In determining appropriate methods to complete the spot beam mapping mission, four constellation types were studied, including Walker Delta Patterns, Single plane constellations with even spacing, Multiple plane constellations with even spacing (Non-Walker), and Single plane constellations using specific spacing angle formations (i.e. non even separation throughout the orbit plane). Close formations were not analyzed, as bunched up CubeSats would not be able to reduce spot beam map coverage gaps as well as synchronized constellations (avoiding repeating ground tracks) would be able to.

Altitude and inclination had a significant impact on the capability of the spot beam mapping CubeSats to produce an accurate ground-based spot beam map. Certain altitudes, most notably when the constellation was simulated at a resonance altitude near a directly repeating ground track orbit, proved very bad for reduction of gaps in coverage within the spot beam maps. Inclination also impacted spot beam mapping capability. For

global coverage of Earth pointing spot beams, the minimum mission inclination was found to be 68 degrees, either prograde or similarly for retrograde orbits. Direct polar orbits increased the latitude size of coverage gaps immensely, making spot beam map generation useless unless significant data was collected.

All facets considered, although the spot beam mapping scenarios presented did not seek to obtain an optimum solution due to the number of customer specific requirements and constraints that must be present, a feasible spot beam mapping orbit and constellation configuration that yields favorable results for the spot beam mapping mission at the Ku- and Ka- bands, assuming the academic assumptions within this research and minimum desired mappable beam widths of 0.5 degrees has been listed below in Table 16.

Table 16: Favorable spot beam mapping configuration for Ku- and Ka-band spot beam map generation, following with research assumptions and derived requirements.

Feature	Recommended
<i>Payload Band</i>	11GHz – 40 GHz
<i>Payload sampling rate</i>	5 Samples per second
<i>Stored GPS data req'd for 24 hours of nonstop collection:</i>	1.37 Mb Maximum
<i>Constellation / Satellites</i>	6-3-2 Walker
<i>Orbit</i>	68 deg inclined, circular, 450 km
<i>Attitude Knowledge</i>	At least 2 degrees
<i>GPS Position Knowledge</i>	10 m orbital position accuracy at 1Hz
<i>Collection time</i>	24 – 72 hours

When simulated, this particular constellation found every single spot beam within the scenario, tracked the mobile spot beam, was shown to have the smallest coverage gaps when compared to other simulations, and was otherwise successful. If a customer

were to today launch 6 spot beam mapping CubeSats with these parameters in place using the mission requirements developed within this research, the mission would no doubt be able to produce spot beam maps with reasonable accuracy in the Ku- and Ka- bands for target GEO comm-sat spot beams.

It was also determined that the spot beam mapping mission absolutely required decent position knowledge of the transmitters out at GEO if the space-centric beam map generated by the CubeSats were to be translated into a ground-centric beam map accurately. GEO position determination was deemed possible through two methods. The best case method would be to have the position of the transmitter already known. Having the position of the transmitter already known means that the CubeSat SBM would not need to perform a position determination calculation of the GEO transmitter onboard. However, if the locations of the desired transmitters are not known, then the CubeSat SBM mission will need to be supplemented with “GEO” location hardware/software in order to create lines of bearing to the transmitter while flying through the spot beams of said transmitter. Based on historic CubeSat attitude knowledge capability of 1-2 deg, it was estimated, with simple filtering, that a CubeSat could generate lines of bearing to determine position of a GEO transmitter within a 100 km covariance, however it must be noted that this estimate does not yet account for losses in the receiver hardware. If CubeSat capability becomes increased, or if the Kalman filtering process is tuned to the mission, this estimated error covariance will shrink, perhaps significantly.

It was additionally concluded that the constellation’s ability to produce an accurate spot beam map within a short amount of time was impacted by the number of CubeSats used within any given formation. For the 24 hour and 72 hour objective and

thresholds set for this mission, respectively, it was found that one CubeSat was not enough to produce a well-defined ground beam map. Once the number of evenly-spaced CubeSats approached 6 CubeSats, the ability of the constellation to produce a well-defined ground beam map was significant when compared with fewer CubeSat amounts in the constellation.

5.1 Recommendations for Future Work

Future work for the spot beam mapping CubeSat mission would involve taking the simulation tools developed within this research, and using them in conjunction with an optimization method to find the best solution in terms of cost. Some additional assumptions and requirements may need to be established in order to appropriately model cost and key requirement needs, since the spot beam mapping mission remains yet as an academic concept. Therefore, any future tool for optimizing this mission constellation and orbit would probably need to be robust enough to account for requirement changes or needs in terms of cost modeling.

A second area for future study would be the effects of utilizing spot beam signal polarity for beam edge and emitter signature identification purposes. Since spot beam signals from GEO can be polarized in different directions, commonly vertical and horizontal polarizations, paying attention to signal polarity would impact antenna and attitude knowledge requirements. Since this work focused on using total received power differential for beam pattern edge detection, further research would be useful by looking into the effects of beam edge mapping when presented with spot beams of differing polarity at the same target frequencies. Analyzing separate signal polarities of beams

would expand on the spot beam mapping mission's capability, by allowing separate beams within a larger beam pattern to potentially be identified and mapped individually.

Additional future work on the potential spot beam mapping CubeSat mission involves various facets of CubeSat hardware and subsystem design and development. The work that was presented in this research was mission level analysis. It is therefore reasonable that follow on work could continue on with mission concept development at the system and subsystem levels. Generally speaking, an appropriate wideband C/X/K-Band software defined receiver with a CubeSat form factor would need to be identified as a baseline payload for this mission. With payload selection, hardware and subsystems can be designed and/or selected from COTS sources to appropriately facilitate the operations of the primary payload, including ADCS components, computing hardware, power hardware, wire harnessing, and any structural or thermal mitigation components.

Future work with position knowledge of the transmitter remains an area for study as well, as additional capability to perform GEO-based location remains as a black-box capability. Further study into additional, different constellation types and configurations such as eccentric orbits or responsive orbits could provide additional capability or knowledge driving the mission capabilities.

Finally, one last (rather sporting) area for future work would be for somebody to design, build, test, and fly a few spot beam mappers in order to compare on-orbit obtained spot beam maps with the results of the simulations presented in this research.

Appendix A: MATLAB Scripts.

Initialize.m (Generate space-beam map from STK scenario)

```
clc
clear all
close all

% 2d Lt Jake LaSarge
% STK/MATLAB data runs for analysis
```

DISCLAIMERS AND/OR WARNINGS

```
% WARNING! -- The directory where initialize.m is run from *MUST NOT* contain
% ANY files of the type *.csv !!!!!!!! If any CSV files are in the same
% directory as initialize.m, they *WILL* be moved and merged/incorporated
% with the data set, which could yield rather bad consequences for an
% oblivious user.

% This program uses windows' DOS commands to make folders and move csv
% files. USE AT OWN RISK. Although I don't believe this to be too
% dangerous.

% This program uses a loaded STK base scenario w/specified directory

% Program designed with STK 10 and Matlab R2013a
```

USER INPUT SECTION

```
outputflag = 1; % set to 1 if you want the spreadsheets output
stkvisibleflag = 0; %set to 0 if you don't want to see STK

altitude = 400; %km --Input the altitude of the CubeSat SBM constellation --- circular
orbit
inclination = 68; %deg
RA = 0; %deg (Right Ascension)
payload_data_rate = 5; %seconds! How often does the payload take a GPS reading &
produce a line of bearing?
num_planes = 3; %How many CubeSat planes do you want?
num_sats = 2; %number of sats per plane. If only one plane desired, then this is the
total number of sats

even_plane_spacing = true; %Should the planes be evenly spaced?
even_spacing = true; %should the CubeSats in the plane be evenly separated?
walker_offset = true; %are you trying to make this a walker constellation? If so, mark
as true
```

```

if even_plane_spacing == true
    plane_spacing = 180/num_planes; %deg
else
    plane_spacing = 10; %deg -- manually set plane spacing if evenly spaced undesired
end

if even_spacing == true
    sat_spacing = 360/num_sats; %deg

    if num_sats == 1
        sat_spacing = 0; %deg
    end

else
    sat_spacing = 20; %deg -- manually sets spacecraft spacing in-plane
end

```

Fire up STK and load test scenario

```

try
    uiapp = actxGetRunningServer('STK10.application'); %Try connecting to STK, in case
it is already running
catch
    uiapp = actxserver('STK10.application'); %If above attempt fails, start a new
instance of STK
end

root = uiapp.Personality2; %This is needed I guess for some reason --- No idea why.
Also nobody else knows why. But... here it is.

uiapp.Visible = stkvISIBLEflag; %Make STK invisible, if desired.

root.CloseScenario; %Close any active STK Scenarios that might be running.

root.LoadScenario('I:\Thesis_Documents\A5 STK\CubeSatSBM_Base.sc') %Loads my totally rad
CubeSat SBM scenario

root.CurrentScenario.SetTimePeriod('1 Oct 2014 04:00:00.00','4 Oct 2014 04:00:00.00');

```

Adding the Spot Beam Mapping CubeSats to the Scenario

```

missionStartDate= root.CurrentScen.StartTime; %Set the mission start date to the current
scenario start time in STK

ctrstart = 1; %starting the Cubesat SBM numbers at 1. How very typical.

```

```

ctr3 = 0; %this is a separate counter I use to deal with spacing between sats in the same
plane

num_total_sats = num_sats*num_planes; %calculates the total number of satellites
utilizing very basic mathematics.

if walker_offset == true
    phasing = 360/num_total_sats;
end

for plane = 1:1:num_planes %This for loop controls the # of planes

    for ctr = ctrstart:1:num_sats %This for loop controls # of sats in the plane

        %Here we're telling STK to add the new satellite in the current scenario. No
idea what the 18 is there for... just go with it.
        SBM(ctr) = root.CurrentScen.Children.New(18, strcat('SBM', num2str(ctr)));

        IS = SBM(ctr).Propagator.InitialState; %Create handle to the Initial states

        %Input the orbital elements of the newly created spacecrafts (Not stored in
memory currently. If you do want to store this later you'll need to use
vertical concatenating or something to make this into an nx6 matrix)
        COE = [6378.14+altitude, 0, inclination, 0, RA, 0+sat_spacing*ctr3]; %Note my
separate counter in there

        if walker_offset == true && plane >= 2
            COE(6) = COE(6) + (phasing*(plane-1));
        end

        IS.Representation.AssignClassical('eCoordinateSystem1CRF',
COE(1), COE(2), COE(3), COE(4), COE(5), COE(6)); %Telling STK to use the Classical Orbital
Elements

        SBM(ctr).Propagator.StartTime = missionStartDate; % Tell STK to set the orbit
Epoch for the mission start time

        SBM(ctr).Propagator.Propagate %Tell STK to propagate the satellite

        clear COE %This loop overwrites the COE's, so I'm going to clear it here for
safety/test reasons.

        ctr3 = ctr3 + 1; %Advance ctr3

        if ctr >= num_total_sats %yes, its a bit of a hack way to break the 'for' loop,
but it works!
            break
        end %if statement

    end %for loop -- num. sats in plane

```

```

ctrstart = num_sats+1; %set the satellite number at which the next 'for' loop will
start

num_sats = (plane+1) * num_sats; %set the satellite number (out of the overall total)
that the next 'for' loop will need to stop at.

RA = RA + plane_spacing; %set the new Right Asc. for the next 'for' loop run.

ctr3 = 0; %reset counter no. 3 for the next plane.

end % for loop -- num. of planes

```

Identify things that exist in the STK scenario that Matlab doesn't yet know about

```

%Identify in MATLAB my GEO birds which were already in loaded scenario
geobird1 = root.CurrentScen.Children.Item(' GALAXY_28_28702 ');
geobird2 = root.CurrentScen.Children.Item(' GEO_Commsat_II ');

%Identifying the INTELSAT Galaxy 28 Spot Beams in MATLAB
BC_beam = geobird1.Children.Item(' Ku-Band_BC ');
Cali_beam = geobird1.Children.Item(' Ku-Band_Cali ');
CentralUS_beam = geobird1.Children.Item(' Ku-Band_CentralUS ');
E_Argentina_beam = geobird1.Children.Item(' Ku-Band_E_Argentina ');
E_Brazil_beam = geobird1.Children.Item(' Ku-Band_E_Brazil ');
Florida_beam = geobird1.Children.Item(' Ku-Band_Florida ');
Hawaii_beam = geobird1.Children.Item(' Ku-Band_Hawaii ');
NC_Coast_beam = geobird1.Children.Item(' Ku-Band_NC_Coast ');
PuertoRico_beam = geobird1.Children.Item(' Ku-Band_PuertoRico ');
QBC_beam = geobird1.Children.Item(' Ku-Band_QBC ');
RioDJ_beam = geobird1.Children.Item(' Ku-Band_RioDJ ');
Uruguay_beam = geobird1.Children.Item(' Ku-Band_Uruguay ');
West_SA_beam = geobird1.Children.Item(' Ku-Band_West_SA ');

%Identifying the GEO Satellite II beams in MATLAB
Steering_beam = geobird2.Children.Item(' Ka-Band_Steering '); % Note Ka-band
Disappearing_beam = geobird2.Children.Item(' Ka-Band_Disappearing ');
Jumping_beam = geobird2.Children.Item(' Ku-Band_Jumping ');
North_beam = geobird2.Children.Item(' Ku-Band_North ');
Equator_beam = geobird2.Children.Item(' Ku-Band_Equator ');
South_beam = geobird2.Children.Item(' Ku-Band_South ');
FP_beam = geobird2.Children.Item(' Ka-Band_FP ');

```

Produce Access Reports for Analysis

```

%Warning, Nested 'for' loops might get rather brutal, but it works.

root.UnitPreferences.Item(' DateFormat ').SetCurrentUnit(' EpSec '); %Set the time units to
be in Epoch Seconds

```

```

scen = root.CurrentScen; %Define the scenario as a variable (for ease of use later)

if outputflag == 1 %If we want the output, do the following

%create new directory called "Beam_map" where the LLA data sets go
dos('MD Beam_map');

%create new directory where flythrough LLA data sets go, for each GEO bird
dos('MD Galaxy28');
dos('MD GEO_Commsat_II');

%For each SBM Cubesat...
for ctr2 = 1:1:num_total_sats

    %Get STK to recognize access to Galaxy 28 Spot Beams
    access(1) = SBM(ctr2).GetAccessToObj ect(BC_beam); %This is inside the 'for' loop...
    so it is overwriting itself for each CubeSat. Do use caution...
    access(2) = SBM(ctr2).GetAccessToObj ect(Cali_beam);
    access(3) = SBM(ctr2).GetAccessToObj ect(Central_US_beam);
    access(4) = SBM(ctr2).GetAccessToObj ect(E_Ar genti na_beam);
    access(5) = SBM(ctr2).GetAccessToObj ect(E_Brazi l_beam);
    access(6) = SBM(ctr2).GetAccessToObj ect(Fl ori da_beam);
    access(7) = SBM(ctr2).GetAccessToObj ect(Hawai i_beam);
    access(8) = SBM(ctr2).GetAccessToObj ect(NC_Coast_beam);
    access(9) = SBM(ctr2).GetAccessToObj ect(PuertoRi co_beam);
    access(10) = SBM(ctr2).GetAccessToObj ect(QBC_beam);
    access(11) = SBM(ctr2).GetAccessToObj ect(Ri oDJ_beam);
    access(12) = SBM(ctr2).GetAccessToObj ect(Uruguay_beam);
    access(13) = SBM(ctr2).GetAccessToObj ect(West_SA_beam);

    %The next beams are from GEO_Commsat_II
    access(14) = SBM(ctr2).GetAccessToObj ect(Steering_beam);
    access(15) = SBM(ctr2).GetAccessToObj ect(Di sappeari ng_beam);
    access(16) = SBM(ctr2).GetAccessToObj ect(Jumpi ng_beam);
    access(17) = SBM(ctr2).GetAccessToObj ect(North_beam);
    access(18) = SBM(ctr2).GetAccessToObj ect(Equator_beam);
    access(19) = SBM(ctr2).GetAccessToObj ect(South_beam);
    access(20) = SBM(ctr2).GetAccessToObj ect(FP_beam);

    %For Each Spot Beam Access Report...
    for ctr4 = 1:1:20 %This is inside the main 'for' loop... so the information contained
    is overwriting itself for each CubeSat. Do use caution...

        access(ctr4).ComputeAccess; %Compute Access for the selected beam

        %Initialize the STK Data Provider for the access of the selected beam
        A_DP(ctr4) = access(ctr4).DataProviders.Item('Access Data').Exec(scen.StartTime,
scen.StopTime);

        %Store (in a Matlab Mtrx) the data I desire from STK's 'Access Data'
        try %I'm using a 'try' command here, since on rare occasion STK data is defective

```

and crashes matlab. Thus if I get a defective STK data point, it will not obliterate matlab calculations

```

        beaminfo_out(:, 1) =
cell2mat(A_DP(ctr4).DataSets.GetDataSetByName('Duration').GetValues);
        beaminfo_out(:, 2) = cell2mat(A_DP(ctr4).DataSets.GetDataSetByName('From
Start Lat').GetValues);
        beaminfo_out(:, 3) = cell2mat(A_DP(ctr4).DataSets.GetDataSetByName('From
Start Lon').GetValues);
        beaminfo_out(:, 4) = cell2mat(A_DP(ctr4).DataSets.GetDataSetByName('From Stop
Lat').GetValues);
        beaminfo_out(:, 5) = cell2mat(A_DP(ctr4).DataSets.GetDataSetByName('From Stop
Lon').GetValues);
        beaminfo_out(:, 6) = cell2mat(A_DP(ctr4).DataSets.GetDataSetByName('Start
Time').GetValues);
        beaminfo_out(:, 7) = cell2mat(A_DP(ctr4).DataSets.GetDataSetByName('Stop
Time').GetValues);
    catch % so... if I have a defective data point from STK, set all the values to
zero. (i.e. lat/lon/time etc will all be set to zero for this defective data point)
        beaminfo_out(:, 1) = 0;
        beaminfo_out(:, 2) = 0;
        beaminfo_out(:, 3) = 0;
        beaminfo_out(:, 4) = 0;
        beaminfo_out(:, 5) = 0;
        beaminfo_out(:, 6) = 0;
        beaminfo_out(:, 7) = 0;
    end %try

    csvwrite(strcat('SBM', num2str(ctr2), '_BEAM', num2str(ctr4), '.csv'), beaminfo_out);

    %Move the .csv file just created into the Beam_map folder
    dos('move *.csv I:\Thesis_Documents\A4_MATLAB\A1_Thesis_Code\Beam_map\');

    %NEXT SECTION OUTPUTS GEO-LOCATION INFORMATION FOR LINES OF BEARING
    %-----

    % For each spot beam flythrough...
    for ctr5 = 1:length(beaminfo_out(:, 6))

        %Initialize the Data Provider for the SBM CubeSat(s)
        SatDP = SBM(ctr2).DataProviders.Item('LLA
State').Group.Item('Fixed').ExecElements(beaminfo_out(ctr5, 6), beaminfo_out(ctr5, 7), payload_data_rate, {'Time'; 'Alt'; 'Lat'; 'Lon'});

        %Store the info/data called from STK in a Matlab Matrix
        GPS_data_out(:, 1) =
cell2mat(SatDP.DataSets.GetDataSetByName('Time').GetValues);
        GPS_data_out(:, 2) =
cell2mat(SatDP.DataSets.GetDataSetByName('Lat').GetValues);
        GPS_data_out(:, 3) =
cell2mat(SatDP.DataSets.GetDataSetByName('Lon').GetValues);
        GPS_data_out(:, 4) =

```

```

cell2mat(SatDP.DataSets.GetDataSetByName('Alt').GetValues);

    %Print that data as a CSV

csvwrite(strcat('GPS_DATA_SBM', num2str(ctr2), '_BEAM', num2str(ctr4), '_PASS', num2str(ctr5),
'.csv'), GPS_data_out);

    clear GPS_data_out

end %flythrough # (ctr5)
clear SatDP

if ctr4 < 14
    dos('move *.csv I:\Thesis_Documents\A4_MATLAB\A1_Thesis_Code\Galaxy28');
else
    dos('move *.csv
I:\Thesis_Documents\A4_MATLAB\A1_Thesis_Code\GEO_Commsat_II');
end

clear beaminfo_out

end %beam # (ctr4)
clear A_DP
clear access

end %sat # (ctr2)

```

Merge created CSV files

```

cd('Beam_map');

dos('copy *.csv beam_map.csv');
dos('move beam_map.csv I:\Thesis_Documents\A4_MATLAB\A1_Thesis_Code');

cd ../;
cd('Galaxy28');

dos('copy *.csv Galaxy28.csv');
dos('move Galaxy28.csv I:\Thesis_Documents\A4_MATLAB\A1_Thesis_Code');

cd ../;
cd('GEO_Commsat_II');

dos('copy *.csv GEO_Commsat_II.csv');
dos('move GEO_Commsat_II.csv I:\Thesis_Documents\A4_MATLAB\A1_Thesis_Code');

cd ../;

end %output flag 'IF'

```

Compute CubeSat Lifetimes Using STK's Lifetime Tool

```
diary('Lifetime_Information');
diary on %Lifetime information should be saved to a file for later viewing.
% Short Case - 12 kg (Fully Loaded 6U)
root.ExecuteCommand('SetLifetime */Satellite/SBMI DragCoeff 2.2');
root.ExecuteCommand('SetLifetime */Satellite/SBMI ReflectCoeff 1.0');
root.ExecuteCommand('SetLifetime */Satellite/SBMI DragArea 0.06');
root.ExecuteCommand('SetLifetime */Satellite/SBMI SunArea 0.06');
root.ExecuteCommand('SetLifetime */Satellite/SBMI Mass 12');
root.ExecuteCommand('SetLifetime */Satellite/SBMI DensityModel MSIS2000');
root.ExecuteCommand('SetLifetime */Satellite/SBMI OrbitLimit 140000');
lifetime_block = root.ExecuteCommand('Lifetime */Satellite/SBMI');
lifetime_out_short = lifetime_block.Item(0) %This displays the lifetime tool result.

% Intermediate (Grav Gradient) Case - 12 kg
root.ExecuteCommand('SetLifetime */Satellite/SBMI DragCoeff 2.2');
root.ExecuteCommand('SetLifetime */Satellite/SBMI ReflectCoeff 1.0');
root.ExecuteCommand('SetLifetime */Satellite/SBMI DragArea 0.03');
root.ExecuteCommand('SetLifetime */Satellite/SBMI SunArea 0.03');
root.ExecuteCommand('SetLifetime */Satellite/SBMI Mass 12');
root.ExecuteCommand('SetLifetime */Satellite/SBMI DensityModel MSIS2000');
root.ExecuteCommand('SetLifetime */Satellite/SBMI OrbitLimit 140000');
lifetime_block2 = root.ExecuteCommand('Lifetime */Satellite/SBMI');
lifetime_out_intermediate = lifetime_block2.Item(0) %This displays the lifetime tool
result.

%Long Case - 12 kg
root.ExecuteCommand('SetLifetime */Satellite/SBMI DragCoeff 2.2');
root.ExecuteCommand('SetLifetime */Satellite/SBMI ReflectCoeff 1.0');
root.ExecuteCommand('SetLifetime */Satellite/SBMI DragArea 0.02');
root.ExecuteCommand('SetLifetime */Satellite/SBMI SunArea 0.02');
root.ExecuteCommand('SetLifetime */Satellite/SBMI Mass 12');
root.ExecuteCommand('SetLifetime */Satellite/SBMI DensityModel MSIS2000');
root.ExecuteCommand('SetLifetime */Satellite/SBMI OrbitLimit 140000');
lifetime_block3 = root.ExecuteCommand('Lifetime */Satellite/SBMI');
lifetime_out_long = lifetime_block3.Item(0) %This displays the lifetime tool result.

% Short Case - 6kg
root.ExecuteCommand('SetLifetime */Satellite/SBMI DragCoeff 2.2');
root.ExecuteCommand('SetLifetime */Satellite/SBMI ReflectCoeff 1.0');
root.ExecuteCommand('SetLifetime */Satellite/SBMI DragArea 0.06');
root.ExecuteCommand('SetLifetime */Satellite/SBMI SunArea 0.06');
root.ExecuteCommand('SetLifetime */Satellite/SBMI Mass 6');
root.ExecuteCommand('SetLifetime */Satellite/SBMI DensityModel MSIS2000');
root.ExecuteCommand('SetLifetime */Satellite/SBMI OrbitLimit 140000');
lifetime_block4 = root.ExecuteCommand('Lifetime */Satellite/SBMI');
lifetime_out_short_light = lifetime_block4.Item(0) %This displays the lifetime tool
result.
```

```

% Intermediate (Grav Gradient) Case - 6kg
root.ExecuteCommand('SetLifetime */Satellite/SBMI DragCoeff 2.2');
root.ExecuteCommand('SetLifetime */Satellite/SBMI ReflectCoeff 1.0');
root.ExecuteCommand('SetLifetime */Satellite/SBMI DragArea 0.03');
root.ExecuteCommand('SetLifetime */Satellite/SBMI SunArea 0.03');
root.ExecuteCommand('SetLifetime */Satellite/SBMI Mass 6');
root.ExecuteCommand('SetLifetime */Satellite/SBMI DensityModel MSIS2000');
root.ExecuteCommand('SetLifetime */Satellite/SBMI OrbitLimit 140000');
lifetime_block5 = root.ExecuteCommand('Lifetime */Satellite/SBMI');
lifetime_out_intermediate_light = lifetime_block5.Item(0) %This displays the lifetime
tool result.

%Long Case - 6kg
root.ExecuteCommand('SetLifetime */Satellite/SBMI DragCoeff 2.2');
root.ExecuteCommand('SetLifetime */Satellite/SBMI ReflectCoeff 1.0');
root.ExecuteCommand('SetLifetime */Satellite/SBMI DragArea 0.02');
root.ExecuteCommand('SetLifetime */Satellite/SBMI SunArea 0.02');
root.ExecuteCommand('SetLifetime */Satellite/SBMI Mass 6');
root.ExecuteCommand('SetLifetime */Satellite/SBMI DensityModel MSIS2000');
root.ExecuteCommand('SetLifetime */Satellite/SBMI OrbitLimit 140000');
lifetime_block6 = root.ExecuteCommand('Lifetime */Satellite/SBMI');
lifetime_out_long_light = lifetime_block6.Item(0) %This displays the lifetime tool
result.

diary off

%G28_Beam_Maps

```

Commands I learned from AGI STK Video (sample variables included in there!)

```

% scenario = root.Children.New('eScenario', 'DIY_MATLAB') [[Create New]]

% root.ExecuteCommand('Animate * Reset') [[[ restarts scenario ]]]

% facility = scenario.Children.New('eFacility', 'Groundsite')
% facility.Position.AssignGeodetic(50, -100, 0)

% satellite = scenario.Children.New('eSatellite', 'LEOSat')
% satellite.Propagator.Propagate

% WARNING, SYNTAX ERROR IN NEXT LINE SOMEWHERE -- I MAY HAVE COPIED SOMETHING SLIGHTLY
% WRONG-ISH!!!!!!!!!!!!!!!!!!!!!!
% cmd = ['SetState */Satellite/LEOSat Classical TwoBody "', scenario.StartTime, '"
"', scenario.StopTime, '" 60 ICRF "', scenario.StartTime, '" 720000 0 90 0 0 0']
% root.ExecuteCommand(cmd)

% access = satellite.GetAccessToObject( facility )
% access.ComputeAccess;

```

```

% accessDP = access.DataProviders.Item(' Access
Data' ). Exec(scenario.StartTime, scenario.StopTime)

% accessStartTimes = accessDP.DataSets.GetDataSetByName(' Start Time' ). GetValues

% SatelliteDP = satellite.DataProviders.Item(' LLA
State' ). Group.Item(' Fixed' ). ExecElements(scenario.StartTime, scenario.StopTime, 60,
{ ' Time' ; ' Alt' })

% satelliteAltitude = SatelliteDP.DataSets.GetDataSetByName(' Alt' ). GetValues

%Alternatively... (i.e. this one is better)
% satelliteAltitude = cell2mat(SatelliteDP.DataSets.GetDataSetByName(' Alt' ). GetValues)

% SatelliteDP.DataSets.ElementNames

```

Published with MATLAB® R2013a

G28_Beam_Maps.m (Generate Ground-Beam Maps for Analysis)

```
clear; clc; close all;
```

Flags

```
tic
% 1 = on
% 0 = off
flag.spacemap = 1;
flag.space2groundmap = 1;
flag.space2groundmap3D = 1;
flag.groundmap = 1;
flag.rawdatamaps = 1;
```

Parameters

```
%Transmitter location
Tx.lat = 0;      %Latitude (degrees) AFIT: 39.782
Tx.lon = -89;    %Longitude (degrees) AFIT: -84.083  GCS_II = -151, G28 = -89

Tx2.lat = 0;
Tx2.lon = -151;

Tx.alt = 35786000; %m

Earth.R = 6378000; %m

SC.xError = 0; %m --- accuracy to which the spacecraft knows its position. (i.e. what's
the GPS position error?)
TX.xError = 0; %m --- accuracy to which we know the position of the transmitter.
```

Import STK

```
%ECEF transmitter location
%[Tx.x, Tx.y, Tx.z] = geodetic2ecef(Tx.lat*pi/180, Tx.lon*pi/180, Tx.alt, Earth);

%Import edges

[GPS.duration, GPS.startlat, GPS.startlon, GPS.stopl原因, GPS.stopl原因, GPS.starttime,
GPS.stoptime] = importBeam_map('beam_map.csv');

%Import Galaxy 28 Flythrough Data
[G28.time, G28.lat, G28.lon, G28.alt] = importSTK('Galaxy28.csv');
```

```

G28.alt = G28.alt * 1000; %CONVERT Km to METERS

%Import GEO_COMMSAT_II Flythrough Data
% [GCII.time, GCII.lat, GCII.lon, GCII.alt] = importSTK('GEO_Commsat_II.csv');
load coast %for figures -- load the feature that adds in coastlines.
if flag.spacemap == 1
    figure

    xlim([-180 180])
    ylim([-90 90])
    grid on
    hold on
    plot(GPS.startlon, GPS.startlat, 'k.')
    plot(GPS.stoplon, GPS.stoplat, 'k.')
    plot(Tx.lon, Tx.lat, 'g*')
    plot(Tx2.lon, Tx2.lat, 'b*')
    plot(long, lat, 'k')
    title('Lat/Lon/Alt spot beam "edge" raw data points as recorded by spacecraft')
    xlabel('Earth Longitude, (deg)')
    ylabel('Earth Latitude, (deg)')
    legend('Beam Entrance Point', 'Beam Exit Point', 'Galaxy 28 Position', 'G-II
Position', 'Location', 'northeast')
end

```

Compute ground map from space points

```

if flag.space2groundmap == 1
    %galaxy28groundmap

    %Convert LLA points to ECEF points
    TX_ECEF = lla2ecef([Tx.lat, Tx.lon, Tx.alt], 'WGS84');
    ECEF = lla2ecef([G28.lat, G28.lon, G28.alt], 'WGS84');

    %Add in GPS sensor noise
    ECEF(:, 1) = ECEF(:, 1) + SC.xError * randn(size(ECEF(:, 1)));
    ECEF(:, 2) = ECEF(:, 2) + SC.xError * randn(size(ECEF(:, 2)));
    ECEF(:, 3) = ECEF(:, 3) + SC.xError * randn(size(ECEF(:, 3)));
    [G28.LLA_noisy] = ecef2lla([ECEF(:, 1), ECEF(:, 2), ECEF(:, 3)]);

    %Add in position knowledge of the transmitter.
    TX_ECEF(:, 1) = TX_ECEF(:, 1) + TX.xError * randn(size(TX_ECEF(:, 1)));
    TX_ECEF(:, 2) = TX_ECEF(:, 2) + TX.xError * randn(size(TX_ECEF(:, 2)));
    TX_ECEF(:, 3) = TX_ECEF(:, 3) + TX.xError * randn(size(TX_ECEF(:, 3)));
    [Tx.LLA_noisy] = ecef2lla([TX_ECEF(:, 1), TX_ECEF(:, 2), TX_ECEF(:, 3)]);

    %Rotation R3 about 3 by x-mitter (G28) longitude (i.e. -89deg)
    R3 = [cosd(89), -sind(89), 0; sind(89), cosd(89), 0; 0, 0, 1];

```

```

%Rotate and apply R3 to matrices
TX_ECEF_Mod = R3 * TX_ECEF';
ECEF_Mod = R3 * ECEF';

%transpose matrices back to the way they were
TX_ECEF_Mod = TX_ECEF_Mod';
ECEF_Mod = ECEF_Mod';

%Glorious amounts of trig and vector math to find delta lat/lon. Brace yourself.

P1 = [0,0,0];
norm_cs = [0,1,0]; %normal vector of 31 plane of coordinate systems

%compute rotation angle of the plane defined by GPS pt and Txmitter
P2 = [ECEF_Mod(:,1), ECEF_Mod(:,2), ECEF_Mod(:,3)];
P3 = [TX_ECEF_Mod(1), TX_ECEF_Mod(2), TX_ECEF_Mod(3)];

normmv = cross(P2, repmat(P3, size(P2,1),1)); %that 'repmat' command is rather nice.
computing normal vectors here

dotp1 = dot(normmv', repmat(norm_cs, size(normmv,1),1)'); %dot products
dotp1 = dotp1'; %rotate to column vector

L1 = norm(TX_ECEF_Mod); %length of major triangle hypotenuse (constant... dist. from
centre of earth to GEO bird)

for ctr = 1:length(ECEF)
    psi = acosd(dotp1(ctr) / (norm(normmv(ctr,:))*norm(norm_cs)));

    %normal vector quadrant checking...
    if normmv(ctr,3) >= 0 && normmv(ctr,2) >= 0
        psi = 360 - psi;
    elseif normmv(ctr,3) >= 0 && normmv(ctr,2) < 0
        psi = 360 - psi;
    elseif normmv(ctr,3) < 0 && normmv(ctr,2) < 0
        psi = psi;
    elseif normmv(ctr,3) < 0 && normmv(ctr,2) >= 0
        psi = psi;
    else
        psi = inf;
    end

    R1 = [1 0 0; 0 cosd(psi) -sind(psi); 0 sind(psi) cosd(psi)]; %plug angle in to
the R1 rot. matrix

    ECEF_Mod2 = (R1 * ECEF_Mod(ctr,:))';

    L2 = sqrt(abs(ECEF_Mod2(1))^2 + abs(ECEF_Mod2(2))^2 + abs(ECEF_Mod2(3))^2); %the
short side of the major triangle

```

```

L3 = pdist([TX_ECEF_Mod; ECEF_Mod2]); %The not-hypotenuse long-ish side

%Law of cosines to find angles.
%A1 = acosd((L1^2 - L2^2 - L3^2)/(-2*L2*L3));
A2 = acosd((L2^2 - L1^2 - L3^2)/(-2*L1*L3));
%A3 = acosd((L3^2 - L1^2 - L2^2)/(-2*L1*L2));

L2_F = Earth.R; %apply surface of earth constraint
A1_F = asind((sind(A2)/L2_F)*L1); %Get angle A1 of the major triangle

%Double solution check for law of sines... applying "obtuse angle only"
constraint.
if A1_F < 90
    A1_F = 180 - A1_F;
end

A3_F = 180 - A1_F - A2; %A3_F is the new combined Lat/Lon angle I want

L1_F = L2_F * cosd(A3_F); % L1_F => Right triangle 'X' component
L3_F = L2_F * sind(A3_F); % L3_F => Right triangle 'Z' component (up)

Coord(ctr,:) = (R3' * (R1' * [L1_F; 0; L3_F]))';
if isreal(Coord(ctr,:)) == 1
    LLACoord(ctr,:) = ecef2lla(Coord(ctr,:), 'WGS84');
else
    LLACoord(ctr,:) = [0, 0, 0]; %throws out 'bad' points
end

end
toc

figure

xlim([-180 180])
ylim([-90 90])
grid on
hold on
plot(LLACoord(:, 2), LLACoord(:, 1), 'k.')
plot(G28.LLA_noi sy(:, 2), G28.LLA_noi sy(:, 1), 'b.')
plot(Tx.LLA_noi sy(2), Tx.LLA_noi sy(1), 'g*')
plot(long, lat, 'k') %plot the coastlines
title('G-28 Lat/Lon/Alt spot beam raw data points overlaid with derived ground-based
map')
xlabel('Earth Longitude, (deg)')
ylabel('Earth Latitude, (deg)')
legend('Derived Ground Lat/Lon Point', 'Space raw data LLA point', 'G-28
Position', 'Location', 'northeast')

```

```

if flag.space2groundmap3D == 1
    h = figure('Color','w');
    JFrame = get(handle(h), 'JavaFrame'); % get the javahandle so we can use java
    commands to manipulate the window
    drawnow % force draw so that there is something to maximize on the next line...
    set(JFrame, 'Maximized', true) % maximize it via the javahandle
    axis off
    axis square
    axis vis3d
    rotate3d on
    set(h, 'ToolBar', 'figure')
    hold on

    %Earth
    [x, y, z] = sphere(36); % 36x36 sphere = 10deg Longitude grid
    % apply the Earth surface image to the RE-diameter sphere
    x = Earth.R*x;
    y = Earth.R*y;
    z = -Earth.R*z;

    hEarth =
surface(x, y, z, 'FaceColor', 'texture', 'CData', imread('earth.jpg'), 'LineStyle', 'none');
    alpha(hEarth, .99)
    clear x y z
%     line([0 1.2*Earth.MeanRadius], [0 0], [0 0], 'Color', 'r');
%     line([0 0], [0 1.2*Earth.MeanRadius], [0 0], 'Color', 'g');
%     line([0 0], [0 0], [0 1.2*Earth.MeanRadius], 'Color', 'b');

%plot3(TX_ECEF(1), TX_ECEF(2), TX_ECEF(3), 'Marker', 'x', 'MarkerEdgeColor', 'y', 'MarkerFaceCol
or', 'y', 'MarkerSize', 10)
    plot3(ECEF(:, 1), ECEF(:, 2), ECEF(:, 3), 'ro')
    plot3(Coord(:, 1), Coord(:, 2), Coord(:, 3), 'yo')
    view(-25, 10)

end

end

if flag.rawdatamaps == 1
    figure

    xlim([-180 180])
    ylim([-90 90])
    grid on
    hold on
    plot(G28.lon, G28.lat, 'b.')
    plot(Tx.lon, Tx.lat, 'g*')

```

```

%plot(Tx2.lon,Tx2.lat,'b*')
plot(long,lat,'k')
title('G-28 space-based spot beam map')
xlabel('Earth Longitude, (deg)')
ylabel('Earth Latitude, (deg)')
legend('Space collected (GPS) LLA point','Galaxy 28 Position','Location','northwest')
hold off

figure

xlim([-180 180])
ylim([-90 90])
grid on
hold on
plot(LLACoord(:,2),LLACoord(:,1),'k.')
plot(Tx.lon,Tx.lat,'g*')
%plot(Tx2.lon,Tx2.lat,'b*')
plot(long,lat,'k')
title('G-28 ground-based spot beam map')
xlabel('Earth Longitude, (deg)')
ylabel('Earth Latitude, (deg)')
legend('Ground LLA point','Galaxy 28 Position','Location','northwest')
hold off

%   figure   (GC_II)
%
%   xlim([-180 180])
%   ylim([-90 90])
%   grid on
%   hold on
%   plot(GCII.lon, GCII.lat,'k.')
%   plot(Tx.lon,Tx.lat,'g*')
%   plot(Tx2.lon,Tx2.lat,'r*')
%   hold off
end

```

Published with MATLAB® R2013a

GCI Beam_Maps.m (Generate Ground-Beam Maps for Analysis)

```
clear; clc; close all;
```

Flags

```
tic
% 1 = on
% 0 = off

flag.spacemap = 1;
flag.space2groundmap = 1;
flag.space2groundmap3D = 1;
flag.groundmap = 1;
flag.rawdatamaps = 1;
```

Parameters

```
%Transmitter location
Tx.lat = 0;      %Latitude (degrees) AFIT: 39.782
Tx.lon = -89;    %Longitude (degrees) AFIT: -84.083  GCS_II = -151, G28 = -89

Tx2.lat = 0;
Tx2.lon = -151;

Tx.alt = 35786000; %m

Earth.R = 6378000; %m
```

Import STK

```
%ECEF transmitter location
%[Tx.x, Tx.y, Tx.z] = geodetic2ecef(Tx.lat*pi/180, Tx.lon*pi/180, Tx.alt, Earth);

%Import edges

[GPS.duration, GPS.startlat, GPS.startlon, GPS.stopl原因, GPS.stopl原因, GPS.starttime,
GPS.stoptime] = importBeam_map('beam_map.csv');

%Import Galaxy 28 Flythrough Data
[G28.time, G28.lat, G28.lon, G28.alt] = importSTK('Galaxy28.csv');
G28.alt = G28.alt * 1000; %CONVERT Km to METERS

%Import GEO_COMSAT_II Flythrough Data
```

```

[GCIi.time, GCIi.lat, GCIi.lon, GCIi.alt] = importSTK('GEO_Commsat_II.csv');
GCIi.alt = GCIi.alt * 1000;

% Move points > 0 longitude by 360 degrees for ease of plotting.
for check = 1:length(GPS.startlat)
    if GPS.startlon(check) > 0
        GPS.startlon(check) = GPS.startlon(check) - 360;
    end
    if GPS.stopl lon(check) > 0
        GPS.stopl on(check) = GPS.stopl on(check) - 360;
    end
end

for check2 = 1:length(G28.lon)
    if G28.lon(check2) > 0
        G28.lon(check2) = G28.lon(check2) - 360;
    end
end

for check3 = 1:length(GCIi.lon)
    if GCIi.lon(check3) > 0
        GCIi.lon(check3) = GCIi.lon(check3) - 360;
    end
end

load coast %for coastline generation in the figures

if flag.spacemap == 1
    figure

    xlim([-360 0])
    ylim([-90 90])
    grid on
    hold on
    plot(GPS.startlon, GPS.startlat, 'k.')
    plot(GPS.stopl on, GPS.stopl at, 'k.')
    plot(Tx.lon, Tx.lat, 'g*')
    plot(Tx2.lon, Tx2.lat, 'b*')
    plot(long, lat, 'k')
    plot(long-360, lat, 'k')
    title('Lat/Lon/Alt spot beam "edge" raw data points as recorded by spacecraft')
    xlabel('Earth Longitude, (deg)')
    ylabel('Earth Latitude, (deg)')
    legend('Beam Entrance Point', 'Beam Exit Point', 'Galaxy 28 Position', 'G-II
Position', 'Location', 'northwest')
end

```

Compute ground map from space points

```
if flag.space2groundmap == 1
    %galaxy2groundmap

    TX_ECEF = ll2ecef([Tx2.lat, Tx2.lon, Tx.alt], 'WGS84');
    ECEF = ll2ecef([GCII.lat, GCII.lon, GCII.alt], 'WGS84');

    %Rotation R3 about 3 by x-mitter (G28) longitude (i.e. -89deg)
    R3 = [cosd(151), -sind(151), 0; sind(151), cosd(151), 0; 0, 0, 1];

    %Rotate and apply R3 to matrices
    TX_ECEF_Mod = R3 * TX_ECEF';
    ECEF_Mod = R3 * ECEF';

    %transpose matrices back to the way they were
    TX_ECEF_Mod = TX_ECEF_Mod';
    ECEF_Mod = ECEF_Mod';

    %Glorious amounts of trig and vector math to find delta lat/lon. Brace yourself.

    P1 = [0, 0, 0];
    norm_cs = [0, 1, 0]; %normal vector of 31 plane of coordinate systems

    %compute rotation angle of the plane defined by GPS pt and Txmitter
    P2 = [ECEF_Mod(:, 1), ECEF_Mod(:, 2), ECEF_Mod(:, 3)];
    P3 = [TX_ECEF_Mod(1), TX_ECEF_Mod(2), TX_ECEF_Mod(3)];

    normv = cross(P2, repmat(P3, size(P2, 1), 1)); %that 'repmat' command is rather nice.
    computing normal vectors here

    dotp1 = dot(normv', repmat(norm_cs, size(normv, 1), 1)); %dot products
    dotp1 = dotp1'; %rotate to column vector

    L1 = norm(TX_ECEF_Mod); %length of major triangle hypotenuse (constant... dist. from
    centre of earth to GEO bird)

    for ctr = 1:length(ECEF)
        psi = acosd(dotp1(ctr) / (norm(normv(ctr, :))*norm(norm_cs)));

        %normal vector quadrant checking...
        if normv(ctr, 3) >= 0 && normv(ctr, 2) >= 0
            psi = 360 - psi;
        elseif normv(ctr, 3) >= 0 && normv(ctr, 2) < 0
            psi = 360 - psi;
        elseif normv(ctr, 3) < 0 && normv(ctr, 2) < 0
            psi = psi;
        elseif normv(ctr, 3) < 0 && normv(ctr, 2) >= 0
```

```

        psi = psi;
    else
        psi = inf;
    end

    R1 = [1 0 0; 0 cosd(psi) -sind(psi); 0 sind(psi) cosd(psi)]; %plug angle in to
the R1 rot. matrix

    ECEF_Mod2 = (R1 * ECEF_Mod(ctr,:))' ;

    L2 = sqrt(abs(ECEF_Mod2(1))^2 + abs(ECEF_Mod2(2))^2 + abs(ECEF_Mod2(3))^2); %the
short side of the major triangle
    L3 = pdist([TX_ECEF_Mod; ECEF_Mod2]); %The not-hypotenuse long-ish side

    %Law of cosines to find angles.
    %A1 = acosd((L1^2 - L2^2 - L3^2)/(-2*L2*L3));
    A2 = acosd((L2^2 - L1^2 - L3^2)/(-2*L1*L3));
    %A3 = acosd((L3^2 - L1^2 - L2^2)/(-2*L1*L2));

    L2_F = Earth.R; %apply surface of earth constraint
    A1_F = asind((sind(A2)/L2_F)*L1); %Get angle A1 of the major triangle

    %Double solution check for law of sines... applying "obtuse angle only"
constraint.
    if A1_F < 90
        A1_F = 180 - A1_F;
    end

    A3_F = 180 - A1_F - A2; %A3_F is the new combined Lat/Lon angle I want

    L1_F = L2_F * cosd(A3_F); % L1_F => Right triangle 'X' component
    L3_F = L2_F * sind(A3_F); % L3_F => Right triangle 'Z' component (up)

    Coord(ctr,:) = (R3' * (R1' * [L1_F; 0; L3_F]))';
    if isreal(Coord(ctr,:)) == 1
        LLACoord(ctr,:) = ecef2lla(Coord(ctr,:), 'WGS84');
    else
        LLACoord(ctr,:) = [0,0,0]; %throws out 'bad' points
    end

end

toc

figure

for check4 = 1:length(LLACoord(:,2))
    if LLACoord(check4,2) > 0
        LLACoord(check4,2) = LLACoord(check4,2) - 360;
    end
end
end

```

```

xlim([-360 0])
ylim([-90 90])
grid on
hold on
plot(LLACoord(:, 2), LLACoord(:, 1), 'k.')
plot(GCII.Lon, GCII.Lat, 'b.')
plot(Tx2.Lon, Tx2.Lat, 'g*')
plot(long, lat, 'k')
plot(long-360, lat, 'k')
title('G-II Lat/Lon/Alt spot beam raw data points overlaid with derived ground-based
map')
xlabel('Earth Longitude, (deg)')
ylabel('Earth Latitude, (deg)')
legend('Derived Ground Lat/Lon Point', 'Space raw data LLA point', 'G-II
Position', 'Location', 'northwest')

if flag.space2groundmap3D == 1
    h = figure('Color', 'w');
    jFrame = get(handle(h), 'JavaFrame'); % get the javahandle so we can use java
commands to manipulate the window
    drawnow % force draw so that there is something to maximize on the next line...
    set(jFrame, 'Maximized', true) % maximize it via the javahandle
    axis off
    axis square
    axis vis3d
    rotate3d on
    set(h, 'ToolBar', 'figure')
    hold on

    %Earth
    [x, y, z] = sphere(36); % 36x36 sphere = 10deg Longitude grid
    % apply the Earth surface image to the RE-diameter sphere
    x = Earth.R*x;
    y = Earth.R*y;
    z = -Earth.R*z;

    hEarth =
surface(x, y, z, 'FaceColor', 'texture', 'CData', imread('earth.jpg'), 'LineStyle', 'none');
    alpha(hEarth, .99)
    clear x y z
%     line([0 1.2*Earth.MeanRadius], [0 0], [0 0], 'Color', 'r');
%     line([0 0], [0 1.2*Earth.MeanRadius], [0 0], 'Color', 'g');
%     line([0 0], [0 0], [0 1.2*Earth.MeanRadius], 'Color', 'b');

%plot3(TX_ECEF(1), TX_ECEF(2), TX_ECEF(3), 'Marker', 'x', 'MarkerEdgeColor', 'y', 'MarkerFaceCol
or', 'y', 'MarkerSize', 10)
    plot3(ECEF(:, 1), ECEF(:, 2), ECEF(:, 3), 'ro')
    plot3(Coord(:, 1), Coord(:, 2), Coord(:, 3), 'yo')

```

```

        view(-90, 0)

    end

end

if flag.rawdatamaps == 1
%     figure    (G28)
%
%     xlim([-180 180])
%     ylim([-90 90])
%     grid on
%     hold on
%     plot(G28.lon, G28.lat, 'k. ')
%     plot(Tx.lon, Tx.lat, 'g*')
%     plot(Tx2.lon, Tx2.lat, 'b*')
%     hold off

    figure

    xlim([-360 0])
    ylim([-90 90])
    grid on
    hold on
    plot(GCII.lon, GCII.lat, 'b. ')
    plot(Tx.lon, Tx.lat, 'g*')
    plot(Tx2.lon, Tx2.lat, 'r*')
    plot(long, lat, 'k')
    plot(long-360, lat, 'k')
    hold off
    title('G-II space-based spot beam map')
    xlabel('Earth Longitude, (deg)')
    ylabel('Earth Latitude, (deg)')
    legend('Space raw data LLA point', 'Galaxy 28 Position', 'G-II
Position', 'Location', 'northwest')

    figure

    xlim([-360 0])
    ylim([-90 90])
    grid on
    hold on
    plot(LLACoord(:, 2), LLACoord(:, 1), 'k. ')
    plot(Tx.lon, Tx.lat, 'g*')
    plot(Tx2.lon, Tx2.lat, 'r*')
    plot(long, lat, 'k')
    plot(long-360, lat, 'k')
    hold off
    title('G-II ground-based spot beam map')
    xlabel('Earth Longitude, (deg)')

```

```
ylabel('Earth Latitude, (deg)')  
legend('Ground LLA point', 'Galaxy 28 Position', 'G-II  
Position', 'Location', 'northwest')  
  
end
```

Published with MATLAB® R2013a

Data_rate_check_script.m (Analyze data rate effects)

```
clc
clear all
close all

alt = 350;

desired = 3; %%desired** minimum number of data points per beam flythrough, assuming
less-than-nominal passes.
c = 35786+6378;

altcheck = 0;

for alt = 350:50:500
    beam_width(1) = 0;
    check = 0;
    altcheck = altcheck+1;

    for ctr = 1:1:150

        if check == 0
            beam_width(ctr) = beam_width(ctr) + 0.1;
        else
            beam_width(ctr) = beam_width(ctr-1) + 0.1;
        end

        check = 1;

        half_beam_width = beam_width(ctr)/2;

        A = half_beam_width;

        a = 6378 + alt;

        C = asind((sind(A)/a)*c);

        B = 180 - A - C;

        Arc_covered = 2*C;

        In_beam_fraction = Arc_covered / 360;

        Orbit_period = 2*pi*sqrt(((6378+alt)^3)/398600);

        Time_in_beam = In_beam_fraction * Orbit_period;

        Time_in_beam_MOD = Time_in_beam / 3; %Safety Factor Applied in order to account for
```

less-than-nominal passes.

```
Sampling_rate(ctr) = Time_in_beam_MOD / desired;

hold on

end

if altcheck ==1
    plot(beam_width, Sampling_rate, 'k. ')
elseif altcheck == 2
    plot(beam_width, Sampling_rate, 'g. ')
elseif altcheck == 3
    plot(beam_width, Sampling_rate, 'b. ')
elseif altcheck == 4
    plot(beam_width, Sampling_rate, 'r. ')
end

end

xlim([0, 10])
legend('350 km alt', '400 km alt', '450 km alt', '500 km alt');

xlabel('Beam width of spot beam, (deg)');
ylabel('Necessary sampling rate (seconds / sample)');
title('Appropriate minimum payload sampling rate for various GEO spot beam sizes, assumes a minimum of 3 data points required per pass');
```

Published with MATLAB® R2013a

Map_Simulation.m (Watch Beam Mapping Progress Visually)

```
clc; clear all; close all

Max_Time = 300000; %duration of mapping simulation, seconds
Step_Size = 1; %seconds. be careful about increasing this too much...

[GPS.duration, GPS.startlat, GPS.startlon, GPS.stopl原因, GPS.stopl原因, GPS.starttime,
GPS.stoptime] = importBeam_map('beam_map.csv');

% Move points > 0 longitude by 360 degrees for ease of plotting.
for check = 1:length(GPS.startlon)
    if GPS.startlon(check) > 0
        GPS.startlon(check) = GPS.startlon(check) - 360;
    end
    if GPS.stopl原因(check) > 0
        GPS.stopl原因(check) = GPS.stopl原因(check) - 360;
    end
end

GPS_Data = [GPS.duration, GPS.startlat, GPS.startlon, GPS.stopl原因, GPS.stopl原因,
GPS.starttime, GPS.stoptime];

GPS_Data = sortrows(GPS_Data, 6); %sort by column 6, which is the 'starttime'

figure
xlim([-270 0])
ylim([-90 90])
grid on
ctr2 = 1; %controls which 'row' in the data will be plotted.
ctr3 = 1;

for ctr = 1:Step_Size:Max_Time %For loop that controls time

    if GPS_Data(ctr2, 6) < ctr; %If the ctr passes the time when the GPS point was
detected...
        hold on
        pause(.3)
        point1(ctr2) = plot(GPS_Data(ctr2, 3), GPS_Data(ctr2, 2), 'g. '); %Then plot the
start point.
        pause(.3)
        point2(ctr2) = plot(GPS_Data(ctr2, 5), GPS_Data(ctr2, 4), 'g. ');
        drawnow
        ctr2 = ctr2 + 1; %Get ready to plot the next point
    end

    if GPS_Data(ctr3, 6) < ctr - 5000; %Fading memory simulation
        hold on
        delete(point1(ctr3))
        delete(point2(ctr3))
    end
end
```

```
    plot(GPS_Data(ctr3, 3), GPS_Data(ctr3, 2), 'k. ') %Then plot the start point.  
    plot(GPS_Data(ctr3, 5), GPS_Data(ctr3, 4), 'k. ')  
    drawnow  
    ctr3 = ctr3 + 1;  
end
```

```
end
```

Published with MATLAB® R2013a

Additionally Used or Required MATLAB Scripts and Functions

- importBeam_Map.m
 - Generated by MATLAB to import beam map spreadsheets
- importSTK.m
 - Generated by MATLAB to import STK data
- STK.m
 - Class definitions useful for linking STK and MATLAB. Created by James Sales [28].
- Main.m
 - Developed in coordination with previous AFIT geolocation research, this script was created to import single spot beam pass information from my simulations, generate simulated lines of bearing (with noise) to the Galaxy 28 transmitter, and pass the data through a simple Kalman filter to perform position location estimation of GEO transmitters.

Bibliography

- [1] US. Government, "National Security Space Strategy Unclassified Summary," US Policy, January 2011.
- [2] J. Garamone, "Shelton Discusses Importance of Space Defense," *Defense News*, 7 January 2014.
- [3] US. Government, "FCC Online Table of Frequency Allocations," Federal Communications Commission Office of Engineering and Technology Policy and Rules Division, 2014.
- [4] H. H. et al., "CubeSat: A new generation of picosatellite for education and industry low-cost space experimentation," in *14th Annual AIAA/USU Small Satellite Conference*, Logan, UT, 2000.
- [5] E. A. Abbate, "Disaggregated Imaging Spacecraft Constellation Optimization with a Genetic Algorithm," MS Thesis, AFIT-ENY-M-14, Graduate School of Engineering and Management, Air Force Institute of Technology (AU), Wright-Patterson AFB, OH, 2014.
- [6] D. a. K. D. Selva, "A Survey and Assessment of the Capabilities of CubeSats for Earth Observation," *Acta Astronautica*, vol. 74, 2012.
- [7] "2013 AFIT 6U EDU CubeSat Bus Interface Control Document (ICD)," Air Force Institute of Technology, WPAFB, OH, 2013.
- [8] M. Blackstun, E. Swenson, S. Hart, J. Black and R. Cobb, "Design, Build, and Test of Engineering Development Unit CubeSats for Satellite Design Courses," in *ASEE International Forum, American Society for Engineering Education*, 2012.
- [9] E. Glennon, J. Gauthier, M. Choudhury, K. Parkinson and A. Dempster, "Project Biarri and the Namuru V3.2 Spaceborne GPS Receiver," in *International Global Navigation Satellite Systems Society (IGNSS) Symposium*, Outrigger Gold Coast, Australia, July 2013.
- [10] P. Gurfil and J. Herscovitz, "The SAMSON Project - Cluster Flight and Geolocation with Three Autonomous Nano-satellites," Technion-Israel Institute of Technology, Haifa, Israel, 2012.
- [11] D. C. Montgomery, *Design and Analysis of Experiments*, Hoboken, NJ: John Wiley & Sons, 2009.
- [12] "Satbeams," IPC BonAnza LLC., 2014. [Online]. Available: <http://www.satbeams.com>. [Accessed 1 October 2014].
- [13] R. Horak, *Telecommunications and Data Communications Handbook*, Hoboken, NJ: John Wiley & Sons, 2012.
- [14] D. Roddy, *Satellite Communications*, 4th ed., New York, NY: McGraw-Hill Companies, 2006.
- [15] SiRF Technology, Inc., "NMEA Reference Manual," SiRF Technology, Inc., San Jose, CA, January 2005.
- [16] A. C. Newell, R. D. Ward and E. J. McFarlane, "Gain and Power Parameter Measurements Using Planar Near-Field Techniques," *IEEE Transactions on*

- Antennas and Propagation*, vol. 36, no. 6, pp. 792-803, 1988.
- [17] M. Schneider, C. Hartwanger and H. Wolf, "Antennas for multiple spot beam satellites," *CEAS Space*, vol. J, no. 2, pp. 59-66, 2011.
 - [18] Y. Henri, "ITU Radiomonitoring," in *ITU Asia-Pacific Regional Workshop on Satellite Launching & Coordination*, Indonesia, 2013.
 - [19] Puig-Suari, et al., "Development of the Standard CubeSat Deployer and a CubeSat-Class PicoSatellite.," *Proc. 2001 Aerospace Conference*, vol. 1, pp. 347-353, 2001.
 - [20] "Canisterized Satellite Dispenser (CSD) Data Sheet, 2002337 Rev B.," Planetary Systems Corp., Silver Spring, MD, 2014.
 - [21] M. Swartwout, "The First One Hundred CubeSats: A Statistical Look," *Journal of Small Satellites*, vol. 2, no. 2, pp. 213-233, 2013.
 - [22] University of New Mexico, "ORS Squared," Cosmiac, 2014. [Online]. Available: <http://cosmiac.org/space-missions/ors-squared/>. [Accessed 18 February 2015].
 - [23] A. J. Small, "Radio Frequency Emitter Geolocation Using CubeSats," MS Thesis, AFIT-ENG-14-M-68. Department of Electrical and Computer Engineering, Air Force Institute of Technology (AU), Wright-Patterson AFB, OH, 2014.
 - [24] Fish, et al., "DICE Mission Design, Development, and Implementation: Success and Challenges," in *26th Annual AIAA/USU Conference on Small Satellites*, Logan, UT, 2012.
 - [25] P. O. Hayne, B. A. Cohen, R. G. Sellar, R. Staehle, N. Toomarian and D. A. Paige, "Lunar Flashlight: Mapping Lunar Surface Volatiles Using a CubeSat," in *USRA Annual Meeting of the Lunar Exploration Analysis Group*, Laurel, MD, 2013.
 - [26] J. R. Claybrook, "Feasibility Analysis on the Utilization of the Iridium Satellite Communications Network for Resident Space Objects in Low Earth Orbit," MS Thesis, AFIT-ENY-13-M-04. Graduate School of Engineering and Management, Air Force Institute of Technology (AU), Wright-Patterson AFB, OH, March 2013.
 - [27] S. P. Ingraham, "Dynamic Constellation Tasking and Management," MS Thesis, AFIT-ENY-13-M-18. Graduate School of Engineering and Management, Air Force Institute of Technology (AU), Wright-Patterson AFB, OH, 2013.
 - [28] J. W. Sales, "Trajectory Optimization for Spacecraft Collision Avoidance.," MS Thesis, AFIT-ENY-13-S-01. Graduate School of Engineering and Management, Air Force Institute of Technology (AU), Wright-Patterson AFB, OH, 2013.
 - [29] R. E. Thompson, J. M. Colombi, J. T. Black and B. Ayers, "Disaggregated Defense Weather System Follow-on (WSF) Conceptual Architecture Optimization," in *AIAA SPACE 2014 Conference and Exposition*, San Diego, CA, August 2014.
 - [30] A. Hatch, "Electrospray Propulsion Interface and Mission Modeling for CubeSats," MS Thesis, AFIT-GA-ENY-12-S47. Graduate School of Engineering and Management, Air Force Institute of Technology (AU), Wright-Patterson AFB, OH, 2012.
 - [31] B. A. Andrews, "A Colony-II CubeSat Mission Modeling Tool," MS Thesis, AFIT-GA-ENY-12-M01. Graduate School of Engineering and Management, Air Force Institute of Technology (AU), Wright-Patterson AFB, OH, 2012.

- [32] B. W. Spanbauer and J. M. Yates, "Geostationary Orbit Development and Evaluation for Space Situational Awareness," MS Thesis, AFIT-GSE-ENV-09-05DL. Graduate School of Engineering and Management, Department of Systems and Engineering Management, Air Force Institute of Technology (AU), Wright-Patterson AFB, OH, December 2009.
- [33] R. T. Bentley, "Experimental investigation of radio frequency (RF) signal geolocation concepts using geostationary satellites," in *AIAA Space Programs and Technologies Conference*, Huntsville, AL, September 1996.
- [34] J. E. D. P. J. Wertz, *Space Mission Engineering, The New SMAD*, Hawthorne, CA: Microcosm Press, 2011.
- [35] Honeywell Aerospace, "Ku vs. Ka, Content Brief Pt. I," *Avionics Magazine*, August 2013.
- [36] K. Singarajah, "Overview of Ka-band Satellite System Development & Key Regulatory Issues," in *ITU Conference on Prospects for use of the Ka-band by Satellite Communication Systems*, Almaty, Kazakhstan, 2012.
- [37] M. W. Tobias, "Cruise Ship Communications for Passengers is About to Change," *Forbes*, 8 March 2013.
- [38] USA Today, "Coming to a cruise ship near you: Fast Internet," *USA Today*, 19 November 2012.
- [39] D. Welch, "Is Ka-Band the Ku- Killer?," *SatMagazine*, February 2013.
- [40] D. Vallado, *Fundamentals of Astrodynamics and Applications*, 3rd ed., New York, NY and Hawthorne, CA: Springer and Microcosm Press, 2007.
- [41] W. E. Wiesel, *Spaceflight Dynamics*, Third Edition, Dayton, OH: CreateSpace Independent Publishing Platform, 2010.
- [42] NASA Ames Research Center, "Small Spacecraft Technology State of the Art," NASA/TP-2014-216648/REV1. National Aeronautics and Space Administration, Washington, DC, 2014.
- [43] R. Ersoy and G. H. Schennum, "INTELSAT VII Spacecraft Antennas," Ford Aerospace, Palo Alto, CA, 1989.
- [44] G. H. Schennum and L. Ersoy, "Antenna Subsystem for the INTELSAT VII Spacecraft," Ford Aerospace, Space Systems Division, Palo Alto, CA, 1989.
- [45] B. R. Castello, "CubeSat Mission Planning Toolbox," MS Thesis. California Polytechnic State University, San Luis Obispo, CA, June 2012.
- [46] L. Qiao, C. Rizos and A. G. Dempster, "Analysis and Comparison of CubeSat Lifetime," Australian Centre for Space Engineering Research, School of Surveying and Geospatial Engineering, University of New South Wales, Sydney, NSW, Australia, 2013.
- [47] H. Voss, "EyeStar: A Paradigm Shift," in *11th Annual CubeSat Developers Workshop*, San Luis Obispo, CA, April 2014.
- [48] L. B. Bastow, "Modeling the Impact of the Payload Alert Communications System (PACS) on the Accuracy of Conjunction Analysis," MS Thesis, AFIT-ENV-13-M-

01. Graduate School of Engineering and Management, Air Force Institute of Technology (AU), Wright-Patterson AFB, OH, 2013.
- [49] R. Votel and D. Sinclair, "Comparison of Control Moment Gyroscopes and Reaction Wheels for Small Earth-Observing Satellites," in *26th Annual AIAA/USU Conference on Small Satellites*, Logan, UT, 2012.
- [50] T. E. O'Brien, "Space Situational Awareness CubeSat Concept of Operations," MS Thesis, Naval Postgraduate School, Monterey, CA, 2011.
- [51] National Science Foundation (NSF), "Annual CubeSat Report, CubeSat Based Science Mission for Geospace and Atmospheric Research," National Aeronautics and Space Administration, Washington, DC, 2013.
- [52] E. R. Dannemeyer, "Design and Analysis of an Attitude Determination and Control Subsystem for AFIT's 6U Standard Bus," Air Force Institute of Technology, WPAFB, OH, 2014.
- [53] S. K. N. S. B. J. D. D. J. L. D. V. D. Eric Bailey, "Anubis ASYS 631 Final Report," Air Force Institute of Technology, WPAFB, OH, 2014.
- [54] C. Le Gaux III, "STARE CubeSat Communications Testing, Simulation, and Analysis," Naval Postgraduate School, Monterey, CA, 2012.
- [55] D. Koks, "Numerical Calculations for Passive Geolocation Scenarios," Electronic Warfare and Radar Division, Defense Science and Technology Organization, Australian Government, Edinburgh, SA, Australia, 2007.
- [56] B. Weeden, "Radio Frequency Spectrum, Interference and Satellites Fact Sheet," Secure World Foundation (SWF), 2013.
- [57] F. Roßberg, "Simulation of the deployment and orbit operations of the NPS-SCAT CubeSat," NPS-SP-08-002. Naval Postgraduate School, Monterey, CA, 2008.
- [58] R. Hodges, B. Shah, D. Muthulingham and T. Freeman, "ISARA - Integrated Solar Array and Reflectarray Mission Overview," in *AIAA/USU Conference on Small Satellites*, Logan, UT, 2013.
- [59] M. Boghosian, "Cost Estimating Methodology for Very Small Satellites, A-PICOMO (Aerospace Picosatellite Cost Model)," in *1st Interplanetary CubeSat Workshop*, Cambridge, MA, 2012.
- [60] K. N. Hale, "Expanding the Use of Time/Frequency Difference of Arrival Geolocation in the Department of Defense," PhD Dissertation. The RAND Corporation, Santa Monica, CA, 2012.
- [61] L. Qiao, "Garada: SAR Formation Flying, Annex 7. Orbit Modelling and Analysis, Simulated Mission Planning," Australian Centre for Space Engineering Research (ACSER), University of New South Wales, Sydney, Australia, June 2013.
- [62] M. Wade, "Encyclopedia Astronautica, FS-1300 Bus," [Online]. Available: <http://www.astronautix.com/craft/fs1300.htm>. [Accessed September 2014].
- [63] Tachyon, Inc, *Tachyon Airborne Satellite Terminal - Power Spectral Analysis Document*, San Diego, CA: Tachyon, Inc., [No Date] est. 2012.
- [64] R. P. Welle and D. Hinkley, "The Aerospace Nano/PicoSatellite Program," in *In-*

- Space Non-Destructive Inspection Technology Workshop*, Houston TX, July 2014.
- [65] K. O. Michael, *Satellite Communication Engineering*, 2nd ed, CRC Press, 2013.
- [66] California Polytechnic State University, "CubeSat," California Polytechnic State University, 2014. [Online]. Available: <http://wsw.cubesat.org>. [Accessed October 2014].
- [67] W. A. Imbriale, S. Gao and L. Boccia, *Space Antenna Handbook*, Hoboken, NJ: John Wiley & Sons, June 2012.

Vita

Second Lieutenant Jacob A. LaSarge graduated from Byron Center High School in Byron Center, Michigan. He then accepted an Air Force ROTC scholarship from Detachment 400 at Michigan Technological University, where he graduated with a Bachelor of Science degree in Mechanical Engineering, with an Aerospace Enterprise Concentration in May 2013. During his undergraduate studies, he worked as the project lead for the Oculus-ASR, a microsatellite project seeking to enhance U.S. space situational awareness as a non-resolved imagery calibration satellite for ground telescopes. For his efforts leading the Oculus-ASR project, Jacob was nationally recognized by the U.S. Air Force as the recipient of the 2012 Cadet Research Award.

His first assignment, upon commissioning as a Developmental Engineering Officer, was to the Air Force Institute of Technology as a direct accession, where he entered the Graduate School of Engineering and Management in August 2013 for his Master of Science degree in Astronautical Engineering. Upon graduation, he will be assigned to the Space and Missile Systems Center in Los Angeles, CA.

REPORT DOCUMENTATION PAGE			Form Approved OMB No. 0704-0188		
<p>The public reporting burden for this collection of information is estimated to average 1 hour per response, including the time for reviewing instructions, searching existing data sources, gathering and maintaining the data needed, and completing and reviewing the collection of information. Send comments regarding this burden estimate or any other aspect of this collection of information, including suggestions for reducing this burden to Department of Defense, Washington Headquarters Services, Directorate for Information Operations and Reports (0704-0188), 1215 Jefferson Davis Highway, Suite 1204, Arlington, VA 22202-4302. Respondents should be aware that notwithstanding any other provision of law, no person shall be subject to any penalty for failing to comply with a collection of information if it does not display a currently valid OMB control number. PLEASE DO NOT RETURN YOUR FORM TO THE ABOVE ADDRESS.</p>					
1. REPORT DATE (DD-MM-YYYY) 26-03-2015		2. REPORT TYPE Master's Thesis		3. DATES COVERED (From — To) Sept 2013 – Mar 2015	
4. TITLE AND SUBTITLE A CubeSat Mission for Mapping Spot Beams of Geostationary Communications Satellites			5a. CONTRACT NUMBER		
			5b. GRANT NUMBER		
			5c. PROGRAM ELEMENT NUMBER		
			5d. PROJECT NUMBER		
6. AUTHOR(S) LaSarge, Jacob A., Second Lieutenant, USAF			5e. TASK NUMBER		
			5f. WORK UNIT NUMBER		
7. PERFORMING ORGANIZATION NAME(S) AND ADDRESS(ES) Air Force Institute of Technology Graduate School of 2950 Hobson Way WPAFB OH 45433-7765			8. PERFORMING ORGANIZATION REPORT NUMBER AFIT-ENY-15-M-247		
9. SPONSORING / MONITORING AGENCY NAME(S) AND ADDRESS(ES) Intentionally Left Blank			10. SPONSOR/MONITOR'S ACRONYM(S)		
			11. SPONSOR/MONITOR'S REPORT NUMBER(S)		
12. DISTRIBUTION / AVAILABILITY STATEMENT DISTRIBUTION STATEMENT A: APPROVED FOR PUBLIC RELEASE; DISTRIBUTION UNLIMITED					
13. SUPPLEMENTARY NOTES This work is declared a work of the U.S. Government and is not subject to copyright protection in the United States					
14. ABSTRACT As space-rated technologies become more compact and more readily available over time, the concept of accomplishing space missions with smaller nanosatellite-class spacecraft becomes increasingly feasible. This research focuses specifically on a CubeSat mission to assist with radio frequency (RF) domain verification; that of characterizing and mapping K-band spot beams from communications satellites in geostationary orbit. By flying a constellation of CubeSats through the edges of spot beams originating from geostationary communication satellites, the spot beam's coverage area will be characterized. This research conducts a mission feasibility assessment, identifies the principle mission requirements to complete a spot beam mapping CubeSat mission, and examines various constellation configurations that are able to complete the spot beam mapping mission. It was found that certain spot beam mapping CubeSat constellations performed well, specifically regarding mapping time, spot beam detection capability, and overall mapping resolution. On the whole, the spot beam mapping mission was deemed feasible under the governing assumptions and requirements. Constellations with CubeSat formations that used specific spacing between themselves in an orbital plane could be synchronized to produce ground-based spot beam maps with excellent resolution; however constellations with a single plane of evenly-spaced CubeSats or particular Walker constellations could produce better results over shorter durations.					
15. SUBJECT TERMS Mapping, CubeSat, Mission, Radio Frequency Signals, Spot Beams, Communications Satellites, Constellation					
16. SECURITY CLASSIFICATION OF:			17. LIMITATION OF ABSTRACT UU	18. NUMBER OF PAGES 168	19a. NAME OF RESPONSIBLE PERSON Dr. Jonathan Black (ENY)
a. REPORT U	b. ABSTRACT U	c. THIS PAGE U			19b. TELEPHONE NUMBER (Include Area Code) (540) 231-0037 jonathan.black@vt.edu

Standard Form 298 (Rev. 8-98)
Prescribed by ANSI Std. Z39.18